

POLITECNICO DI TORINO

Master's Degree in Mechanical Engineering

Master's Degree Thesis

**Executive design, implementation  
and operation of the Naples Test  
Facility cryogenic system for the  
DarkSide-20k experiment**



**Supervisors**

Prof. Maurizio SCHENONE  
Prof.ssa Giuliana FIORILLO

**Candidate**

Marco CARLEO

DECEMBER 2021



# ABSTRACT

The PDU Naples Test Facility is a dedicated installation located inside the Naples Cryolab cleanroom. The facility is a large cryogenic system that works with liquid nitrogen and was designed specifically for the Photo Detecting Units (PDU) cryogenic test. PDU are the main technology of the DarkSide-20k project. The project is a direct detection dark matter search experiment, which will be assembled inside the Laboratori Nazionali del Gran Sasso in Italy.

The aims of this thesis is the description and commissioning of the Naples Test Facility starting by introducing, first of all, a context to the DarkSide-20k project, its main technologies and the great collaboration involved in this experiment. The Test Facility pursues to be a cryogenic system that works both for long periods and independently. I started this thesis by approaching the design and the layout choice, thanks to 2D and 3D models of the facility, and I analyzed and described the operating phases of the system and the cryogenic test. At this point the main design objectives setting was done.

The second part of this study focuses on the design and production regulations of the Cryostat, the main component of the system, within which will be inserted the PDU in order to be tested. The research was possible following and studying the EN regulations for unfired vessel and PED directive. In addition to this, an in-depth study carried out on Ansys Workbench software is presented in this thesis, focusing on the mechanical behaviour of the cryostat subject to the mechanical and thermal loading conditions.

Finally, the proposed study ends with the assembly and commissioning of the system focusing on the description of the individual components and the description of the first operating tests. The ultimate objective of this study a comparison was made between the test results and the design expectations.

# INDEX

1. DarkSide-20k .....	10
1.1. Cryogenics .....	11
1.1.1. Urania .....	12
1.1.2. Aria .....	13
1.2. WIMPs detection .....	15
1.3. DarkSide 20k features .....	16
1.3.1. Cryogenic system .....	17
1.3.2. Silicon Photomultipliers .....	22
1.4. PDM Test Facility .....	25
2. Test Facility general description .....	27
2.1. Cryogenic System .....	28
2.1.1. Outdoor System .....	29
2.1.2. Clean Room .....	31
2.2. Electrical and optical connections .....	41
2.3. Slow control & data handling .....	43
2.4. Test Facility process .....	46
3. Mechanical assessment of the cryostat based on EN 13445 and finite element analyses .....	54
3.1. Pressure Equipment Directive .....	54
3.2. Conformity assessment with regulatory EN13445 code .....	58
3.2.1. Maximum allowed values of the nominal design stress for pressure parts .....	59
3.2.2. Shell under internal pressure .....	60
3.2.3. Shell under external pressure .....	62

3.2.4. Flanges .....	66
3.2.5. Vertical vessels with skirts .....	70
3.3. Finite Element Analysis .....	75
4. Assembly and commissioning .....	83
4.1. Assembly work.....	83
4.2. Slow Control System .....	93
4.3. Test Facility's tests.....	100

# LIST OF FIGURES

1.1. DS-20k experiment rendering.....	10
1.2. P&ID of Urania Project.....	12
1.3. Aria project Block Diagram.....	14
1.4. distillation column in Seruci(SU).....	14
1.5. Dual phase TPC process.....	15
1.6. LAr TPC & Veto system.....	16
1.7. Schematic of the DarkSide-20k cryogenics system.....	18
1.8. DS-20k cold box design, fabrication and assembly.....	19
1.9. LAr condenser inside the cold box.....	20
1.10. 3D rendering of DS-20k cryostat (red).....	21
1.11. Warm vessel (red).....	22
1.12. SiPM scheme.....	23
1.13. Single channel photodetector module (PDM) consisting of a 5050 mm <sup>2</sup> tile of 24 SiPMs and a front-end board.....	23
1.14. 3D rendering of DS-20k LAr TPC and PDUs.....	24
1.15. Motherboard's prototype.....	25
1.16. CleanRoom layout.....	26
1.17. DarkSide laboratory, Naples.....	26
2.1. Test Facility P&ID.....	27
2.2. The transfer line on the outside of the INFN laboratory(clean room). ....	28

2.3. LN <sub>2</sub> Outdoor Tank .....	29
2.4. Gas lines from LN <sub>2</sub> bottle and tank.....	30
2.5. 3D rendering of INFN Naples' laboratory: on the right Lab 1; on the left Lab 2, Clean room. ....	32
2.6. Clean room overview .....	32
2.7. Test Facility P&ID clean room .....	33
2.8. Cryostat's drawing from Demaco.....	34
2.9. Upper Flange.....	35
2.10. 3D SolidWorks rendering: VCO fittings (in red); Safety valves (in blue). .	35
2.11. Cold box's sketch by Criotec.....	37
2.12. 3D rendering of the inner cold box part.....	38
2.13. 3D layout of Test Facility .....	38
2.14. PDU Box (motherboard).....	39
2.15. The 3D rendering of PDUs holding structure .....	39
2.16. Capture of 3D sectioned cryostat .....	40
2.17. Optical splitter from one to 16 available for the light distribution .....	41
2.18. LV & HV Layout.....	42
2.19. The example of the interface window of the MIDAS run controller .....	43
2.20. Schematic view of the DAQ architecture of the PDU Test Facility .....	44
2.21. PT100s distribution.....	45
2.22. Gas lines from the outdoor system- 2D sketch .....	47
2.23. Gas lines from PRs panel- 2D sketch.....	47
2.24. Clean room:LN <sub>2</sub> direction, blue arrow; N <sub>2</sub> direction from cryostat, green arrow; All metal manual valve VN1, green circle. ....	48

2.25. Electro Valve EV03 in the blue circle; LN <sub>2</sub> way to the clean room, blue arrow; discharge line, red arrow. ....	49
2.26. Filling phase, cold box view .....	50
2.27. Globe valve RV2.....	51
2.28. LN <sub>2</sub> 's way to the vent.....	52
2.29. Discharge line: NVR02 in red; Evaporator VA02 before the electro-valve EV02 in yellow.....	53
3.1. Conformity assessment's chart.....	55
3.2. Conformity assessment table for fluid group 2.....	56
3.3. Conformity assessment modules table .....	57
3.4. Testing groups for steel pressure vessels .....	61
3.5. Torispherical ends; CR crown radius; KR knuckle radius.....	61
3.6. Parameter $\beta$ for torispherical end - rating.....	62
3.7. Cylinder with heads .....	63
3.8. Value of $\epsilon$ .....	64
3.9. Values of $\frac{P_m}{P_y}$ versus $\frac{P_r}{P_y}$ .....	65
3.10. Bolts size .....	67
3.11. Skirt connection in knuckle area .....	70
3.12. Cryostat's 3D modelling and development .....	75
3.13. Analysis settings .....	76
3.14. Equivalent stress solution.....	77
3.15. Total deformation solution.....	78
3.16. Steady-state thermal solution .....	79
3.17. Equivalent stress solution.....	80

3.18. Deformation solution .....	81
3.19. Buckling analysis solution .....	82
4.1. Test Facility's first 3D layout .....	83
4.2. Cryostat and profile tower layout .....	84
4.3. KF flange connection mode .....	85
4.4. Johnston coupling .....	85
4.5. Double-wall transfer line between coldbox & cryostat .....	86
4.6. CoFlat flange assembly .....	86
4.7. Plastic line to the vent .....	87
4.8. Actual inner structure .....	87
4.9. Fittings on the upper flange .....	88
4.10. Pressure indicator (PI1) on the left; pressure transducer (PT1) on the right .....	88
4.11. PT100 installation .....	89
4.12. 3-way fitting with two manual valves VN2 & VN3 .....	90
4.13. Swagelok's VCR fitting .....	90
4.14. Relief valve RV2 .....	91
4.15. CF40 for optical fibers .....	91
4.16. KF40 metal hose from 4 safety valves .....	91
4.17. Manual angle valve VN1 .....	92
4.18. Solenoid-valve EV03 .....	94
4.19. Proportional valve VC1 linked to the PXIe and controlled by Slow Control .....	94
4.20. Electro-valve EV02 and the vent .....	96

4.21. Control loop .....	96
4.22. LabView's interface .....	97
4.23. Proportional valve VC1 linked to the PXIe and controlled by Slow Control .....	98
4.24. Slow control station .....	99
4.25. Proportional valve VC1 linked to the PXIe and controlled by Slow Control .....	100
4.26. Heating cable .....	101
4.27. LN <sub>2</sub> and N <sub>2</sub> heat exchanges .....	102
4.28. MIDAS's interface, data handling 22 October .....	103
4.29. Pressure's trend, data handling 27 October .....	103
4.30. Temperature's trend, data handling 27 October .....	104

# LIST OF TABLES

1. Linde Dewar; List of components.....	31
2. Cryostat Demaco; technical specifications.....	36
3. mechanical properties of AISI 304L.....	58
4. Joint coefficient and corresponding testing group [7].....	60
5. Load multiplier values.....	81
6. Facility's electronic components.....	93
7. Set point values.....	95

# 1

## DARKSIDE-20K

The DarkSide-20k is the successor of the DarkSide-50 experiment, a direct-detection dark matter search experiment, based on a Liquid Argon Time Projection Chamber (LAr-TPC). It is located at the Laboratorio Nazionale del Gran Sasso (LNGS) in Italy. The goal is to perform a background-free dark matter search using low radioactivity argon extracted from underground sources (UAr). The DarkSide-20k experiment proposed by INFN (Istituto Nazionale di Fisica Nucleare) will be developed by the Global Argon Dark Matter Collaboration (GADMC) and deployed at LNGS.

GADMC is an international collaboration that collects scientists from all the major groups currently working with an argon target (ArDM, DarkSide-50, DEAP-3600, and MiniCLEAN). The main technologies of the GADMC program are: the argon target obtained from the extraction of low-radioactivity argon naturally depleted in  $^{39}\text{Ar}$  from underground sources via the Urania plant; the Ar purification and active isotope separation via the Aria project; light detection via large-area cryogenic photodetector modules (PDMs) made of custom-designed silicon photomultipliers (SiPMs); operation of a LAr-TPC detector within an active veto using liquefied atmospheric argon (AAr) as scintillator.

The objective of DarkSide-20k experiment is to push the sensitivity for dark matter direct detection several orders of magnitude beyond current levels.

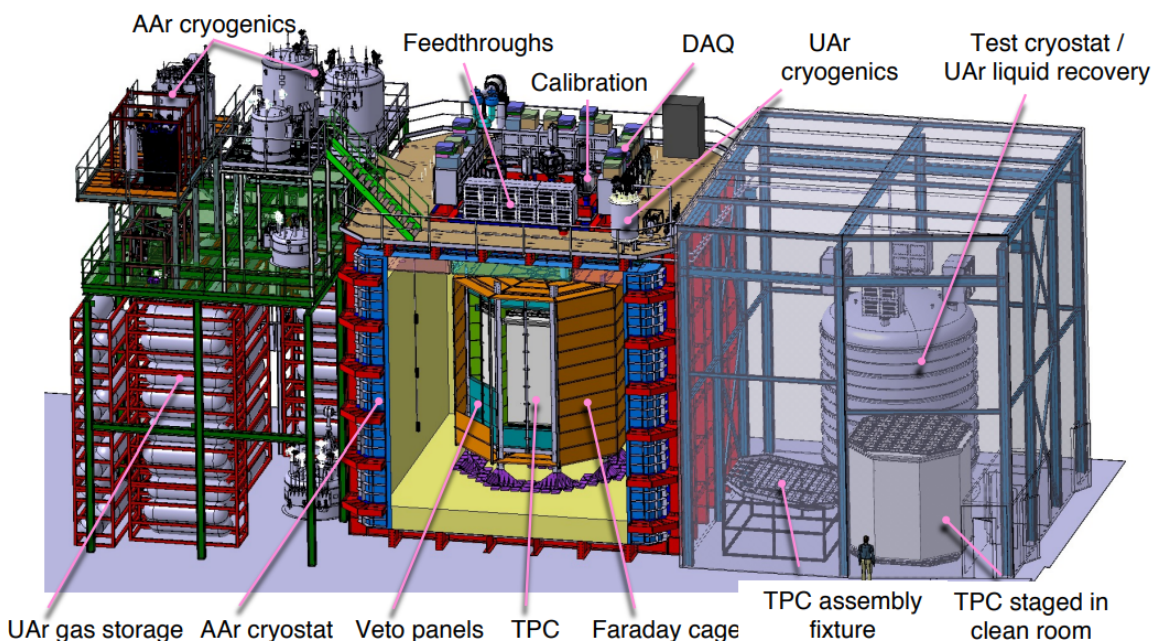


Figure 1.1: DS-20k experiment rendering

This goal can be reached by the DS-20k two-phase LAr detector, Fig. 1.1 shows the DS-20k experiment as it will be installed in the Hall C of LNGS. As shown in the picture the LAr TPC is placed inside a large Cryostat (in red) while on the side is placed the cryogenic system for UAr.

In this section we are going to describe the general design of the detector and we are going to explore how cryogenics technologies are so important for these experiments and why it is necessary to operate in specific conditions with all the devices that will be used by the experiment in particular the Silicon Photomultipliers (SiPMs), that will be tested on Test Facility.

## 1.1 CRYOGENICS

A direct detection experiment aims to detect a direct interaction of a dark matter particle with a detector and because of the extremely low event rate expected for a dark matter search, it is essential to create a low background environment in which the detectors can operate. Many are the aspects that have to be considered in order to create the correct environment. Is important to operate in deep underground laboratories, even though this location is far from sufficient. The experiment must also be placed in extremely quiet environments: shielded from the natural radioactivity of their immediate surroundings. For these reasons DS-20k has been located Hall C of LNGS, a tunnel large 14 m x 26 m and located at a depth of 3800 m.w.e.. Trace radioactivity in detector materials can be a dominant background for direct dark-matter searches. In addition to bulk contamination, a major source of background can be caused by surface contamination. A strategy for material selection and well-defined protocols for machining, storing, transporting and assembly of detector components is mandatory in order to control the backgrounds and maximize the sensitive range of DS-20k.

DS-20k employs argon as target for dark matter detection. In its liquid phase, argon (at  $T \approx 87^\circ \text{K}$ ) is outstanding medium for building large and compact detectors which can reach ultra-low backgrounds at their cores. The simultaneous detection of light and charge produced in the target leads to the identification of the primary particle interacting in the liquid. Working with noble fluids, like Liquid Argon (LAr) and Liquid Nitrogen (LN<sub>2</sub>), leads us to talk about cryogenics, in fact these fluids need specific technologies and environments to maintain their low-temperature conditions and keep a safe working condition. Another challenge with noble liquids is their purification from radioactive isotopes which are also present in the atmosphere, in fact argon derives from the atmosphere, which is predominately stable <sup>40</sup>Ar, contains radioactive isotopes of argon (like <sup>39</sup>Ar). These isotopes are at high enough concentrations in the atmosphere to be a significant background for low-background argon-based radiation detectors, and because all commercial argon is produced from air, these isotopes can represent irreducible backgrounds. However, after a campaign of extracting and purifying argon from deep CO<sub>2</sub> wells in Southwestern Colorado in the United States, the

DarkSide-50 dark matter search experiment demonstrated that this unique argon contained an  $^{39}\text{Ar}$  concentration 0.073% of the one in the atmosphere. This site of low-radioactivity underground argon has sparked an interest on the DS collaboration which focus on increasing the production of UAr to procure the target required for DarkSide-20k giving special attention to his extraction and purify process.

### 1.1.1 Urania

Urania is the project in charge of extracting and purifying the UAr from the  $\text{CO}_2$  extraction sites of Kinder Morgan (company that have an agreement with the DS collaboration) Doe Canyon Facility located in Cortez, CO. The Urania project will extract at least 100 t of low-radioactivity UAr, providing the required 51, 1 t of UAr to fill DarkSide-20k. The goal of the Urania project is to build a plant capable of extracting and purifying UAr at a maximum rate of 330 kg/day, from the same source of UAr that was used for the DarkSide-50 detector. Argon from active  $\text{CO}_2$  wells in southwestern Colorado have been found to contain low levels of the radioactive isotope  $^{39}\text{Ar}$ . The Urania feed gas stream is more or less 95%  $\text{CO}_2$ , plus a few percent of  $\text{N}_2$ , one percent  $\text{CH}_4$ , and 440 ppm of UAr. The processing scheme of the UAr extraction plant is optimized for this feed composition in order to achieve an UAr purity of better than 99.9%.

The cryogenics system of Urania is divided in three units, as we can see from Fig. 1.2.

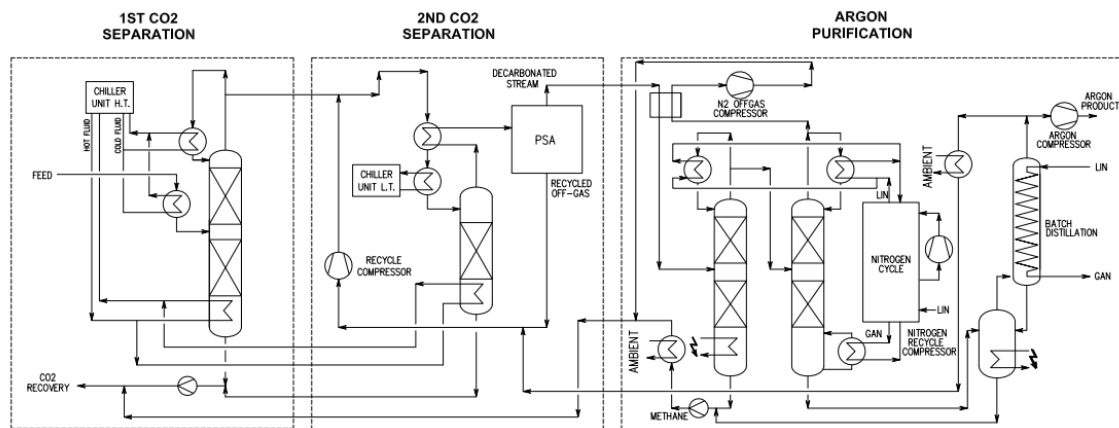


Figure 1.2: P&ID of Urania Project

The 1st and 2nd units are two  $\text{CO}_2$  liquefier/strippers followed by a pressure swing adsorption unit (PSA). The first liquefier accepts gas at 50 bar, with a flow rate of 20000 std  $\text{m}^3/\text{h}$  and a temperature of  $5^\circ\text{C}$ . At these conditions the  $\text{CO}_2$  partially condenses and the stream is separated into 2-phases (gas/liquid) as it goes to the first stripping tower. In the column a controlled quantity of heat is given by a hot fluid working between the chiller condenser and the column reboilers. The light products are vaporized and recovered from the top of the column in gas phase. The heavy products (mainly  $\text{CO}_2$ ) are collected from the bottom, compressed to 50 bar and returned to Kinder Morgan as a gas. The light

products coming from the column head are cooled down in the second step to approximately  $-50^{\circ}\text{C}$  and sent to the second stripper. The first column produces  $3300\text{ std m}^3/\text{h}$  of product flow, a factor of 5 reduction in the amount of gas to be processed by the more complex downstream units. Then in second unit there is a similar process, it ends with a re-heated of the product gas that is sent to the PSA unit, which separates the light fractions, including the argon, from the remaining  $\text{CO}_2$ .

The  $\text{CO}_2$ -free product coming from the PSA plant is sent to the final unit, which is divided in three cryogenic distillation columns. The gas firstly is pre-cooled and sent to the first column, which works at a lower pressure (9 barg), for the removal of  $\text{CH}_4$ . The second column is used to remove the remaining light fractions from the resulting  $\text{N}_2$ -rich stream, and the third to perform the final purification of the UAr using a batch distillation process. The final product, 99.9% pure UAr, will be taken in liquid form from the top of the last column and a small portion collected into a tank to check the quality of the argon. The majority of the liquid UAr will be sent in appropriate cryogenic vessels by boat to Sardinia, where it will undergo final chemical purification by another plant called Aria.

### 1.1.2 Aria

The UAr extracted by Urania arrives in Sardinia to perform his final chemical purification in the Aria plant. It also test a method for active depletion of  $^{39}\text{Ar}$  from the UAr, and it can be described as an isotopic distillation process.

Aria consists of a 350 m tall distillation column, Seruci-I, capable of separating isotopes by means of cryogenic distillation, a process that exploits the tiny difference in volatility due to the difference in isotopic mass. Aria is to be installed in underground vertical shaft of diameter 5 m and depth 350 m, located at the Seruci mine of CarboSulcis, a mining company owned by the Regione Autonoma della Sardegna (RAS).

Cryogenic distillation is an effective method for the production of stable isotopes, in fact the goal of this project is to obtain the purification of Argon-40, in particular the separation of Argon-39 from Argon-40. The Argon-39 unlike Argon-40 which is stable, decays through radioactive processes very slowly. The natural radioactivity of this isotope becomes a problem in dark matter experiments, where attempts are made to eliminate any factor that could affect the measurements. Fig. 1.3 illustrates conceptually the Aria plant. The process consists primarily of two loops: the process loop where the argon is distilled and the  $^{39}\text{Ar}$  is separated from the  $^{40}\text{Ar}$ , the refrigeration loop where nitrogen gas and liquid is used to evaporate and to condense the argon. In block diagram shown in Fig. 1.3 we can see all the sub-parts of the plant like: Feed station, to filter and regulate the feed to the column; Compressor station, to bottle the distillate at the bottom; Vacuum system, to keep a good vacuum in the cold-box, in order to minimize the heat losses;  $\text{LN}_2$  storage; Nitrogen condenser system, consisting of 4 Stirling cryo-refrigerators needed to re-condense the nitrogen, used in a close loop. The main feature of the facility is the column, called Seruci-I, consist-

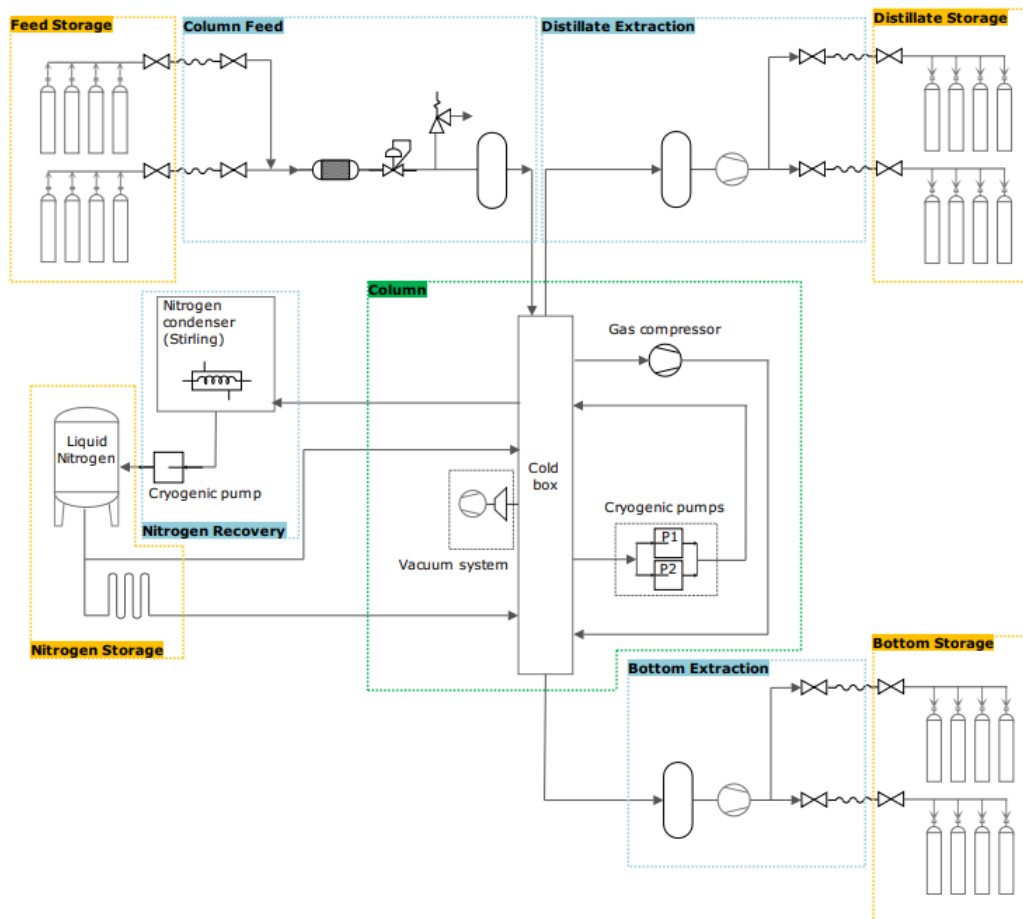


Figure 1.3: Aria project Block Diagram

ing of 28 modules of 12 m height, plus a top module (condenser) and a bottom module (reboiler). Seruci-0, instead, is a test column made by top (condenser) and bottom (reboiler) modules and a single central module and installed in an outdoor hall at the mine site, see Fig.1.4.



Figure 1.4: distillation column in Seruci(SU)

## 1.2 WIMPS DETECTION

Weakly Interacting Massive Particles (WIMPs) are dark matter candidates that may have been produced in the early Universe but are so massive and weakly interacting that they have yet to be observed in a terrestrial experiment. WIMPs constitute a model-independent class of particles that have a very low masses and an interaction cross section that goes from  $10^{-41}$  to  $10^{-51}$  cm<sup>2</sup>. What DS-20k is looking for is a nuclear recoil NRs, obtained by the scattering of a WIMPs from an Ar nucleus. Fig 1.5 describes what should happen during DS-20k experiment in the LAr-TPC.

This NRs excites the liquid argon which then produces scintillation light (called S1). Moreover ionized electrons are produced, and drifted, thanks to an electric field, through the liquid argon towards a gaseous argon region, where they are extracted. The extracted electrons accelerated by another electric field produce additional excitation and a delayed scintillation signal (S2).

These signals are detected by photodetectors' arrays made of SiPMs. Thanks to the S2 position, the time between S1 and S2 and drift velocity of electrons it is possible to know the position of the interaction. Sensors used in DS-20k are able

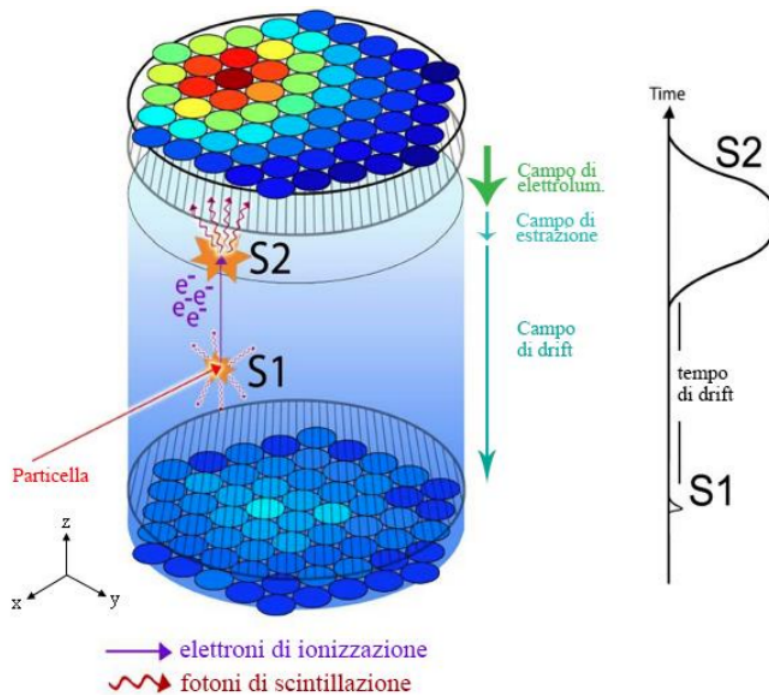


Figure 1.5: Dual phase TPC process

to separate this type of interaction from other events, called background events.

There are two types of background's sources: Electronic Recoil Background ERs, the primary source of background in a WIMPs detection experiment, are electronic recoils caused by natural radioactivity. The recoil is caused by  $\gamma$ -backgrounds and electron interactions. This is a common source of background event because  $\gamma$ -backgrounds are present in the shielding materials or an produced by cosmic ray interactions with nucleons of the detector structure and surrounding materials.

Nuclear Recoil Background NRs result from neutrons scattering off nuclei in the detector and have the major impact on the average detector background because neutrons may produce a signal identical to what we expect from WIMPs.

### 1.3 DARKSIDE 20K FEATURES

In this section I am going to describe the main elements of DS-20k experiment, in particular focusing on the cryogenic system and photodetectors used for the experiment. DS-20k is designed to operate for 10 years and, as I said, is the DS-50 successor with which it has many common features. The main features are:

- LAr TPC: a dual-phase Time Projection Chamber of 20 t, shown in Fig.1.6 (grey)
- The Veto system: a separate detector surrounding the TPC in which the neutrons from both internal and external sources are detected with very high efficiency, and the corresponding recoil events in the LAr TPC are identified and rejected (in Fig.1.6 orange and green).
- The cryogenic system: the cryogenic chamber (Cryostat), GAR and LAr handling system and LN<sub>2</sub> reserve system.
- Photoelectronics: photodetector unit PDU the DS-20K's detector composed by SiPMs silicon photomultipliers, capable to work at cryogenic temperature of LAr (89 K)

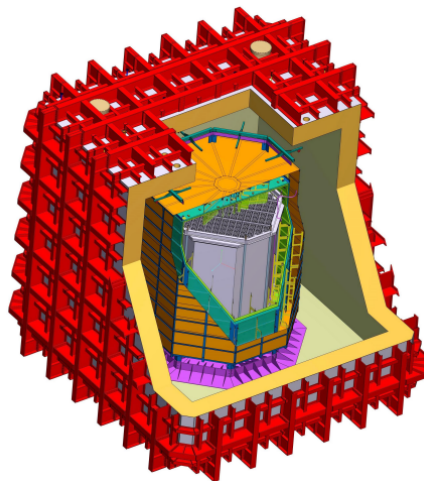


Figure 1.6: LAr TPC & Veto system

### 1.3.1 Cryogenic system

The design of the cryogenic system is largely based on the success of the DarkSide-50 system, with added improvement and scaling to handle much larger argon mass. The robust safety features of the DarkSide-50 cryogenic system will be implemented fully in the DarkSide-20k system. The cryogenic system has two main objectives to reach:

- It must be able to efficiently cool and purify 50 t of LAr to a purity level better than in DarkSide-50, in particular it should have a total gas recirculation flow equivalent to 1000 std l/min to initially reach the desired purity of LAr during the course of about one month (oxygen contamination in LAr of less than 0,06 ppb).
- It must be able to maintain a very stable detector pressure (0,1 psi).

A complete overview of the system is shown in Fig.1.7. Important components of the system are: the heat exchangers used to recover cooling power during fast purification loop; a new custom-designed argon condenser that gets a cooling power of 5 kW max; a SAES heated-Zr getter with a flow-rate capacity > 1000 std l/min for the purification of argon gas (GAr).

As shown by Fig.1.7 the cryogenic system could be divided in these subsections:

- LAr handling system
- LN<sub>2</sub> reserve system
- UAr purification system
- Cold box
- Radon trap
- Gas circulation pump
- Heat exchanger system
- UAr recovery and storage system

The LAr handling system delivers the clean radon-free UAr, which is initially stored in the recovery storage system capable of storing the full target of UAr for DS-20k.

The cold source of the entire system is provided by LN<sub>2</sub>. The LN<sub>2</sub> cooling loop is a closed system that consists of a 30 t LN<sub>2</sub> source supply tank outside Hall C, a local reserve tank capable of storing 3 days worth of cooling power in emergency mode, a LN<sub>2</sub>/argon condenser, and a set of heat exchangers to recycle the spent N<sub>2</sub> cold gas to pre-cool the incoming argon. The spent N<sub>2</sub> gas is then returned to the LN<sub>2</sub> recycling system and the re-liquefied LN<sub>2</sub> returned to the large source tank.

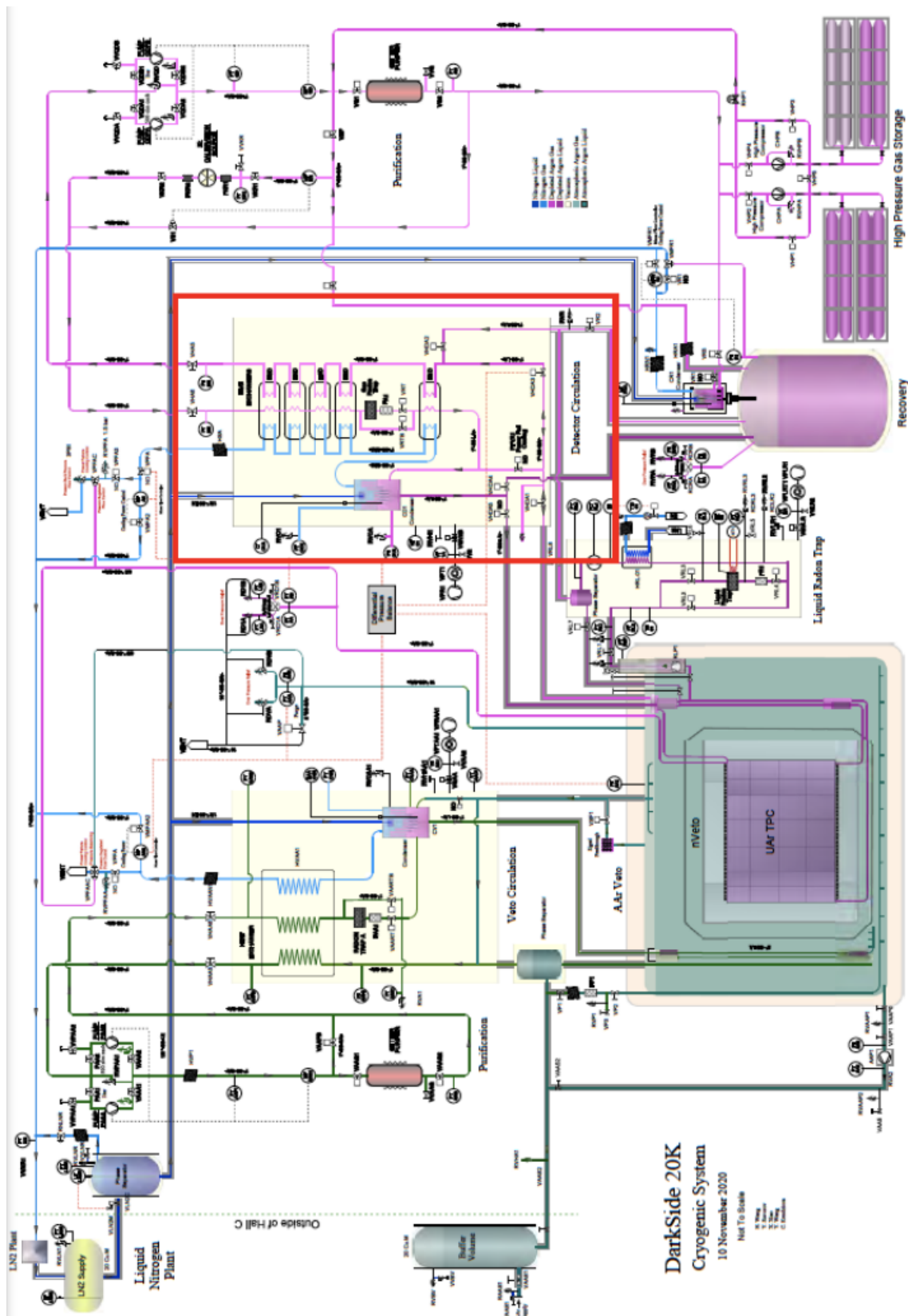


Figure 1.7: Schematic of the DarkSide-20k cryogenics system

The UAr purification system, with its Zr-based getter system, purifies the argon in gas phase during the circulation.

The cold box, as shown in Fig.1.8 , is one of the key components of the DS-20k cryogenics system, as the Test Facility's cold box, which contains all the major cryogenic handling components. Apart from the condenser, the cold box contains five heat exchanger modules to efficiently pre-cool the argon gas by cold nitrogen gas and cold outgoing argon gas. In this way the necessary cooling power is reduced dramatically. The radon trap is a volume filled with activated



Figure 1.8: DS-20k cold box design, fabrication and assembly.

synthetic charcoal in which the clean argon from the getter must pass through, prior to returning to the detector. Radon originating from any warm surfaces of the cables or the gas handling system will be efficiently removed by the radon trap.

The LAr condenser is the key part of the cryogenics system and there will be three of it, one for the detector and one each for the two recovery systems.

The 100% stainless steel condenser shown in Fig. 1.9 has a main heat exchange surface composed of the walls of many short stainless steel tubes (61 tubes of 0.5" diameter, with two different lengths, 5" and 3"). The bottoms of these tubes are welded onto a three-step holder above that and outside the tubes the purple region in Fig. 1.9 is filled with LN<sub>2</sub> at a level that depends on the cooling power requirement, while the volume below the region and inside the tubes, isolated from the LN<sub>2</sub> section, is filled with incoming GAR. LN<sub>2</sub> is fed into the condenser through a half-inch line that ends in a feature called the "chicken feeder" and controls the flow of LN<sub>2</sub> into the volume automatically by the pressure balance. The chicken feeder does not allow gas to flow back into the liquid supply line which provides flow stability. Otherwise the GAR is fed in the lower part of the condenser and liquefy thanks to the heat exchange with LN<sub>2</sub>, then it drops down to the bottom of the condenser and flows into a vacuum-insulated transfer line that transports the liquid to the detector. The length of LAr output is important. This design prevents the over-cooling of LN<sub>2</sub> side. When the LAr drops down it stops cooling and thanks to the length of the output line the LAr is quickly replaced with incoming GAR, which continuously sends heat through the wall to the LN<sub>2</sub> side. On the LN<sub>2</sub> side, the spaces between the tubes are carefully

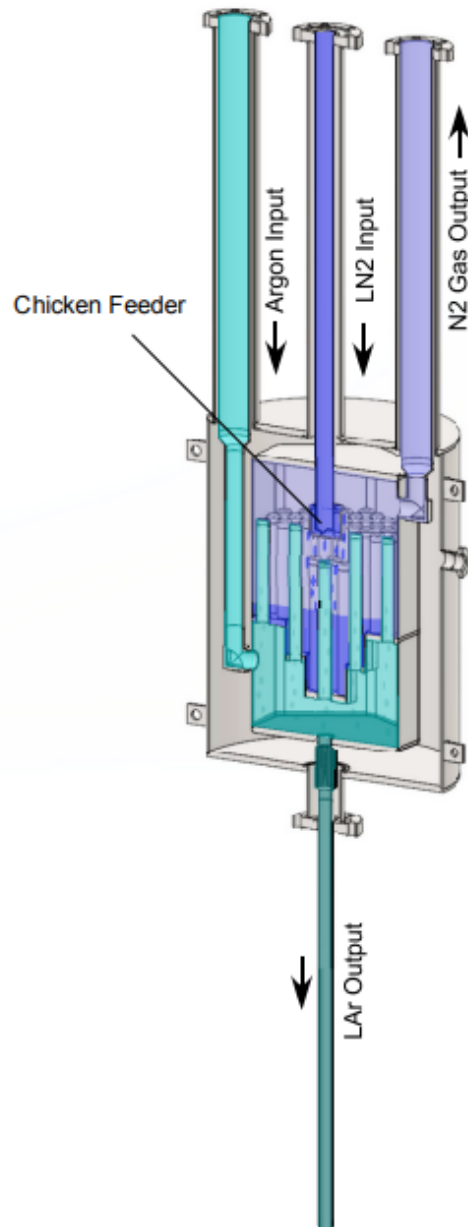


Figure 1.9: LAr condenser inside the cold box

determined such that the boil off gas is constrained and pushes away LN<sub>2</sub>, so the surface of the tube is not covered by LN<sub>2</sub> 100% of the time.

The gas circulation pump provides a speed up to 50 std L/min and relies on two components: linear motors and reed valves. The linear motors, consisting of a piston and cylinder pair, can provide a continuously adjustable pumping power. The reed valves guide the gas flow direction when the linear motors go back and forth. The combination of the linear motors and the reed valve allows the pump to work in a friction-less condition, resulting in a long lifetime. The initial fast circulation requires a speed of 1000 std l/min to achieve a good UAr purity level, and then the circulation speed can be decreased to only maintain the purity and stability. To achieve such a high circulation speed, flexibility

of operations, as well as the ease of the pump development, two individual circulation pumps will be placed in parallel, each providing a circulation rate up to 500 std l/min.

The heat exchangers close to the TPC are basically large heat exchangers using many tubes as the thermal exchanging parts, similar to the concept of the LAr condenser described above, but with a much increased thermal exchanging surface area.

The UAr recovery and storage system consists of a set of high pressure gas containers as delivered to LNGS and of a vacuum insulated cryostat for liquid phase recovery from the TPC.

The large number of elements show us an important feature of this cryogenics system design, its flexibility. Once the desired purity is reached during the commissioning phase, it will be possible to turn off or to reduce the total cooling power to the minimum amount required for the operation of the detector with its anticipated 350 std l/min GAr flow.

After this general description of the cryogenic system lets focus the cryostat. The DS-20k detector will be located inside a cryostat, shown in Fig. 1.10 operating with an atmospheric argon fill refrigerated with the AAr cryogenic system. The two-phase Time Projection Chamber (TPC) serving as the dark matter detector operates with a fill of low-radioactivity underground argon (UAr) at the center of the liquefied AAr bath. The TPC is surrounded by the active veto detector.

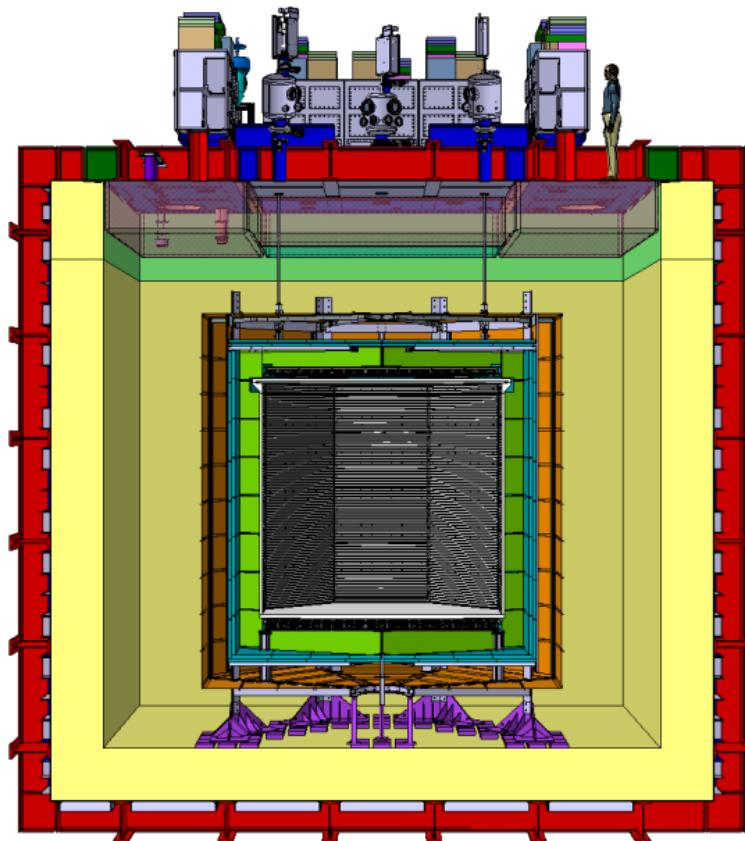


Figure 1.10: 3D rendering of DS-20k cryostat (red)

The cryostat will be divided in these elements: the stainless steel inner cold membrane that contains the cryogenic liquid; the foam insulation panels and a warm steel supporting outer structure. The cold primary membrane tank is made of a stainless-steel, a special carbon steel alloy (S460ML 1.8838), able to maintain its mechanical properties down to 220 K, 1,2 mm thick leak-tight liner that contains the cryogenic liquid. This membrane liner has a special corrugation that allows it to expand and contract in both transverse directions to provide mechanical relief to strains resulting from temperature changes. The overall outer dimensions are: width 11410 mm, length 11410 mm, height 10760 mm, see Fig.1.11.

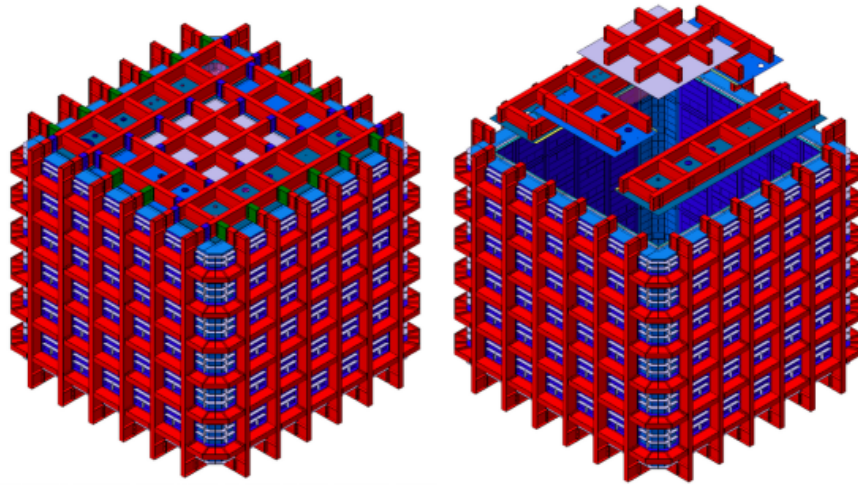


Figure 1.11: Warm vessel (red)

The cold vessel is installed inside the warm support structure. It consists of a primary corrugated stainless steel membrane, two layers of thermal insulation separated by a secondary membrane which provides secondary liquid containment. Thermal requirements determine the minimum thickness of insulation. A 10 mm thick carbon-steel skin, just behind the insulation, provides an effective gas enclosure, permitting proper handling of the argon atmosphere inside the cryostat. While the liquid argon is contained by the primary stainless steel corrugated membrane, the second membrane is present as a safety backup should the innermost membrane experience a leak.

### 1.3.2 Silicon Photomultipliers

Silicon Photomultipliers (SiPMs) constitute a new technology for dark matter research and have a number of performance advantages over traditional PMTs, used in DS-50, including higher photon detection efficiency (PDE) and much better single-photon resolution, all while operating at much lower bias voltage. For these reasons DS Collaboration committed to building the next detectors of its dark matter research programs with SiPM-based photosensors.

Silicon-PhotoMultipliers (SiPMs) are detectors based on semiconductor technology, they have single-photon sensitivity. A schematic of a SiPM is shown in

Fig. 1.12; we see that the antireflective layer favors the entry of photons in the apparatus.

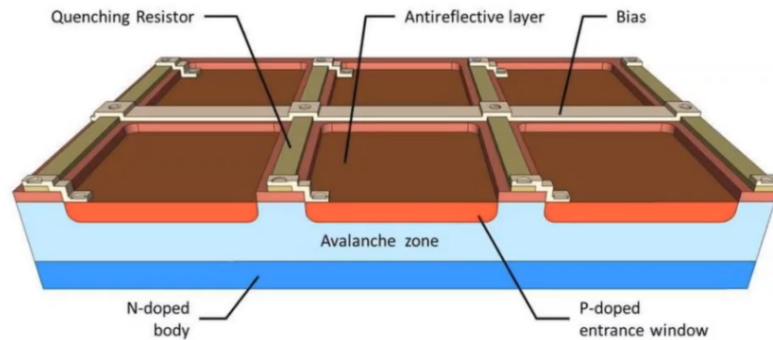


Figure 1.12: SiPM scheme

The PDM, shown in Fig. is built from an array of  $6 \times 4$  SiPMs large  $50 \times 50 \text{ mm}^2$  and will be the basic unit for photon detection in the LAr TPC. The PDM acts like a single detector. On the back side of the tile, each PDM contains a cryogenic amplifier board in the immediate proximity of the sensor. Any individual PDM can be disabled by a signal provided by the slow control system through the Steering Module (SM) in case of failure. The PDM mechanical structure required to keep in place all the components and to protect them during the integration phase makes use of molded acrylic cages and high purity copper to efficiently dissipate heat in the LAr, minimizing the production of bubbles.

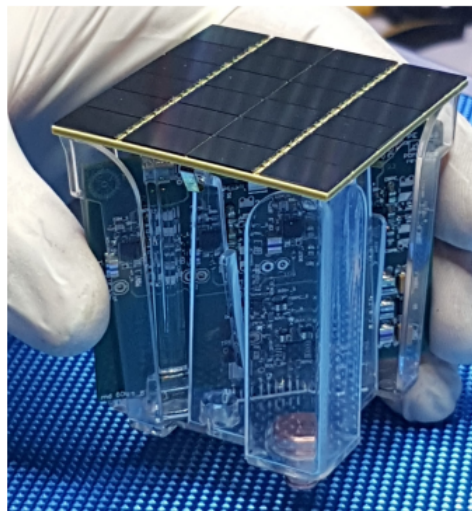
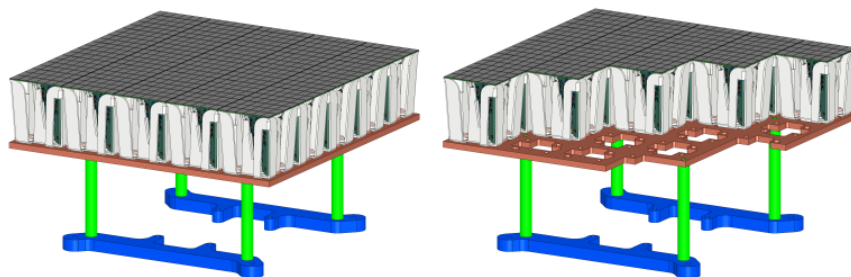


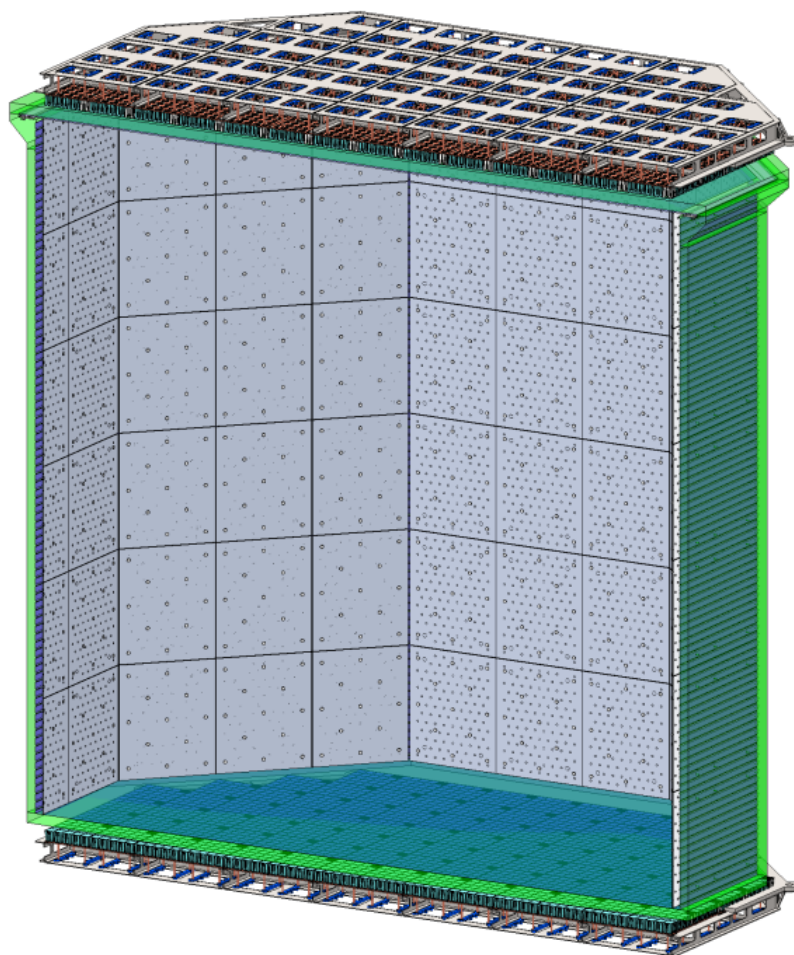
Figure 1.13: Single channel photodetector module (PDM) consisting of a  $5050 \text{ mm}^2$  tile of 24 SiPMs and a front-end board

PDMs cover the top and the bottom sides of the TPC, to detect S1 and S2 signals; the total number of PDMs in the TPC is 8280, half per side, covering a  $21 \text{ m}^2$  area. The top and the bottom optical planes will consist of 4140 PDMs each. To speed up the integration of the optical planes, multiple PDMs are integrated into a single unit to provide a larger building block called the Photo Detector Unit (PDU), shown in Fig. 1.14. The PDU comprises 25 PDMs, the electrical drivers

needed to convey the signals from the PDMs to the outside of the cryostat and the Steering Module (SM) that distributes across the PDMs in the PDU the low voltage power supply, the high voltage needed to bias the SiPMs and the slow control signals. The PDU uses a support structure obtained by milling a high purity oxygen free copper sheet known as a ‘motherboard’ to hold in place all the components and to provide the mechanical interface to the LAr TPC.



(a) Schematic drawings of the DS-20k PDM Photon Detector Unit arrangement.



(b) LAr-TPC equipped with PDUs on the top & on the bottom

Figure 1.14: 3D rendering of DS-20k LAr TPC and PDUs

## 1.4 PDM TEST FACILITY

Focusing on the PDUs, main component of the experiment, the next step in the photo-electronics schedule (The DS-20K experiment's part regarding SiPMs) is the production of about 350 PDUs. NOA, Nuova Officina Assergi, is a new facility founded for the characterization and packaging of SiPM-based detectors for DarkSide-20k. The main goal is to process about 125000 SiPMs in 2 years. This remarkable goal requires a large clean room, relying on cutting edge technology equipment and trained personal. The GADMC selected for the NOA DS-20k SiPM packaging facility a clean room to be built inside the LNGS surface laboratory in the so-called Hall di Montaggio (Assembly Hall), with surface exceeding 700 m<sup>2</sup>.

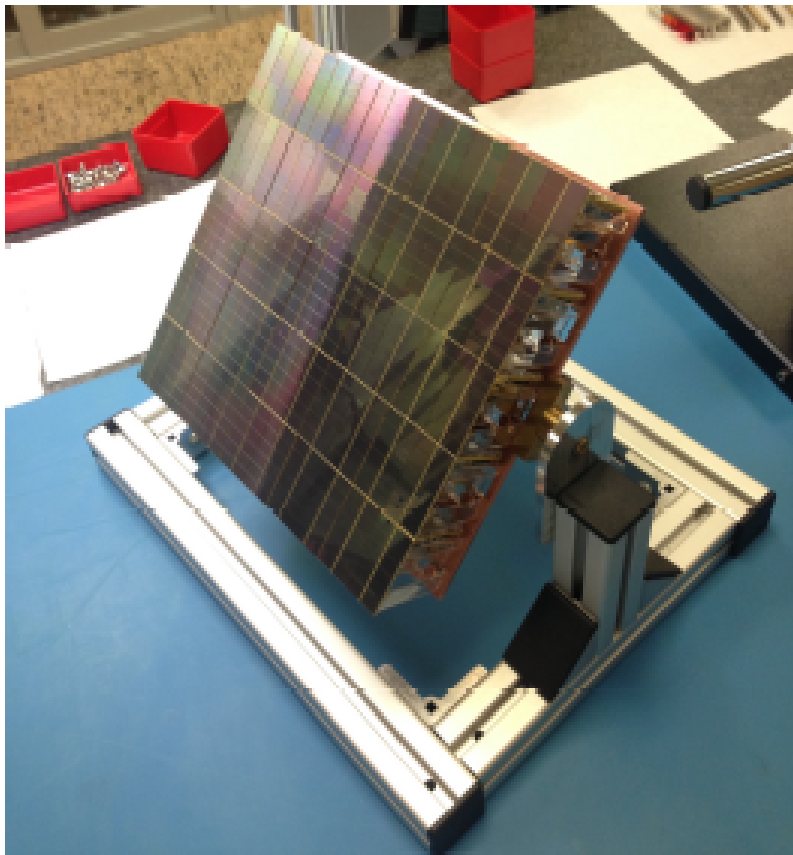


Figure 1.15: Motherboard's prototype.

In order to test 350 PDUs that will cover the DS-20k's TPC, the DS collaboration designed a dedicated installation, the Naples Test Facility.

Test Facility is a wet test station, fed with LN<sub>2</sub> directly by storage tank. It consists of a cylindrical cryostat, 173 cm high and 110 cm in diameter, an holding structure for 12 PDUs and the cryogenic plant to fill the cryostat with LN<sub>2</sub>. This system will also be equipped with the necessary feedthroughs for the individual illumination, voltage supply and signal readout of the PDMs. The Facility is installed in a clean room environment not to compromise the devices with radioactive background. The Test Facility is actually located in a clean room of the University of Naples Federico II, Professor Giuliana Fiorillo's laboratory.

Motherboards prototype, see Fig. 1.15, were assembled and tested at cryogenic temperature in Test Facility during this work.



Figure 1.16: CleanRoom layout

The clean room, shown in Fig. 1.17, hosts several prototyping activities of the DS collaboration other than the PDU Test Facility. The general layout of the laboratory is shown in Fig. 1.16.

Outside hangars, where the clean room and employees offices are located, a dedicate facility hosts the LAr tank supply and LN<sub>2</sub> tank supply, necessary to use these noble liquids in cryogenic experiments.

In the following chapters will describe the process, the general and mechanical characteristics of single components of the PDU Test facility, focusing on the cryostat. I will also report the commissioning showing the results of the first tests that I and my work team carried out.



Figure 1.17: DarkSide laboratory, Naples

# 2 | TEST FACILITY GENERAL DESCRIPTION

The Naples Test Facility is an installation designed specifically for the test of the Photo Detecting Unites (PDU) for the DarkSide-20k experiment produced in NOA.

The PDU Test Facility was designed to test and characterize 12 PDUs in Liquid Nitrogen. The test's duration for each batch is one entire week, during which the PDUs inside the cryostat need to be continuously kept in LN<sub>2</sub>. For this reason the level of LN<sub>2</sub> needs to be monitored and restored if needed. Therefore, the Test Facility is a constantly operating system.

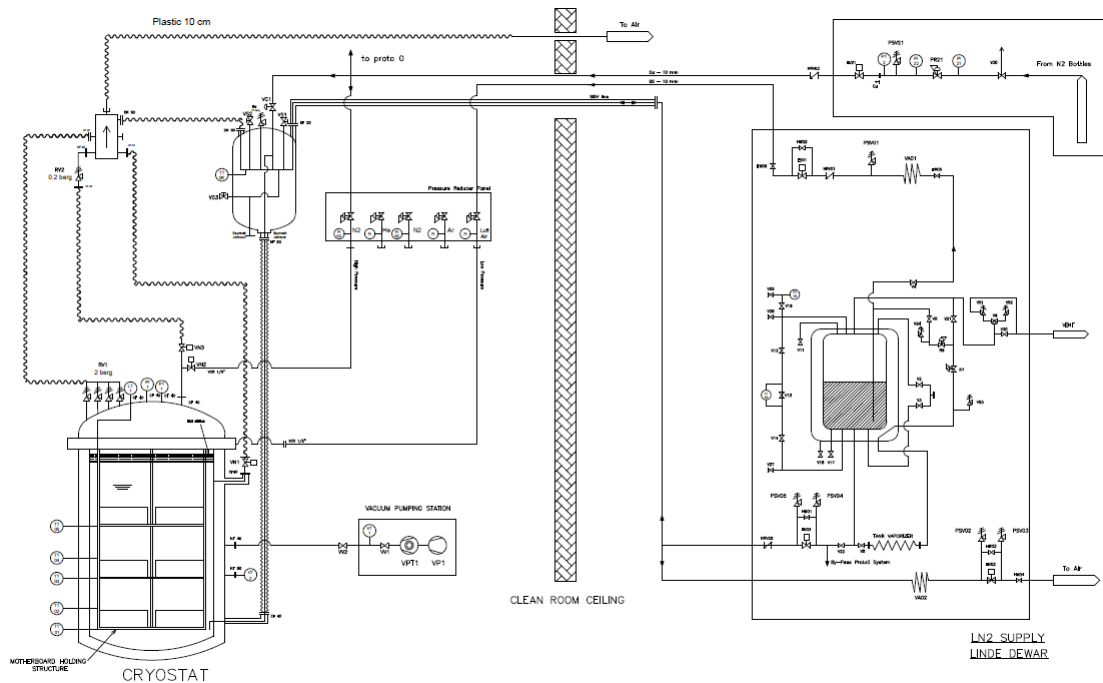


Figure 2.1: Test Facility P&ID

The P&ID, shown in Figure 2.1, describes the installation located in University of Naples Federico II Physics Department. This facility has been subject to many improvements and redesigns during this last year which were carried out by a team, leaded by Prof. Giuliana Fiorillo, and committed to set up it on time within the deadlines provided by DS collaboration.

The one test cycle of the facility includes three phases: filling phase, which is meant to be a fast filling of  $0,5 \frac{cm}{min}$  maximum; a testing phase that is the longest part where we expect to maintain operational conditions for 1 ~ 2 days; a draining phase to empty the cryostat. The main purpose of the cryogenic system is to fill and drain the cryostat, and maintain the LN<sub>2</sub> stable (up to the upper PDU) during the testing phase. Keeping the cryostat filled and monitoring LN<sub>2</sub> level for a long period is the key, specially with the aim of doing it automatically.

To this purpose, the Test Facility equipped with a remote control system and a data handling system.

The key elements of the facility can be summarized as follows:

- Cryogenic System: composed of the entire installation, shown in Fig 2.1.
- The Mechanical Structure inside the Cryostat able to support the 12 PDU on 3 different levels during the test.
- Slow Control electronics to manage the cryogenic system remotely: PT100 thermal sensors, PXI system and readouts.
- Data acquisition electronics, data handling and lasers pulse.

## 2.1 CRYOGENIC SYSTEM

The cryogenic system, shown in Fig. 2.1, is divided in 2 macro-installations, an outdoor part located outside (include the LN storage tank provided by Linde, the leading industrial gas and engineering company, that also provides the Test Facility with Liquid Nitrogen) and one inside the clean room (including the Test Facility cryostat designeb and built by Demaco). The two dewars are linked by a double wall transfer line, provided by Criotec.

The transfer lines are intended for transferring cryogenic fluids between two cryogenic devices, in this case between the two dewars. The two Dewars are at a height of 6 meters from each other, so the transfer line, shown in Fig. 2.2, results very long and starting from the LN<sub>2</sub> supply dewar outside the laboratory it crosses all the hangar to reach the cryostat located in to the clean room. The transfer line is the AISI316L 10x1 mm vacuum insulated line with a delivery capacity of 600 l/h at 2 bar.



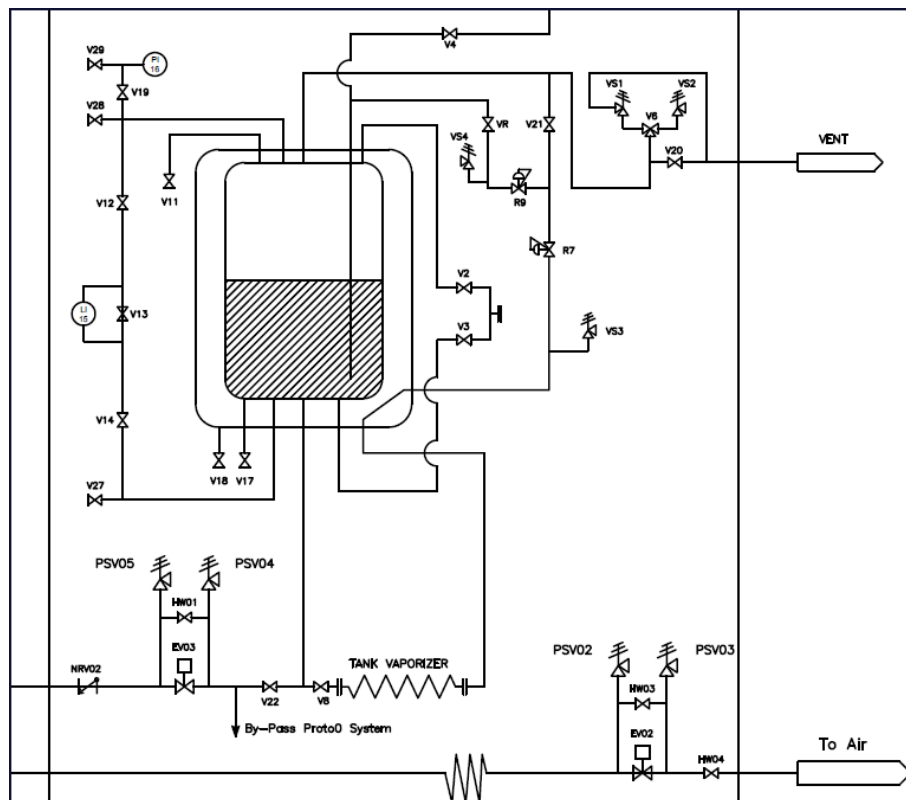
Figure 2.2: The transfer line on the outside of the INFN laboratory(clean room).

### 2.1.1 Outdoor System

The outdoor system is a big facility that includes two  $N_2$  supplies: a big  $LN_2$  dewar, shown in Fig. 2.3 and  $N_2$  canister linked to clean room. This is a fenced area, reserved to qualified stuff, in order to respect safety regulations of facilities that work with dangerous materials, in this case cryogenic liquids.  $LN_2$  Dewar is a big tank large 3300 liters, it contains liquid nitrogen with a pressure of 2.6 bar.



(a)  $LN_2$  Supply Tank



(b) Tank P&ID

Figure 2.3:  $LN_2$  Outdoor Tank

The  $LN_2$  dewar was provided by Linde with all its component, shown in Fig. 2.3 (pic "b") and in Table 1. The P&ID shows how the outdoor installation is fully

equipped with safety valves, evaporators to discharge gas in the ambient, non-return valve in order to intercept multiple lines and electro-valves to remotely control the system. The dewar is periodically filled by Linde which delivers LN<sub>2</sub> by truck and fills it through the V2 and V3 filling valves. The main line lets the LN<sub>2</sub> flow from the bottom of dewar to the clean room; its access is controlled by the shut-off Valve V22 which is normally open. Then by the electro-valve EV03, activated remotely, the LN<sub>2</sub> can finally flow through the double-wall main line. The non-return valve NVR02 prevents the LN<sub>2</sub> to flow back to the dewar and directs the flow, after a evaporation through the VA02, to the vent.

The outdoor system provides also to flow of N<sub>2</sub> gas to the clean room from two different lines with two different pressures. From the LN<sub>2</sub> supply tank starts N<sub>2</sub> gas line (Stainless Steel single wall line of 10 mm) where the LN<sub>2</sub> from the dewar get withdraw, pushed through the dedicated aluminum evaporator and sent through a low pressure transfer line to the clean room. There is another dedicated space outside the laboratory where is located a N<sub>2</sub> gas high pressure (250 bar) bottle as an alternative supply of gas for the facility. The gas from the bottle is linked to the clean room by a Cu line of 10 mm where the gas is sent at high pressure. Both are linked to the clean room in order to supply N<sub>2</sub> gas at different pressure thanks to suitable valves, as shown if Fig. 2.4

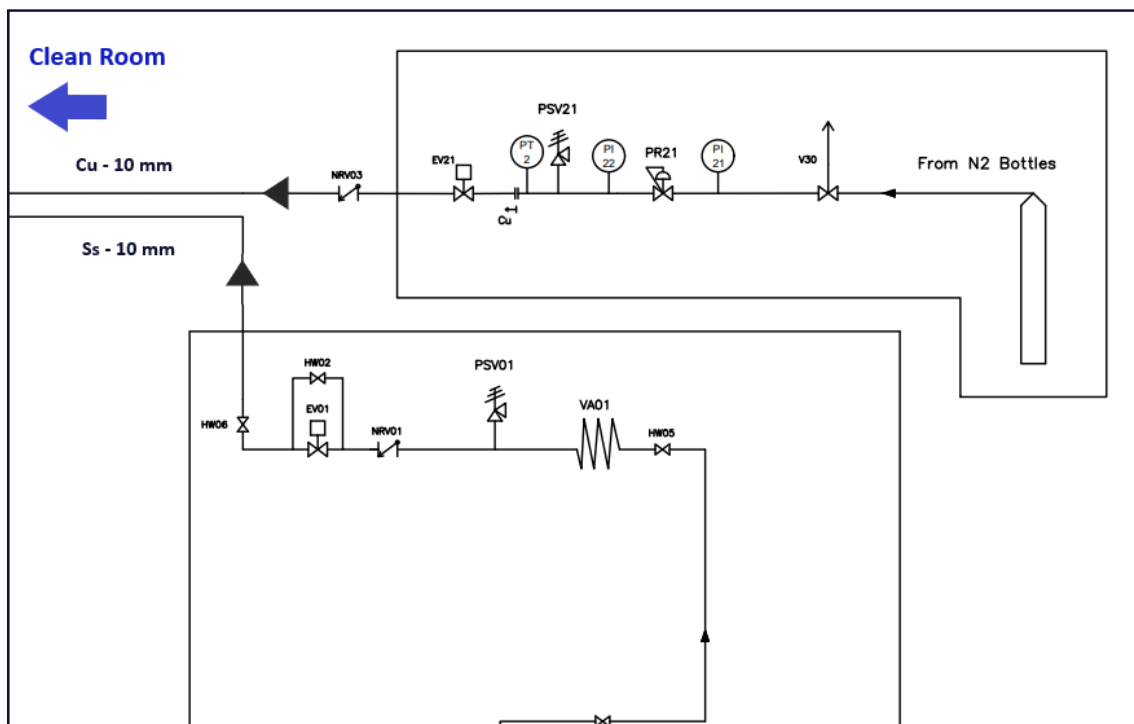


Figure 2.4: Gas lines from LN<sub>2</sub> bottle and tank

Table 1: Linde Dewar; List of components.

<b>Linde Dewar / LN<sub>2</sub> Supply</b>	
<b>Component</b>	<b>Description</b>
V2	Filling Valve (Gas)
V3	Filling Valve (Liquid)
V4	Dispensing
V6	Diverter Valve
R7&9	Pressure Reducer
V8	Shut-off Valve
VA01&02	Evaporator
V11	Overflow Valve
V12&14	Shut-off Valve
V13	By-pass
LI15	Level Gauge
PI16	Pressure Gauge
V17&18	Drain Valve
V19	Shut-off
V20	Exhaust Valve
V21	Press Control
V22	Shut-off LN <sub>2</sub>
V27 – 29	Shut-off Gauge
VS1&2	Safety V. Dewar
VS3&4	Safety Valve Pipe
VR	Check Valve
PSV	Pressure Safety V.
HW0	Handwheel Valve
NRV01 – 3	Non-return V.
EV	Electro-Valve
PI21&22	Pressure Gauge

### 2.1.2 Clean Room

Inside the Physics Department of University of Federico II is located the clean room of the cryogenic laboratory for the direct dark matter researches, one of the most advanced research centers of the INFN in Naples, managed by Professor Giuliana Fiorillo, see Fig.2.6. A number of small scale experiments and experimental activities related to DarkSide Collaboration take place in this laboratory. In fact during autumn INFN of Naples hosted researchers from all part of the world that participate to DS activities. Prof. Giuliana Fiorillo's laboratory is one of the biggest of campus and it is divided in two laboratories: Lab 1, on the right of Fig.2.5, dedicate to the office where people can work remotely on the clean room's activities; Lab 2 is the ISO 6 clean room with a roof 4 meters high equipped with a roof rail where is installed an electric hoist.

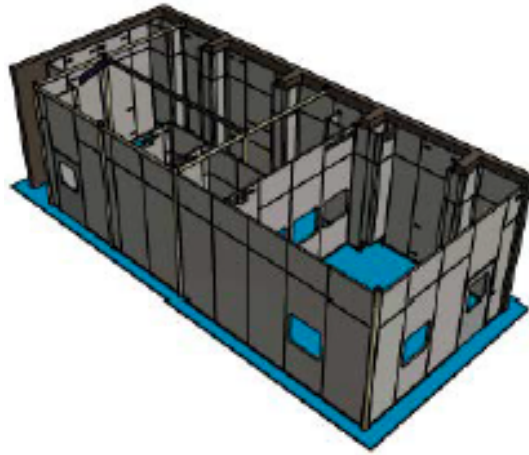


Figure 2.5: 3D rendering of INFN Naples' laboratory: on the right Lab 1; on the left Lab 2, Clean room.

In order to respect safety regulations of a clean room the ambient conditions, like temperature and  $N_2$  presence, are constantly monitored from outside it in Lab 1 and it also provided by emergency exit.

As shown in Fig 2.7 the Test Facility contains many components described in this section. The main component of the facility is the cryostat, in fact it is linked to other features of the installation like: the cold box, a sort of phase separator of  $LN_2$ ; the pressure reducers panel where the  $N_2$  gas input is controlled; the manifold, where all  $N_2$  gas is collected to be vented to the drain line.



Figure 2.6: Clean room overview

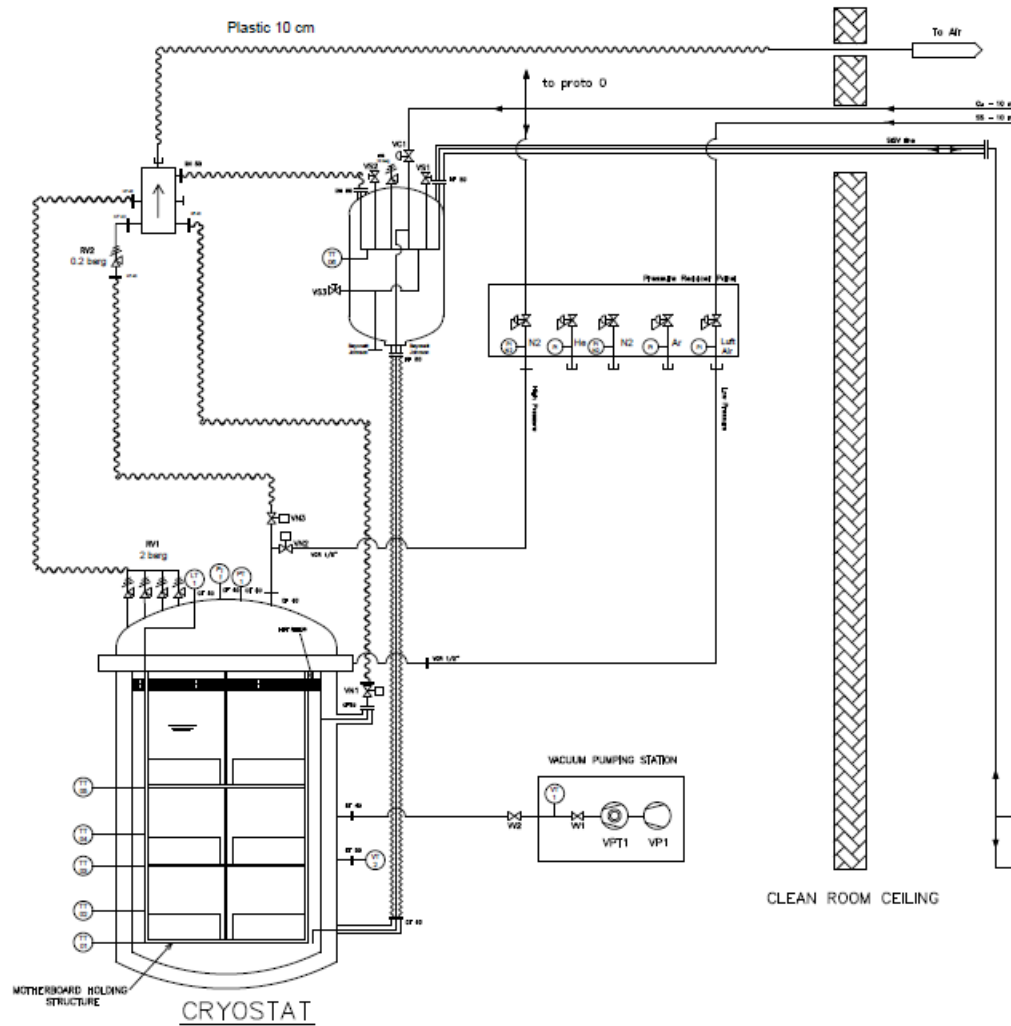


Figure 2.7: Test Facility P&ID clean room

### *Cryostat*

The Cryostat was custom designed by Demaco, a Dutch company who is an expert in the field of cryogenic technology, it is shown in Fig.2.8 also showing the safety devices and temperature sensors PT100, bi-directional transfer line for LN<sub>2</sub> (for the fill and drain), cold vent line, flexible insulated line to connect cryogenic elements together and the external LN<sub>2</sub> storage. The cryostat dimensions and features are designed following the space limits of the clean room. The dimensions have been chosen both to respect the ceiling height of the clean room, which is 4 meters, and to contain the preset number of PDUs (12). The roof rail sets an important building boundary, the electric crane needs to have enough space to lift the internal structure, therefore, in order to be able to extract safely the internal structure with PDUs from the cryostat, the overall available vertical distance should be no less than two heights of the cryostat. For these reasons the cryostat height was fixed to 1730 mm from ground to the i-bolt on its upper flange.

The Demaco cryostat is made of stainless steel, the specific material is AISI 304L a Cr-Ni austenitic stainless steel, it is similar to AISI 304 but the "L" stand

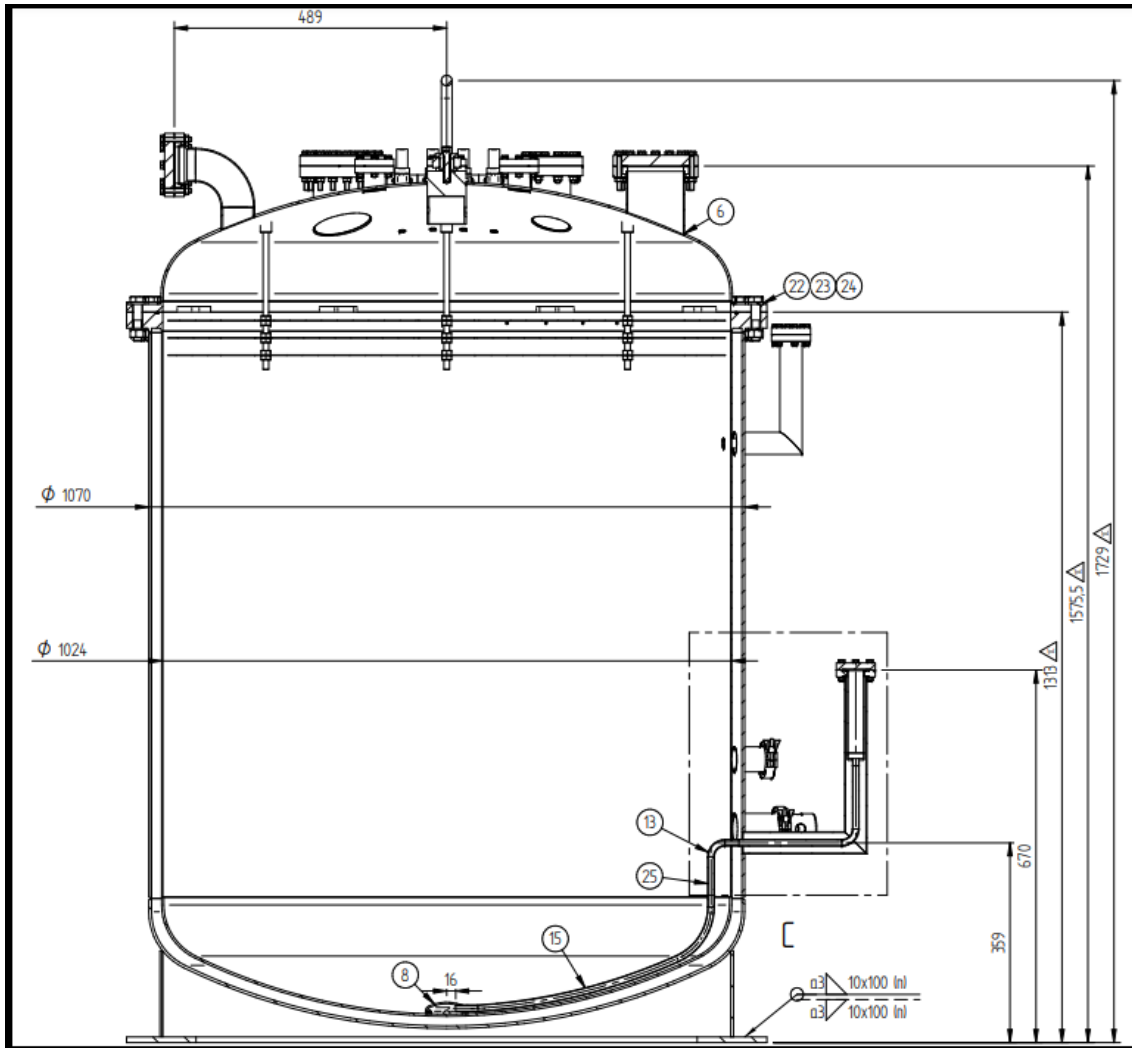


Figure 2.8: Cryostat's drawing from Demaco

for "Low Carbon". Thanks to the lowest presence of carbon AISI 304L is mostly utilized by components with high thickness and the reduced percentage of Cr gives a heavy resistance to corrosion. This feature makes 304L steels particularly suitable for welding even in very grave corrosive conditions and can be used in a cryogenic environment and up to 700 degrees.

The cryostat has the capacity of 930 liters. As we can see the inner vessel has two main exits which are linked to different  $N_2$  supplies, one is a double wall pipe linked with the external  $LN_2$  tank by the dedicated double wall transfer line with the bayonet connection, the other one is a one wall pipe that would be linked with the discharge line. There two other exits on the external vessel dedicated to create vacuum jacket between inner and outer vessel. A vacuum jacket provides insulation, minimizing cold/heat loss from the vessel and so improving efficiency. Thanks to this the outer surface of the vessel does not reach such extreme temperatures, plus there is reduced frosting and condensation. The type connection of vacuum fittings are KF 40 (Klein Flansche in German, or Quick Flange). The outside surface of the inner vessel (inside vacuum insulated

volume) is covered with 30 layers of Multi-Layer Insulation (MLI) to reduce the radiation heat flow.

On the top of the cryostat there is the top dome flange, shown in Fig 2.9, large 1150 mm and attached to the vessel with an elastomeric o-ring in NBR (diameter 1035 mm) and with 44 M16x70 bolts (stainless steel A2 – 70). The

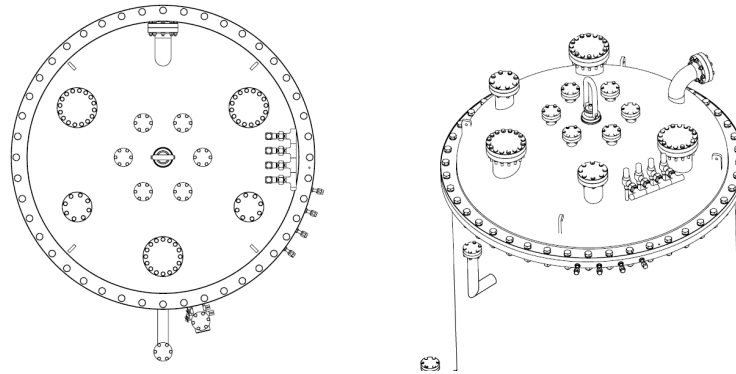


Figure 2.9: Upper Flange

top of the cryostat is equipped with many different flanges and connections to make the installation flexible and in order to set up pneumatic and manual valves, instrumentations and safety devices that allow to control the flows of the  $N_2$  Gas and Liquid in secure way and provide the equipment placed inside the cryostat with power and signal cables by means of the dedicated feedthroughs. The full equipped top flange has not to exceed 200 kg to respect the electric crane's specifications. There are 6 CF 40 flanges dedicated to feedthroughs and sensors, 3 CF 63 and other 3 CF 100. On the flange side there are 4 VCO fittings that could be use as a  $N_2$  gas inlet giving more flexibility to the cryostat's setting.

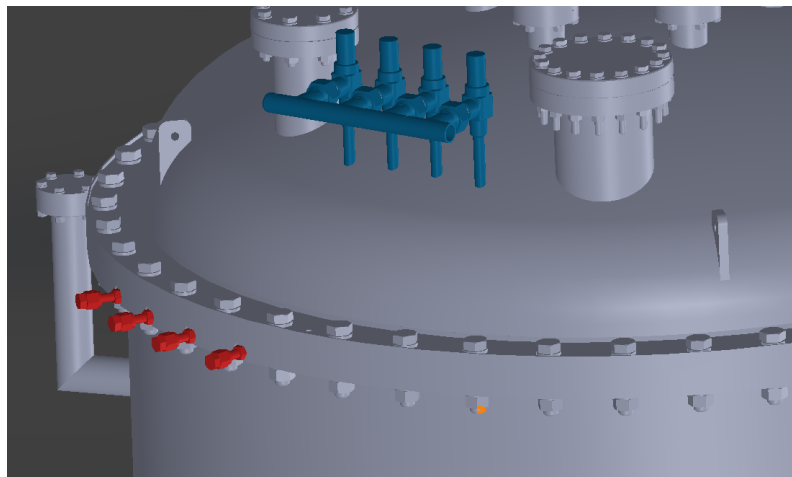


Figure 2.10: 3D SolidWorks rendering: VCO fittings (in red); Safety valves (in blue).

To ensure safe work conditions of the cryostat the design includes four safety valves on the top flange, see Fig. 2.10. Equipment designed to work at high pressure conditions necessitate a particular certification, PED (Pressure equipment directive) Certification. The Test Facility was designed and fully certificated, also

with PED certification, by Demaco. On Table 2 there are technical features of the cryostat provided by Demaco.

Table 2: Cryostat Demaco; technical specifications

EN 13445 / PED 2014/68/EU	
Design code	EN 13445
Medium	Nitrogen/Argon
Design pressure inner vessel	2/ - 1 barg
Design temperature	-196 / +40 °C
Corrosion allowance	0
Testing group	3b
Welding methode	141 (TIG)
NDE	Visual examination 100%
	Radiographic test: 1x Circumferential welds
	Radiographic test: 1x Longitudinal welds
	Dye penetrant test: Nozzle 10%
Testing pressure without vacuum	$1.43 * (2 + 1) = 3.4$ barg
Testing pressure with vacuum	$1.43 * (2 + 1) - 1 = 2.4$ barg
Test medium	Nitrogen
Volume inner vessel	930 l
Diameter $D_e$ inner vessel	1024 mm
Diameter $D_e$ outer vessel	1070 mm
Total height	1729 mm
Inlet connection	CF40
Outlet connection	CF40
Blow off	4x12x2
Type inner bottom	Klopper head $D=\text{Ø}1024$ H=215 d=3
	m.a.f. - DIN 28011
Tare weight	438 kg

### *Cold box*

The first component of the facility that LN<sub>2</sub> reaches is the Cold box, clearly shown in the P&ID in Fig. 2.7. Cold box is a small box in which are installed several valves, see Fig. 2.11, designed and provided by Criotec. Criotec is an Italian company, located in Chivasso (To), specialized in vacuum and cryogenic techniques.

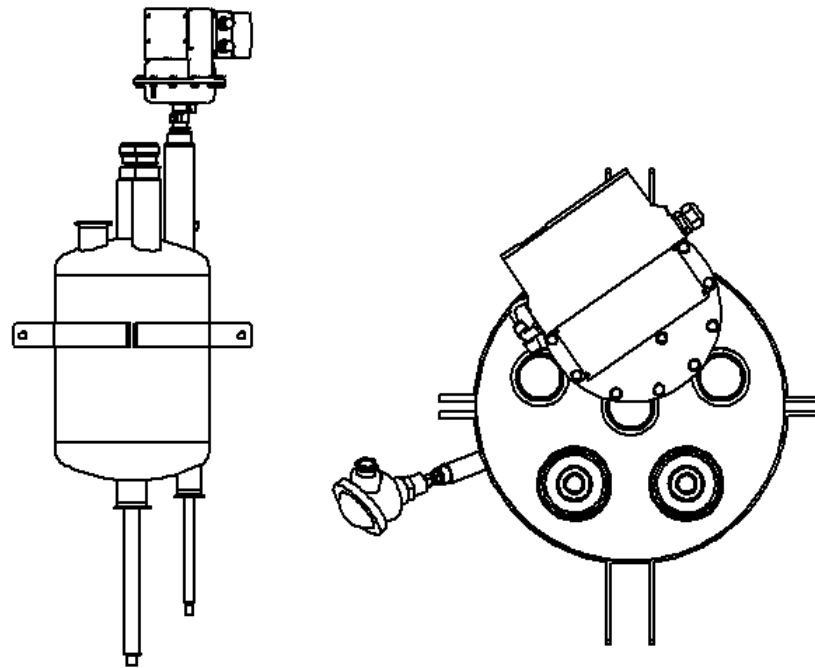


Figure 2.11: Cold box's sketch by Criotec

The main feature of the cold box is controlling the LN<sub>2</sub> flow in to the cryostat through the proportional valve installed on the top of the box. It is composed by one inlet fitting (on the top) for the double wall line that delivers LN<sub>2</sub> from the outer tank and three outlet fittings: the one on the top is a DN50 fitting used to vent lines from exceed N<sub>2</sub> gas; two fittings on the bottom with Johnston male bayonet are used to connect the cryostat or additional systems.

On the top of the box there are three manual valves used to let the N<sub>2</sub> to flow into the box. More precisely, the blue manual valve, illustrated in Fig. 2.12, lets the LN<sub>2</sub> to flow through the blue line up to the cryostat by the double wall transfer line. The red one is used to separate the gas from the main line and the green is an alternative line with another Johnston bayonet outlet.

The cold box is equipped with safety features such as the relief valve (set to 10 bar) and the temperature transducer to monitor the temperature inside the

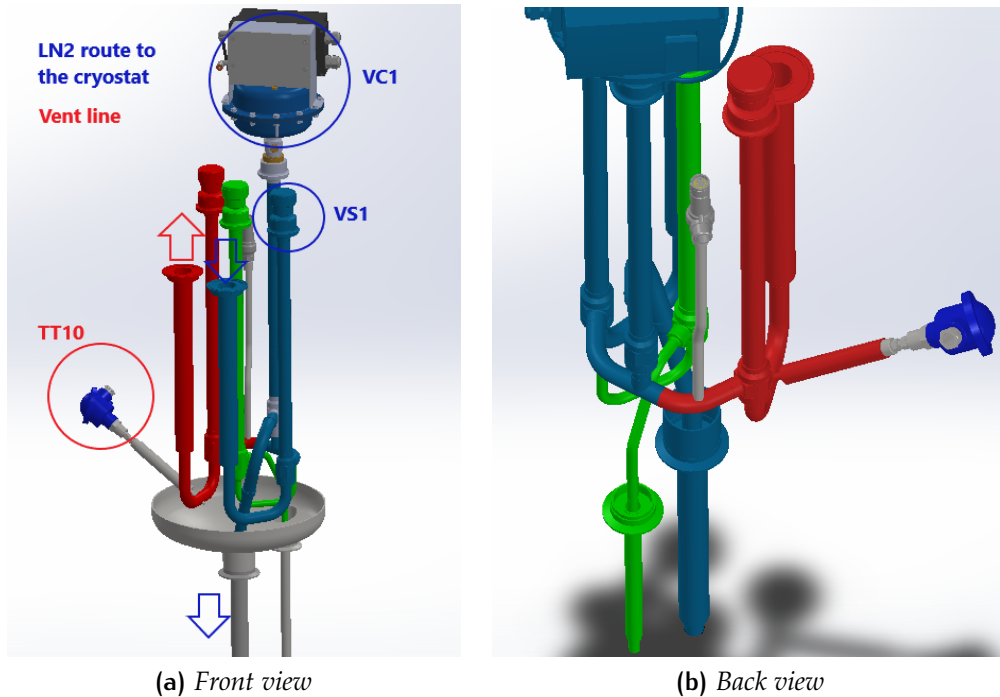


Figure 2.12: 3D rendering of the inner cold box part

cold line. There is one last component of the cryogenic system, the manifold which is a little discharge box, provided by Criotec. All lines of the Test Facility are connected to the manifold with KF 40 fittings and allow to collect all  $N_2$  gas from the system (from the cold box and from the cryostat) and carries to the vent outside the clean room through a flexible plastic line of 10 cm diameter.

The Fig.2.13 illustrates a 3D rendering of the Test Facility, made with Solid-Works 3D, inside the clean room. The CAD was used to organize a the layout based on the available space of the clean room.

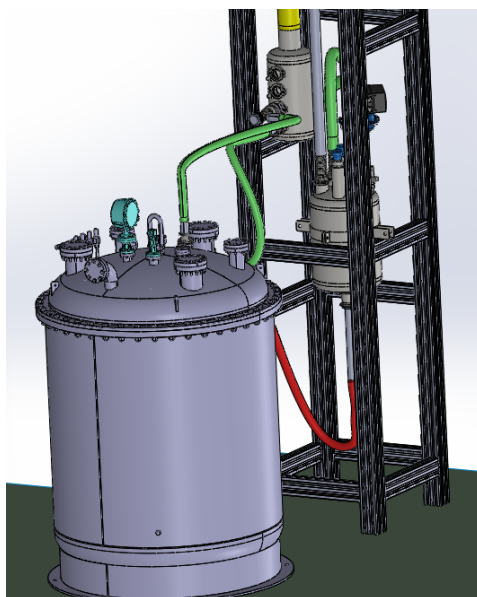


Figure 2.13: 3D layout of Test Facility

### Mechanical Structure

The mechanical system of the facility is composed of: the PDUs holding structure that has to be attached to the cryostat top flange; the working table made of aluminum profiles in order to low and fix the holding structure for the loading and unloading with PDUs; and the electrical crane. One of the elements of this structure will be the PDU Box, see Fig.2.14.

The PDU is the object of 25x25x9 cm size consisting of 25 Photo Detecting Modules (PDM) which are made of a 5x5cm tile coupled with a Front End Board (FEB). Tile and FEB are connected orthogonally. Once produced in NOA, the PDU will be locked inside the Box designed for the transportation and test 12

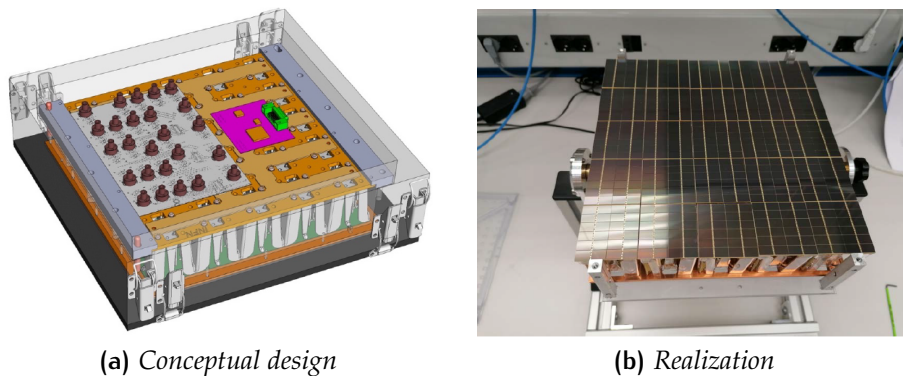


Figure 2.14: PDU Box (motherboard)

PDUs will be hosted inside the dedicated mechanical aluminum structure in three levels (700x900 mm) with four PDU at each level with the overall height of about 900 mm. The structure is rigidly attached to the dome top flange with the central vertical stainless steel profile. The Cryostat together with its top flange is shown on the Fig. 2.15. To seal the cryostat for duration of the test the reusable silicon O-ring (NBR 71) suitable for the low temperature applications is foreseen. The three levels of aluminum plates are designed to be 30 cm far from each other.

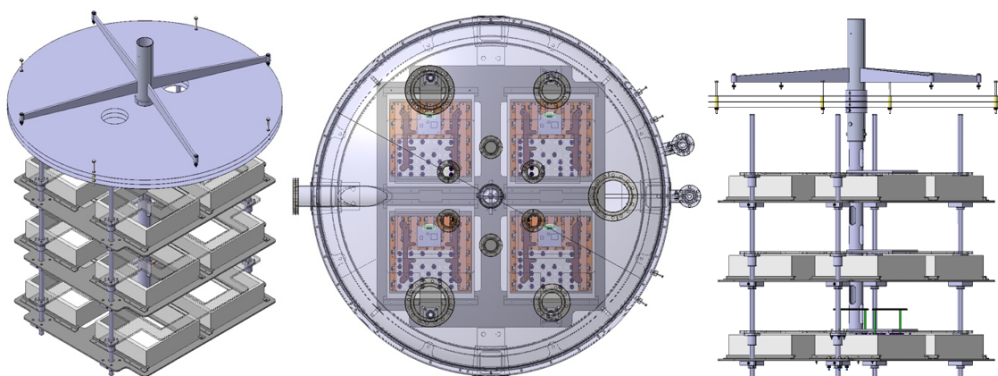


Figure 2.15: The 3D rendering of PDUs holding structure

The top level is designed to be at least 30 cm (max 40 cm) from the top dome, as we can see from Fig. 2.16. The main reason of this design is the level of LN<sub>2</sub>,

that has to cover all the three PDUs levels during the test. We set the liquid level to 30 cm from the flange in order to keep PDUs covered during the LN<sub>2</sub> evaporation. It is also important that the LN<sub>2</sub> is under the elbow CF40 fitting, located 20 cm from the flange, that is used to discharge N<sub>2</sub> gas from the cryostat during the phase of fill. To reduce the evaporation rate there will be installed, as we can see in Fig. 2.15, three metal discs that work as thermal shields.

The aperture of the top flange will be done by electrical hoist that has a fine speed regulation in order to provide smooth movement, so all the structure has to weight no more than 200 kg.

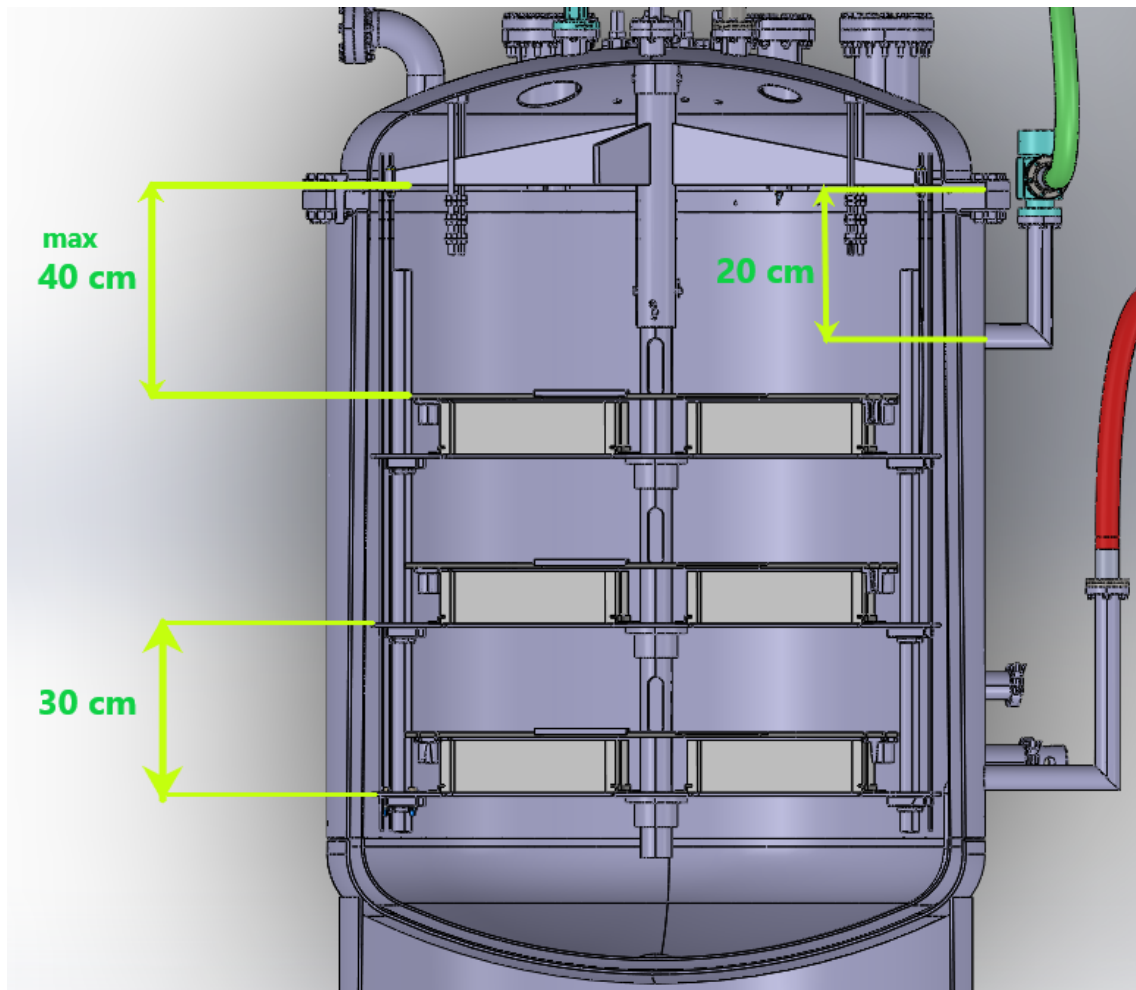


Figure 2.16: Capture of 3D sectioned cryostat

## 2.2 ELECTRICAL AND OPTICAL CONNECTIONS

Test Facility is equipped with the necessary feedthroughs for the individual illumination, voltage supply and signal readout of the PDMs.

The Naples Test Facility will use low and high voltage power supplies as well as the power lines filter boxes and digitizers. The Low and Bias voltage will be provided by power supplies of CAEN, company that provides complete range of High/Low Voltage Power Supply systems and Front-End/Data Acquisition modules which meet IEEE Standards for Nuclear and Particle Physics.

In order to test the PDU the light pulses, generated by the Hamamatsu laser head PLP C8898, will be delivered inside the cryostat by means of 16 ports optical feedthrough coupled with the CF40 flange located on the top of the cryostat, Fig.2.17. The primary fiber connected to the laser head will be splitted into 12 fibers and then connected to 12 individual optical SMA connectors on the optical feedthrough mounted on the top domed flange. Inside the cryostat from the feedthrough 12 SMA-SMA fibers of 2 m (one for each PDU) will be further splitted into 4 so that every PDU will be covered by 4 fibers.

The reason why in the Facility we want to illuminate PDMs with optical fibers in a controlled way, with very low light levels, is the necessity to excite the individual PDM within the PDU with single photo electron signals and acquire their responds in form of the waveforms. Analysis of collected waveform will tell us about the PDU overall performance and will allow us to qualify these devices for the installation on the DarkSide-20k detector.



Figure 2.17: Optical splitter from one to 16 available for the light distribution

The holding structure together with the feedthroughs mounted on the top domed flange are the key elements of the Facility. They will allow to connect the 12 PDUs positioned inside the cryostat with the electronics boards mounted on the racks outside in order to power them ON and be able to readout the signals during the test.

The Steering Modules (SM) mounted on the PDUs will receive the Low & High voltages cables shown on the Fig. 2.18.

A warm interface (external device) handles the communication at room temperature with the Steering Modules. In addition, all the PDU tiles will need the bias voltage (up to 65V) supplied by a power supply board in order to be able to

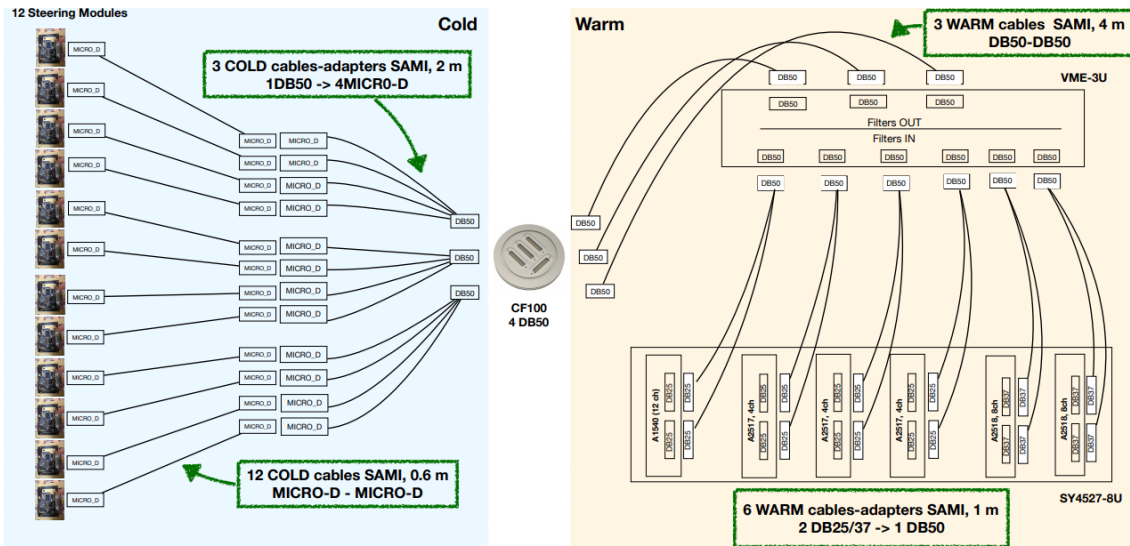


Figure 2.18: LV &amp; HV Layout

feed the SiPMs and read the cold signals. All this will result in lines which will be routed from the electronic rack to the cryostat. The signals on the warm side will be grouped into main multiline cables and for both, cold and warm cables, the SAMI cables can be used (for cold in particular). In between the warm and cold side, we will use the CF100 x 4DB50 feedthrough mounted on the cryostat top flange. The approximate length of the power cables will be of 2m on the cold side and 4m on the warm one.

## 2.3 SLOW CONTROL & DATA HANDLING

The data storage and offline processing system must support transfer, storage, and analysis of the data recorded by the DAQ system, for the entire lifespan of the experiment. Necessary components for data storage and offline systems are the software framework and services, as well as the data management system, user-support services, and the world-wide data access and analysis job-submission system.

The Maximum Integrated Data Acquisition System (MIDAS), shown in Fig. 2.19, has been chosen as a framework for developing the DAQ readout and related online control software for the Test Facility. The MIDAS DAQ package has been used extensively within other experiments and will be utilized on DS-20k and together with the CAEN hardware provides a nice baseline for the digitization and recording of the raw data.

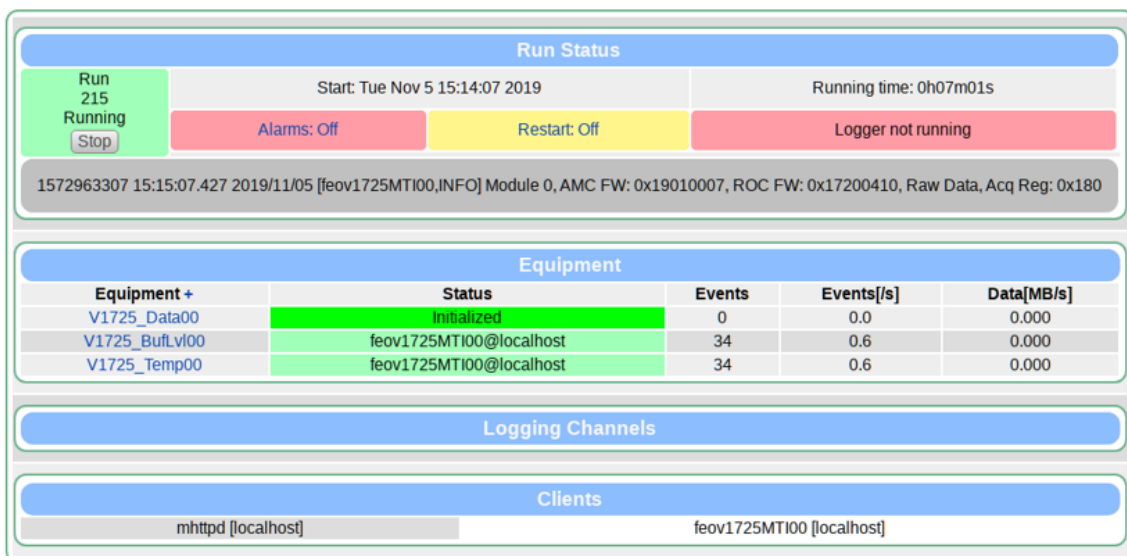


Figure 2.19: The example of the interface window of the MIDAS run controller

Naples test system will rely on the dedicated computing architecture consisting of the two server machines and over 600 Tb storage. It consists of:

- DAQ readout server: MIDAS software framework acquires events and store them on remote mounted Network File System (NFS) partition on DAQ storage server;
- DAQ storage server: on this server a set of disks are available to store events. The disk space is available to DAQ readout server and DAQ controller server by Network File System protocol in order to allow remote read/write of data event files;
- DAQ controller server: MIDAS DAQ system is controlled by a web interface available on this server. Other DAQ services are also available on this machine in order to allow these tasks: Run Control, Online Analysis plots and Offline Analysis plots;

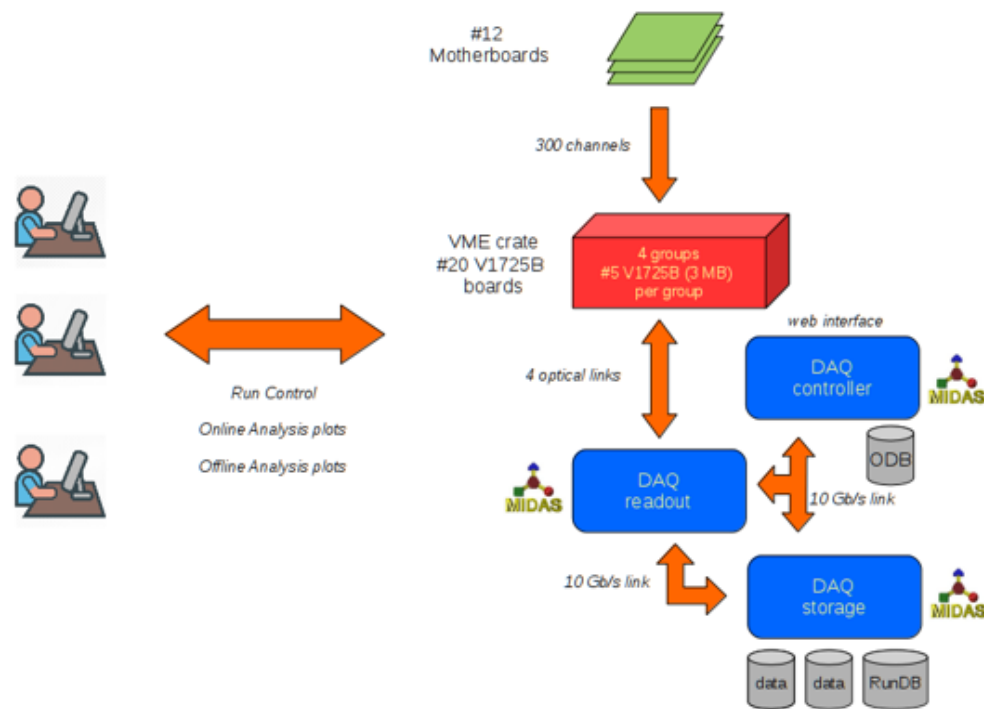


Figure 2.20: Schematic view of the DAQ architecture of the PDU Test Facility

A Run Database is available on DAQ storage in order to store all details on each run:

- run number
- run type
- start time
- stop time
- duration
- L&H voltage configuration

The Run Database is filled simultaneously by MIDAS-DAQ and Slow Control subsystem. For some runs the Slow Control subsystem can be acquired by MIDAS-DAQ to store and plot data useful for PDUs characterization.

The test facility will be controlled by the NI PXIe-8861 based Slow Control system. All the dataflow will be handled by the dedicated MIDAS based DAQ.

The PT100 temperature sensors distributed at different levels inside the cryostat, see Fig.2.21, will be read-out by the NI PXI inlet module RTD PXIe-4357 controlled by the Slow Control software based on Labview.

The PT100 thermo-resistors (commonly called “PT100 probes”) are thermosensitive elements suitable for measuring the temperature considering their particular sensitivity, precision and reliability.

Available in any shape, size and material, PT100 probes are commonly applied in all those application fields in which the maximum working temperature is  $\leq 650$  °C. Also suitable for use in immersion and cryogenic environments, the PT100 resistance thermometers can also be supplied complete with a connection head, suitable for generic measurements and adjustments on systems. Their fixing takes place through a threaded fitting welded directly on the sheath (fixed) or through special compression joints or sliding flange, in this case the PT100 are inserted in the cryostat without using probes and connecting head.

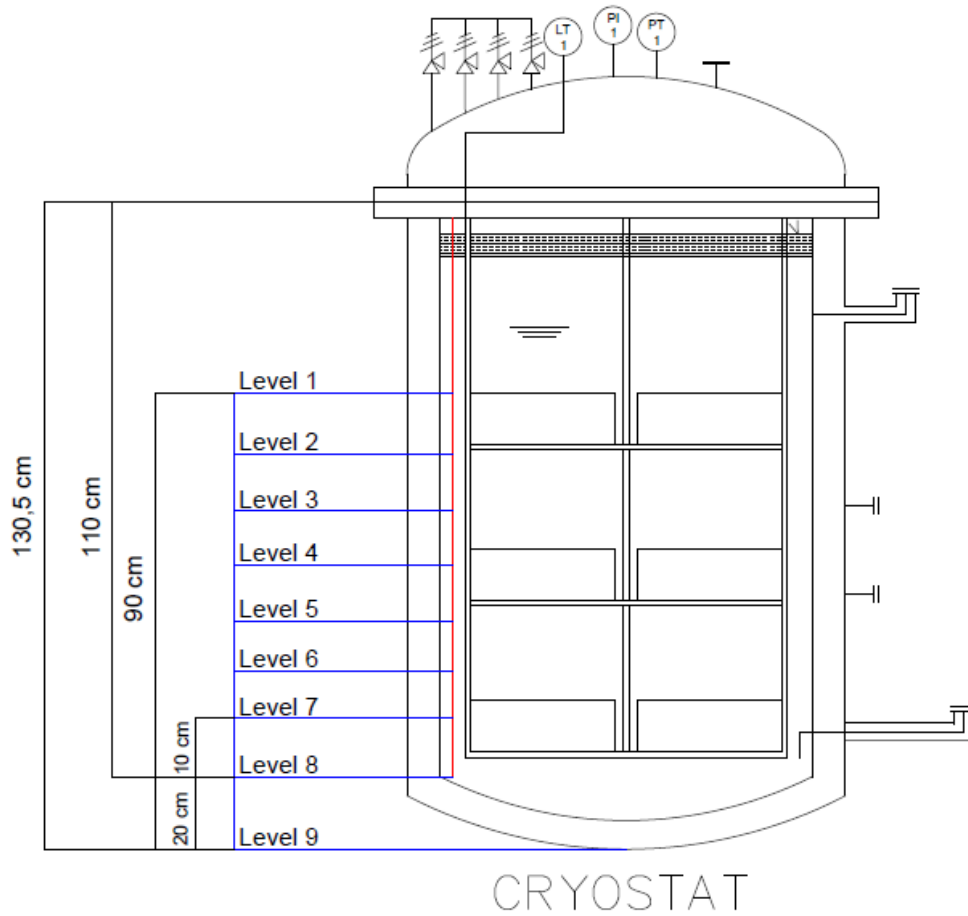


Figure 2.21: PT100s distribution

To reach the goal of keeping all PDUs covered by  $\text{LN}_2$  we need to monitor its level inside the cryostat. For this reason it is necessary to put the first PT100 at the same level of the upper PDUs level. The PT100s' distribution was designed to be like the Fig.2.21 shown. In this configuration the 1st sensor, put on level 1, will show when the cryostat will reach the desired filling. Other PT100s will be distributed every 10 cm on a threaded rod, mounted to the upper flange, until the last one that will be on the bottom of the cryostat in order to know when the test start.

The graphical pages of the Slow Control are based on the NI LabView framework. The key features of the Slow control are:

- the monitoring of the temperature sensors and pressure of the cryostat;

- the monitoring of liquid level and the pressure in external LN<sub>2</sub> tank;
- the monitoring of the vacuum in the insulation jacket;
- the control of the filling and draining processes by means of the regulation of the valves aperture;
- the control of the CAEN boards of the Low and High voltages needed for PDUs;

## 2.4 TEST FACILITY PROCESS

Now it is possible, having a first knowledge of all the components, to give a description of the whole process.

The process can be divided in series of operations that we can outline as follows:

- Pump & purge
- Filling phase
- Testing phase
- Emptying phase

The very first step of the test procedure will start with the positioning of 12 PDUs and their coupling with the light distribution plates in the dedicated slots of the holding structure attached to the cryostat top flange. All the cables and fibers will arrive from the feedthroughs mounted on the top flange and therefore will be present for the individual connections on each PDU. The fibers for the readout from the receiver channels will be connected to the single optical drivers on 12 PDUs. Once all the PDUs are properly installed and all the connections are done and verified, we pass to the closure of the cryostat with the O-ring seal and bolts.

### *Pump & purge*

Before starting the filling phase of the LN<sub>2</sub> in the vessel we purge with N<sub>2</sub> gas from the external tank, see Fig.2.22. This phase starts thanks to our input on the EVs (Solenoid Valve) so the N<sub>2</sub> gas can flow from the Tank or Bottle at 2,5 bar. Then N<sub>2</sub> gas goes through Cu or Ss line to the Pressure Reducer Panel inside the clean room. We use the PR to set the pressure of the N<sub>2</sub>.

Both gas lines can be used to purge the cryostat. The two lines let the gas flow at two different pressures, the PR (pressure reducer), on the PRs panel, of the bottle line sets the pressure up to 4 bar. The gas can flow inside the cryostat in many ways thanks to the flexibility of the facility. An example is shown on Fig.2.23 where the inlet gas can enter from a VCO fitting, by the low pressure

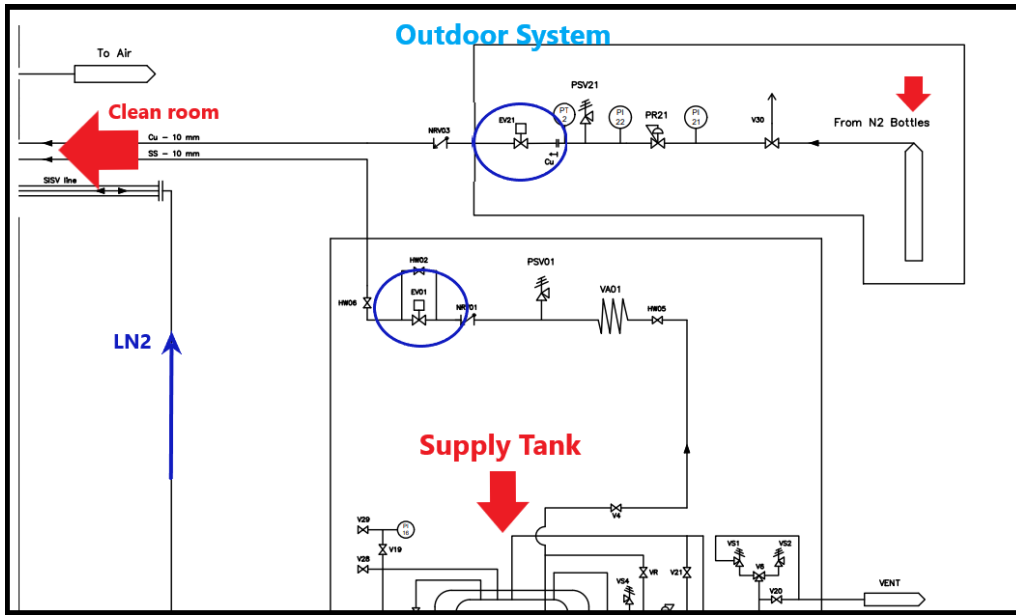


Figure 2.22: Gas lines from the outdoor system- 2D sketch

line, on the side of the cryostat; or opening the manual valve VN2 on the top of the cryostat, by the high pressure line. To prepare the cryostat for the LN<sub>2</sub> it will be flushed with warm N<sub>2</sub> gas in order to remove the humidity (as an option we can also do a three - four Pump & Purge cycles pumping the cryostat down to 10<sup>-2</sup> mbar), after that we can prepare the cryostat to the filling phase flushing the cold N<sub>2</sub> in order to precool the system and avoiding thermal shock.

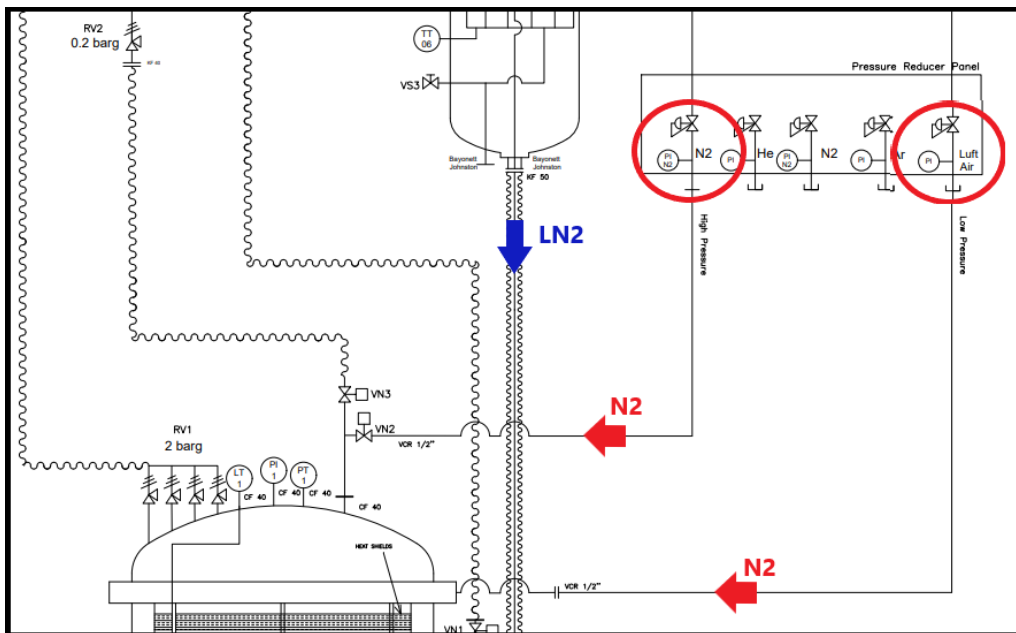


Figure 2.23: Gas lines from PRs panel- 2D sketch

### Filling phase

As first step we need to precool the cryostat, the cool down occurs with the same  $N_2$  that comes out from the  $LN_2$  storage, when the transfer line will all be filled with  $LN_2$  we will pass to the actual fill of the vessel (during all the process of the cool down and filling the temperature at different levels inside will be monitored with the slow control by means of the PT100 sensors readings).

The filling will be done slowly, at the rate of approximately few cm per minute (5 – 6 hours in total). The filling consists in controlled delivery of the  $LN_2$  directly to the bottom of the cryostat. The overall level of  $LN_2$  above the upper PDUs has to be at least 20 cm (not exceed 25 cm) in order to guarantee enough time to perform the measurements without the additional filling. Once the cryostat is filled at the desired level, we can start the test measurements.

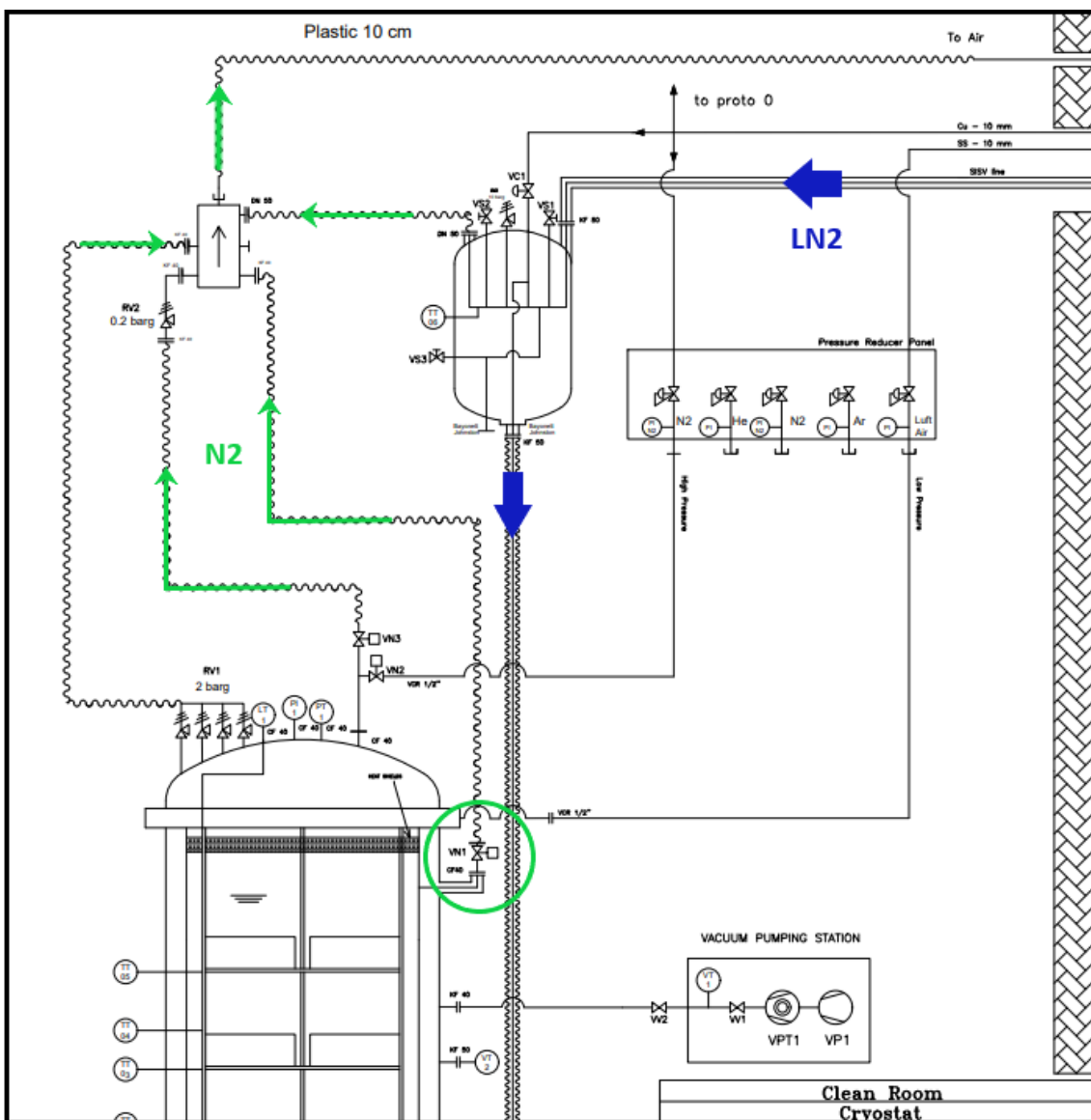


Figure 2.24: Clean room:  $LN_2$  direction, blue arrow;  $N_2$  direction from cryostat, green arrow; All metal manual valve VN1, green circle.

LN<sub>2</sub> arrives in the clean room through the transfer line (bi-directional line) from the Outdoor Tank, see Fig. 2.24. Firstly LN<sub>2</sub> evaporates through double-wall line, Coldbox & Cryostat because of heat exchanges. When the Cryostat cools down thanks to the cold gas, LN<sub>2</sub> could slowly fill it. The gas in the Cryostat is vented thanks to the all metal manual valve VN1 during this phase.

To start the filling phase we open, remotely by LabView or manually, the EV03 (Electro Valve) keeping the shut-off valve of the LN<sub>2</sub> supply tank completely open (V22), see Fig. 2.25.

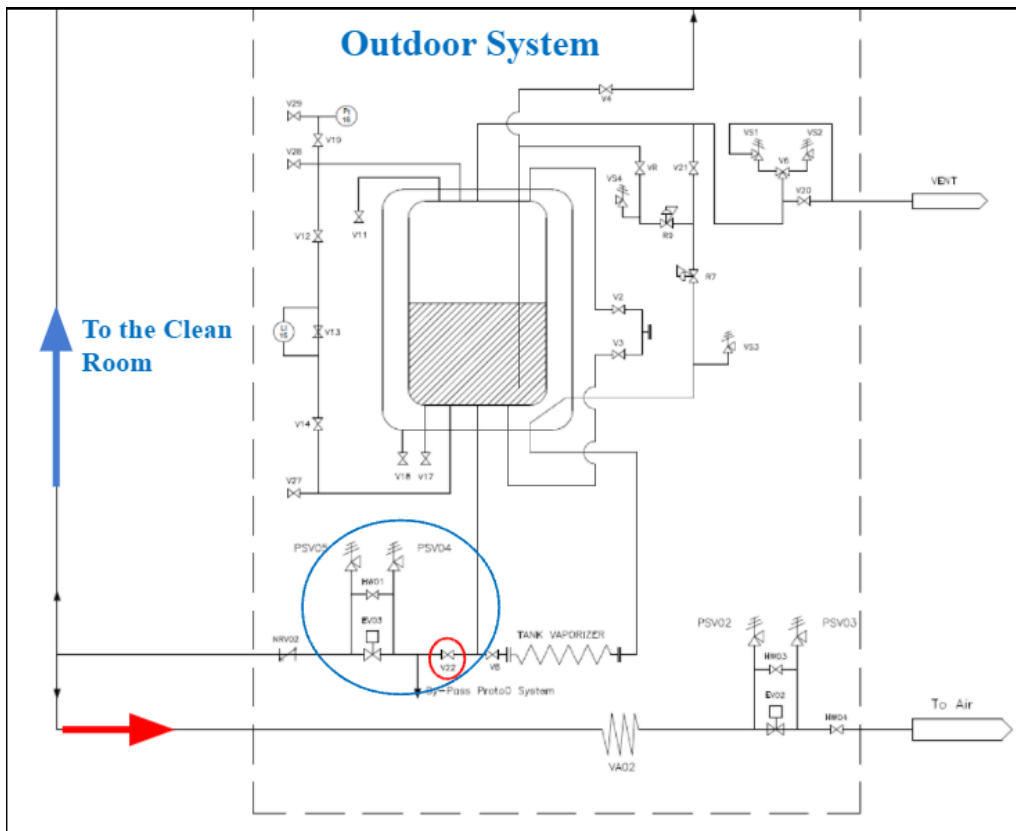
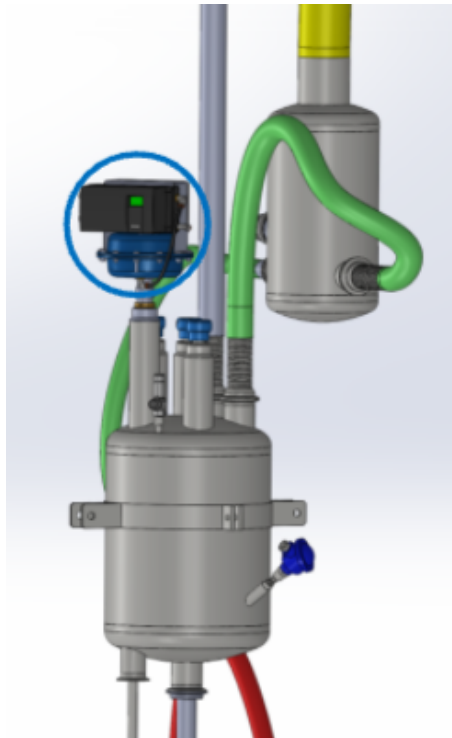


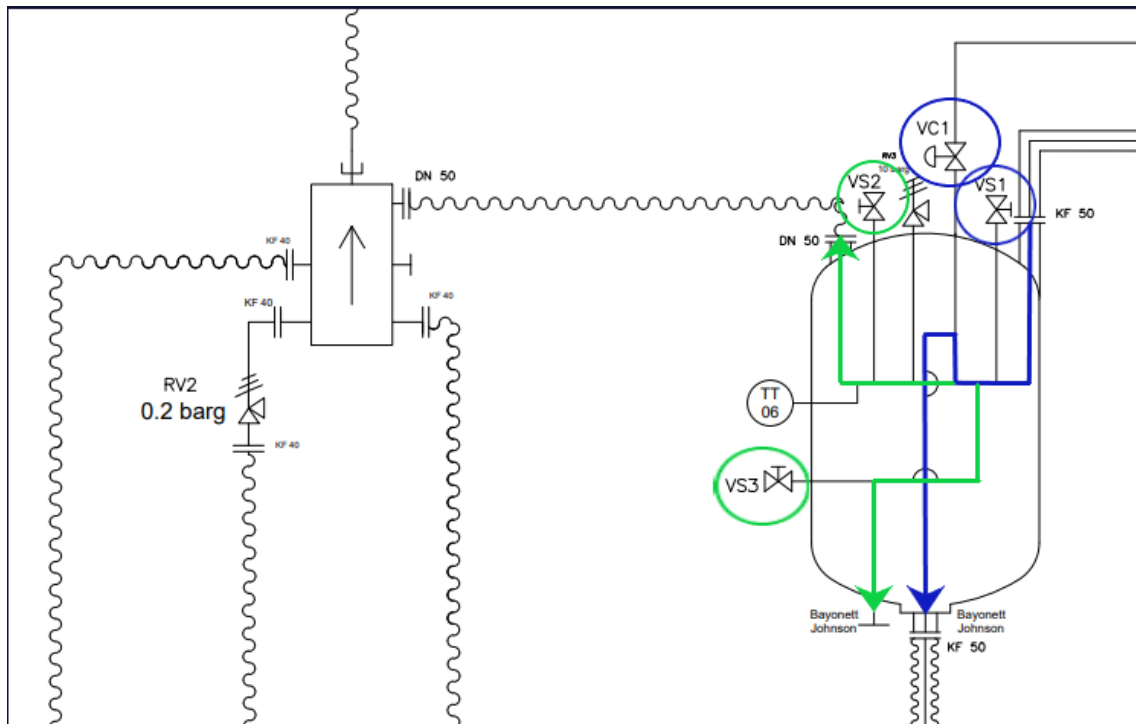
Figure 2.25: Electro Valve EV03 in the blue circle; LN<sub>2</sub> way to the clean room, blue arrow; discharge line, red arrow.

After that, LN<sub>2</sub> flows through the blue line in Fig. 2.26 and it is possible to regulate the flow thanks to the proportional valve on the top of the cold box VC1, it is possible to control the LN<sub>2</sub> flow further with manual valve VS1. VS2 & VS3 manual valves separate the N<sub>2</sub> gas from the LN<sub>2</sub>, the first one through the manifold and VS3 in the clean room. With TT6 (T transducer) we read the temperature in the green line (gas fluid).

After setting the VC1 opening rate the N<sub>2</sub> flows in the cryostat as gas, caused by the heat exchange between warm cryostat and the cold fluid, starting the cool down of the cryostat. When the double wall transfer line will all be filled with LN<sub>2</sub> we will pass to the actual fill of the vessel, it is possible read out this moment thanks to the PT100 located in the bottom of the cryostat. During the filling we expect a pressure of 1500 mbar maximum, it can be checked thanks to the level and pressure transducer linked with LabView or directly with the pressure indicator (PI1) located on the top of the cryostat. Acting on the all



(a) 3D rendering of proportional valve VC1



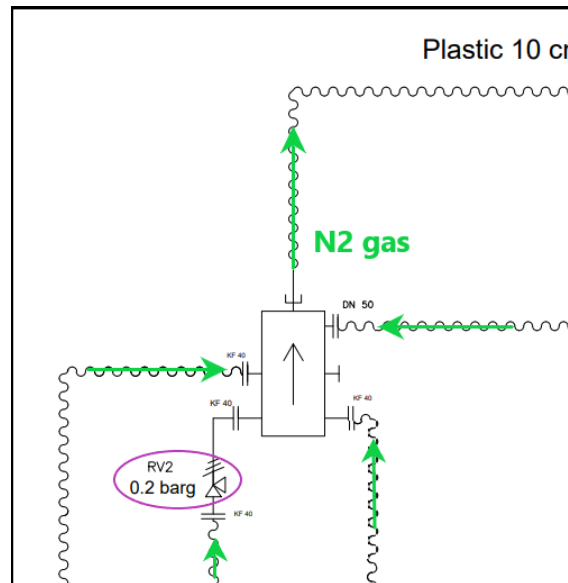
(b) LN<sub>2</sub> direction, blue line; N<sub>2</sub> gas direction, green line; VS1, VS2 & VS3 manual valve.

Figure 2.26: Filling phase, cold box view

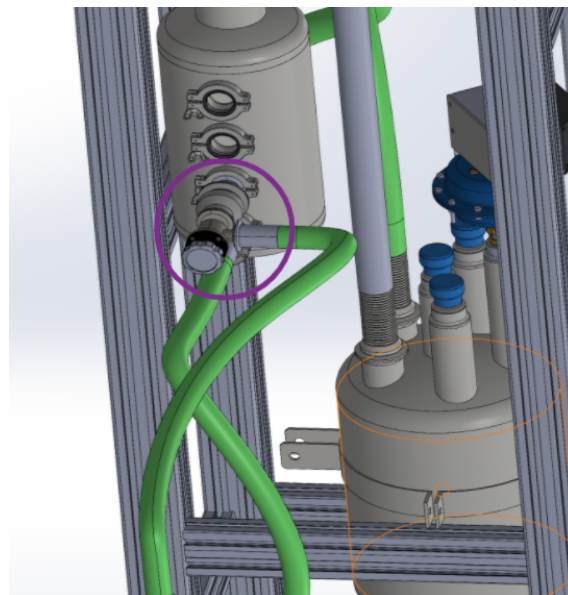
metal manual valve VN1, see Fig. 2.24 during the filling we set the pressure at the measure we want until the last PT100 will be reach the LN<sub>2</sub> temperature (77K).

### Testing phase

This phase starts when the LN<sub>2</sub> level in the inner vessel reaches the upper PT100. After that, the all metal valve VN1 need to be closed, the manual valve located on the top of the cryostat VN3 has to be manually opened. The VN3 links the cryostat to the manifold through a flexible line in which should be located a globe valve RV2, see Fig.2.27. RV2 guarantees a pressure in the cryostat of 1200 mbar maximum.



(a) 2D sketch



(b) 3D rendering

Figure 2.27: Globe valve RV2

### Emptying phase

As the final step of the test cycle the LN<sub>2</sub> has to be removed from the cryostat by use of the pressure buildup. The estimated necessary overpressure is less than 1 bar in order to remove the liquid and deliver it to the evaporator located outside the clean room close to the LN<sub>2</sub> storage tank at height of 8 m above the clean room. The LN<sub>2</sub> will be removed with the same transfer line used previously for the filling, see Fig.2.28.

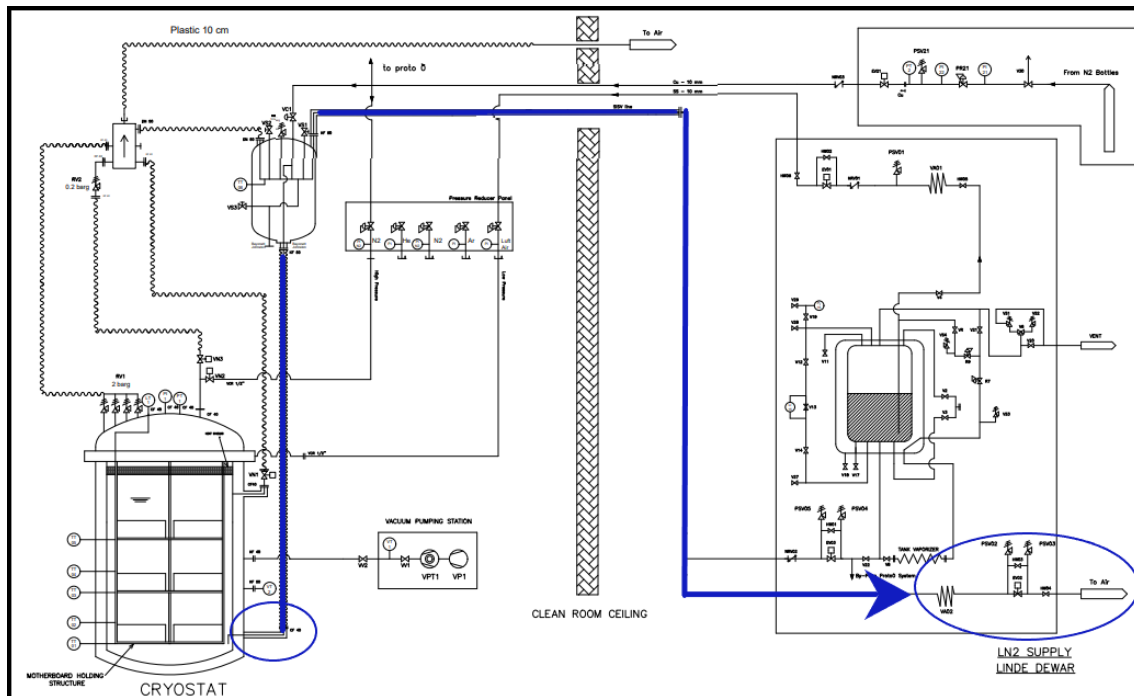


Figure 2.28: LN<sub>2</sub>'s way to the vent

To increase the pressure in the cryostat VN3 needs to be closed. This phase could be done forcing the discharge, fluxing N<sub>2</sub> into the cryostat through the PR panel, or leaving the LN<sub>2</sub> to evaporate through the vent naturally. As first step we need to close the electro-valve EV03 near the output fitting of the supply tank then we can open the other electro-valve EV02 linked to the vent.

The LN<sub>2</sub> will not flow back to the supply dewar thanks to the non return valve NVR02, see Fig.2.29, but it will evaporate inside the VA02 then it will be flow out through the vent. After the LN<sub>2</sub> removal the cryostat will be flushed with N<sub>2</sub> gas for warm up to the room temperature, then the top flange will be opened, and all PDUs will be removed to make room for the next ones.

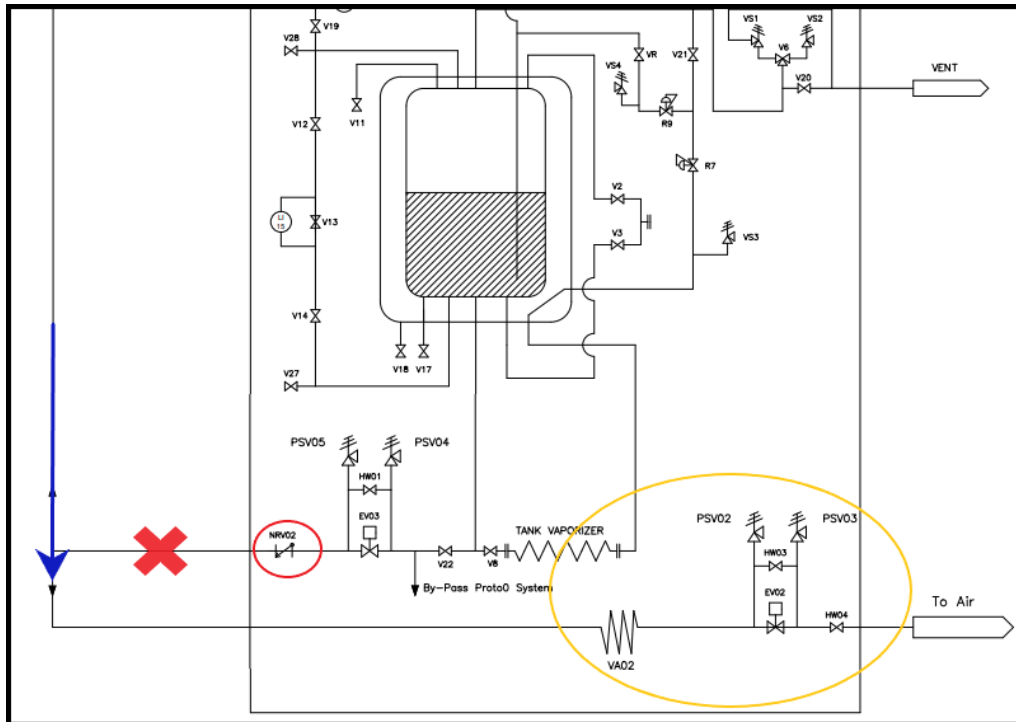


Figure 2.29: Discharge line: NVR02 in red; Evaporator VA02 before the electro-valve EV02 in yellow.

This short description of the Test Facility should illustrate how it was designed and how the Collaboration expects it to work, in the next sections assembly and commissioning will be shown in order to compare design expectations to effective results.

# 3

## MECHANICAL ASSESSMENT OF THE CRYOSTAT BASED ON EN 13445 AND FINITE ELEMENT ANALYSES

The cryostat is the main element of the Test Facility, during this section many aspects of its design will be analyzed.

The requirements for design, construction, inspection and testing will be considered in detail according to the European standard EN 13445 [5] [6] [7] [8].

An in-depth study carried out on Ansys Workbench software will be shown focusing on the mechanical behaviour of the cryostat subject to the mechanical and thermal loading conditions. As already mentioned the cryostat operating conditions are such that it shall conform to the Pressure Equipment Directive (PED) [3]. The PED covers all components that are generally over one liter in volume and having a maximum pressure more than 0.5 bar gauge (1.5 bar). The cryostat far exceeds these limits, in fact it could work as far as 2 bar gauge and its volume is 930 liters. As a first step in the following section the general content of the Pressure Equipment Directive (PED) and the Unfired Pressure Vessel code (EN 13445) are described.

### 3.1 PRESSURE EQUIPMENT DIRECTIVE

The PED covers the design, manufacturing of pressure equipment and assemblies with a maximum allowable pressure greater than 0.5 bar. It also sets the administrative procedures requirements for the "conformity assessment" of pressure equipment, for the free placing on the European market without local legislative barriers. It has been mandatory throughout the EU since 30 May 2002, with 2014 revision fully effective as of 19 July 2016.

Equipment that does not fall under the scope of the PED includes: pipelines, water distribution, equipment for cars, nuclear equipment, machinery, ships, aircraft, and carriage of dangerous goods (for a complete list, refer to Article 1 of the PED, [3]).

According to [4] there are several steps to be followed in order to define the PED category, which defines the design, manufacturing, documentation, quality assurance and testing procedures.

**1. DEFINE EQUIPMENT TYPE (ARTICLE 2 OF THE PED)** There are six types of pressure equipment that will be CE marked in accordance with the PED:

- Vessel: A housing designed and built to contain fluids under pressure including its direct attachments up to the coupling point connecting it to other equipment. A vessel may be composed of more than one chamber.
- Steam Generator or Pressure Cookers or Otherwise Heated Pressure Equipment
- Piping
- Safety Accessories
- Pressure Accessories
- Assemblies

In this case I will refer to the vessel as pressure equipment.

**2. DETERMINE GAS OR LIQUID** For the PED if vapor pressure of liquid is at maximum allowable temperature greater than 0.5 bar above normal atmospheric pressure, treat as a Gas and if a vessel or chamber contains more than one fluid, base the classification on the fluid that requires the higher hazard category. The fluid used in the facility is LN<sub>2</sub>, hence is treated as gas, being its vapor pressure much greater than 0.5 barg at maximum allowable temperature.

**3. CHOOSE THE FLUID GROUP** In the article 13 of the PED [3] fluids are divided in two groups:

- Group 1: Fluids defined as: explosive, extremely flammable, highly flammable, flammable (where the maximum allowable temperature is above flashpoint), very toxic, toxic, or oxidizing.
- Group 2: All fluids not referred to in Group 1.

**4. SELECT CONFORMITY ASSESSMENT TABLE** Next step is to find the conformity assessment table according to the Annex III of the PED, as shown in the chart in Fig.3.1.

	Vessel				Steam Generator	Piping			
State of contents	Gas		Liquid		N/A	Gas		Liquid	
Fluid group	1	2	1	2		1	2	1	2
Table*	1	2	3	4	5	6	7	8	9

Figure 3.1: Conformity assessment's chart

For the Test Facility we have a gas and a fluid Group 2 so the table that will be used is Table 2 shown in Fig.3.2 . Table 2, according to article 4 of [3], belongs to liquids with a vapor pressure at the maximum allowable temperature greater than 0.5 bar over the normal atmospheric pressure (1013 mbar), within the following limits: fluids of group 2; the volume is greater than one liter and the product  $PS \times V$  is greater than 200 bar x liter; the pressure  $PS$  is less than 3 bar.

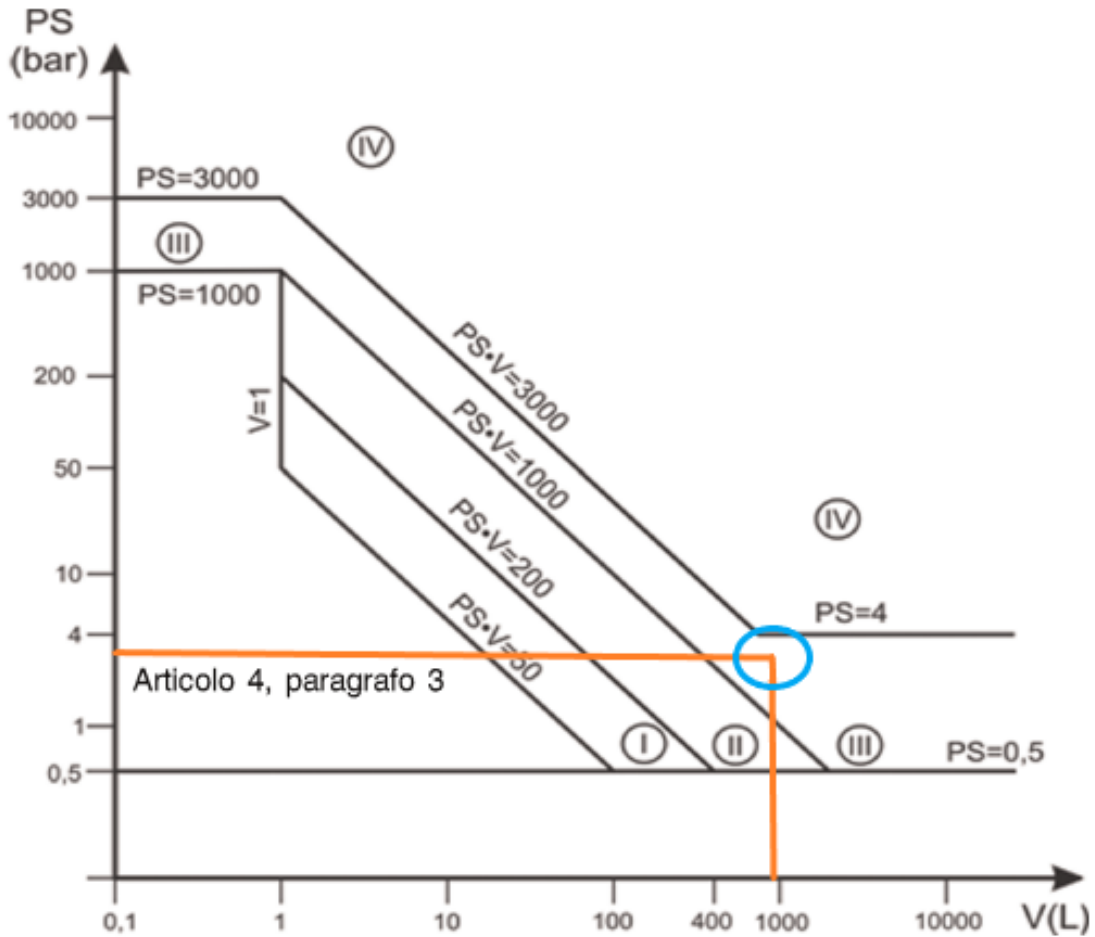


Figure 3.2: Conformity assessment table for fluid group 2

**5. SELECT HAZARD CATEGORY FROM THE TABLE** On the X axis of Table 2 there is Volume (liters) and on the Y axis there is Pressure (bar). To find Hazard Category, use the maximum allowable pressure (bar), volume (liters or nominal diameter DN). The demarcation lines in the tables indicate the upper limit for each category. In this case the maximum allowable pressure is 3 bar and the cryostat is 930 liters big. The cryostat belongs to the category "III".

6. **DETERMINE THE CONFORMITY ASSESSMENT MODULE** Choose the desired conformity assessment module for the category according to the following table:

Hazard Category	With no QA system		With QA ISO 9000 system or equivalent	
	Serial Production	Unit Production	Serial Production	Unit Production
I	<b>Modules</b>			
	<b>A</b> Technical documentation and internal production control			
II	<b>A1</b> Technical documentation and internal manufacturing checks with monitoring of the final assessment		<b>D1</b> Technical documentation and production quality assurance	<b>E1</b> Technical documentation and product quality assurance
III	<b>B</b> EC type examination + <b>C1</b> Conformity to type	<b>B1</b> EC Design examination + <b>F</b> Product verification	<b>B</b> EC type examination + <b>E</b> Product quality assurance	<b>B1</b> EC Design examination + <b>D</b> Quality assurance for final inspection, testing & production  <b>H</b> Full quality assurance for design, final production, inspection & testing
IV	<b>B</b> EC type examination + <b>F</b> Product verification	<b>G</b> EC unit verification	<b>B</b> EC type examination + <b>D</b> Quality assurance for final inspection, testing & production	<b>H1</b> Full quality assurance with design examination and special surveillance of the final assessment

Figure 3.3: Conformity assessment modules table

One of the possible modules for category III is Module H: Conformity based on full quality assurance. This module is a conformity assessment procedure with which the manufacturer complies to the obligations, referred to following points, as well as verifying and declaring, under its sole responsibility, that the pressure equipment meets the requirements of this directive.

- **Quality system**

The manufacturer submits an application for verification of his quality system for the pressure equipment to be approved by an external regulator body. Technical documentation, allowing to assess the compliance of the pressure equipment with the relevant requirements and includes risk analysis and assessment. It specifies the applicable requirements to be met in the design, manufacture and operation of the pressure equipment. The technical documentation contains at least the following elements:

- a general description of the pressure equipment
- design and manufacturing drawings

- the descriptions and explanations about drawings and diagrams
  - a list of standards applied
  - the results of the design calculations, examinations, etc.
  - the reports on the tests carried out
- **Manufacturing**  
The manufacturer shall operate an approved quality system for design, manufacture, final product inspection and testing of the pressure equipment referred to the previous point.
  - **CE marking and EU conformity assessment**
    - The manufacturer signs the CE marking to each item of pressure equipment that satisfies the requirements of this one directive.
    - The manufacturer has to write an EU declaration of conformity for a model of pressure equipment which keeps at the disposal of the national authorities for ten years from the placing on the market date.

### 3.2 CONFORMITY ASSESSMENT WITH REGULATORY EN13445 CODE

EN13445 specifies the requirements for design, construction, inspection and testing of unfired pressure vessels.

The analyzed vessel has a volume of 930 liters and is approximately 1.7 m high. The cryostat material is stainless steel AISI 304L which mechanical properties are shown in Table 3.

<b>Density</b>	7,9	kg/dm <sup>3</sup>
<b>E (elastic modulus)</b>	200	GPa
<b><math>\lambda</math> (Thermal conductivity)</b>	14,6	W/mK
<b><math>c_p</math> (specific heat capacity)</b>	500	J/kgK
<b><math>\alpha</math> (Coefficient of thermal expansion)</b>	16,5	mm/m°C
<b><math>R_{p0.2}</math> (yield stress)</b>	180	MPa
<b><math>R_{p1.0}</math> (yield stress)</b>	205	MPa
<b><math>R_m</math> (tensile strength)</b>	500 – 700	MPa

Table 3: mechanical properties of AISI 304L

In this section, the vessel design will be verified according to EN 13445 – 3 [7].

This Part specifies requirements for the design of unfired pressure vessels covered by EN 13445 – 1 : 2014 [5] and constructed of steels in accordance with

EN 13445 – 2 : 2014 [6] and it applies to design in vessels before putting into service. In particular, Cap. 6 – 7 – 8 – 11&16 of [7] will be examined. They concern pressure vessel, maximum allowed design stress, stress applied between the top flange and bolts and additional non-pressure loads.

### 3.2.1 Maximum allowed values of the nominal design stress for pressure parts

This part specifies maximum allowed values of the nominal design stress for pressure parts other than bolts and physical properties of steels. For the specific AISI 304L the applicable part is austenitic steels with a minimum rupture elongation from 35%.

#### *normal operating load cases "f<sub>d</sub>"*

The nominal design stress for normal operating load cases **f** shall not exceed **f<sub>d</sub>** the greater of the two values:

- a) the minimum 1% yield stress at calculation temperature, see Tab.3, divided by the safety factor 1,5.

$$f_d = 136,7\text{MPa} \quad (3.1)$$

- b) if a value of  $R_m$  is available, the smaller of two values:

- the minimum tensile strength  $R_m$ , see Tab.3.3, at calculation temperature, divided by the safety factor 3,0;

$$f_d = 166,7\text{MPa} \quad (3.2)$$

- the minimum 1% yield stress at calculation temperature divided by the safety factor 1,2.

$$f_d = 170,8\text{MPa} \quad (3.3)$$

The nominal design stress is the 3.2, the greater between the two values.

#### *testing load cases "f<sub>t</sub>"*

The nominal design stress for testing load cases **f** shall not exceed **f<sub>test</sub>**, the greater of the two values:

- a) the minimum 1% yield stress at test temperature, divided by the safety factor 1,05.

$$f_t = 195,2\text{MPa} \quad (3.4)$$

- b) the minimum tensile strength  $R_m$  at test temperature, divided by the safety factor 2.

$$f_t = 250 \text{ MPa} \quad (3.5)$$

Testing load cases  $f$  has not to exceed the 3.5, the greater between the two values.

### 3.2.2 Shell under internal pressure

This part provides requirements for design against internal pressure of shells. The calculation pressure  $P$  shall be based on the most severe condition of coincident differential pressure and temperature. It shall include the static and dynamic head where applicable, and shall be based on the maximum possible differential pressure in absolute value between the inside and outside of the vessel (or between the two adjacent chambers). The vessel has a 1024 mm external diameter and a 1020 mm internal diameter, with a thickness of 2 mm. The inner vessel has been divided into three parts, analyzed singularly: cylindrical shell and the top & bottom of the cryostat considered as a torispherical ends.

#### *Cylindrical shell*

For a given geometry the equation for maximum pressure allowed is:

$$P_{\max} = \frac{2f \cdot z \cdot e_a}{D_m} \quad (3.6)$$

$f$  represents  $f_d$ ,  $D_m$  the medium diameter of the inner vessel,  $e_a$  is the thickness and  $z$  is the joint coefficient of the governing welded joint(s) of the component. For the normal operating load cases, the value of  $z$  is given in Table 4. It is related to the testing group of the governing welded joints. Testing groups are specified in EN 13445 – 5 : 2014, Clause 6 [8].

<b>z</b>	1	0,85	0,7
<b>Testing group</b>	1;2	3	4

Table 4: Joint coefficient and corresponding testing group [7]

According to the testing group there will be several non-destructive testing NDT that need to be done from producers to verify vessel compliance, the cryostat belongs to steels group 8.1 (Austenitic stainless steels with  $Cr \leq 19\%$ ) according to EN 13445 – 5 [8]. From Fig.3.4 we see that group 8.1 steels belong to testing group 3b.

However, the maximum pressure allowed by the inner cylinder is 0,55 MPa.

#### *Torispherical ends*

Lets consider the top and bottom flange having same dimensions. In Fig.3.5 there are dimension features of a torispherical end: inner diameter 1020 mm,

Requirements	Testing group <sup>a</sup>						
	1a	1b	2a	2b	3a	3b	4 <sub>b,d</sub>
Permitted materials <sup>g</sup>	1 to 10	1.1, 1.2, 8.1	8.2, 9.1, 9.2, 9.3, 10	1.1, 1.2, 8.1	8.2, 9.1, 9.2, 10	1.1, 1.2, 8.1	1.1, 8.1
Extent of NDT for governing welded joints <sup>e,h</sup>	100 %	100 %	100 % - 10% <sup>g</sup>	100 % - 10% <sup>g</sup>	25 %	10 %	0 %
NDT of other welds	Defined for each type of weld in Table 6.6.2-1						
Joint coefficient	1	1	1	1	0,85	0,85	0,7
Maximum thickness for which specific materials are permitted	Unlimited <sup>f</sup>	Unlimited <sup>f</sup>	30 mm for groups 9.1, 9.2 16 mm for groups 9.3, 8.2 <sup>f</sup> , 10	50 mm for groups 1.1, 8.1 30 mm for group 1.2	30 mm for groups 9.2, 9.1 16 mm for groups 8.2, 10	50 mm for groups 1.1, 8.1 30 mm for group 1.2	12 mm for groups 1.1, 8.1
Welding process	Unlimited <sup>f</sup>	Unlimited <sup>f</sup>	Fully mechanical welding only <sup>c</sup>		Unlimited <sup>f</sup>	Unlimited <sup>f</sup>	Unlimited <sup>f</sup>
Service temperature range	Unlimited <sup>f</sup>	Unlimited <sup>f</sup>	Unlimited <sup>f</sup>	Unlimited <sup>f</sup>	Unlimited <sup>f</sup>	Unlimited <sup>f</sup>	Limited to (-10 to +200) °C for group 1.1 (-50 to +300) °C for group 8.1

Figure 3.4: Testing groups for steel pressure vessels

same as the inner cylindrical vessel; outer diameter 1028 mm, for this reason we have a different thickness, 4 mm; R is the Crown Radius and is 512 mm large; r is the Knuckle Radius and is 102,4 mm large.

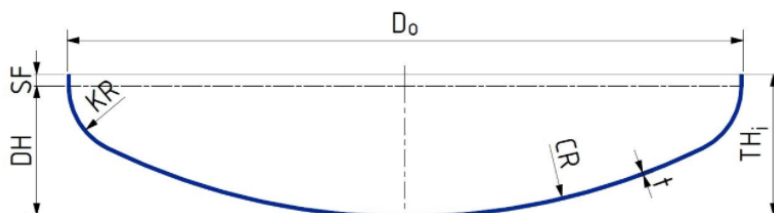


Figure 3.5: Torispherical ends; CR crown radius; KR knuckle radius.

The following calculations have been carried out for both flanges. For a given geometry  $P_{max}$  shall be the least of  $P_s$ ,  $P_y$  and  $P_b$ , where:

$$P_s = \frac{2f \cdot z \cdot e_a}{R + 0,5e_a} \quad (3.7)$$

$$P_y = \frac{f \cdot e_a}{\beta(0,75R + 0,2D_i)} \quad (3.8)$$

$\beta$  is found from Fig.3.6 where  $\frac{r}{D_i} = 0,1$  and  $\frac{e_a}{R} = 0,0078$ .

$$P_y = 111f_b \left( \frac{e_a}{0,75R + 0,2D_i} \right)^{1,5} \left( \frac{r}{D_i} \right)^{0,825} \quad (3.9)$$

Taking the least between 3.7, 3.8 and 3.9 we obtain a value of  $P_{max} = 0,57$  MPa.  $P_{max}$  equals internal pressure for both top and bottom torispherical ends.

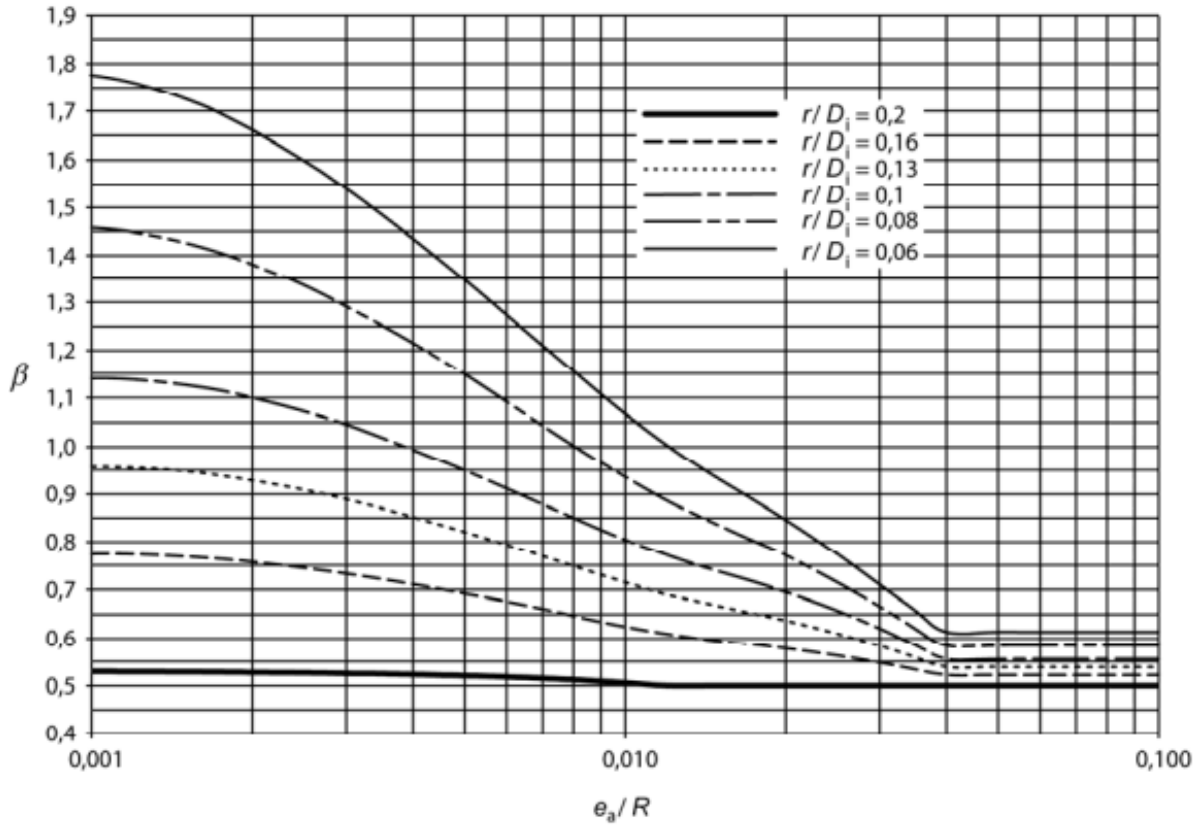


Figure 3.6: Parameter  $\beta$  for torispherical end - rating

### 3.2.3 Shell under external pressure

As the previous section these calculations provide requirements for the design of shells under external pressure loading. They apply to stiffened and unstiffened cylinders and cones, spheres and dished ends. The outer vessel dimensions are: outer diameter of 1070 mm; inner diameter of 1060 mm;  $e_a = 5$  mm.

#### *Cylindrical shells*

For unstiffened cylinders and unsupported length the vessel  $L$  is given by the following equation and taken from Fig.3.7.

$$L = L_{\text{cyl}} + 0,4h' + 0,4h'' \quad (3.10)$$

Considering  $R$  as mean radius of the outer vessel,  $\sigma_e$  as the nominal elastic limits for shell calculated as  $\frac{R_{p0,2/T}}{1,25}$ , for austenitic steel shells and with a given  $e_a$ ,  $P_y$  has been calculate as:

$$P_y = \frac{\sigma_e \cdot e_a}{R} \quad (3.11)$$

It is the pressure at which mean circumferential stress in a cylindrical or conical shell midway between stiffeners, or in a spherical shell, reaches yield point. Then calculate  $P_m$ , that is the theoretical elastic instability pressure for collapse

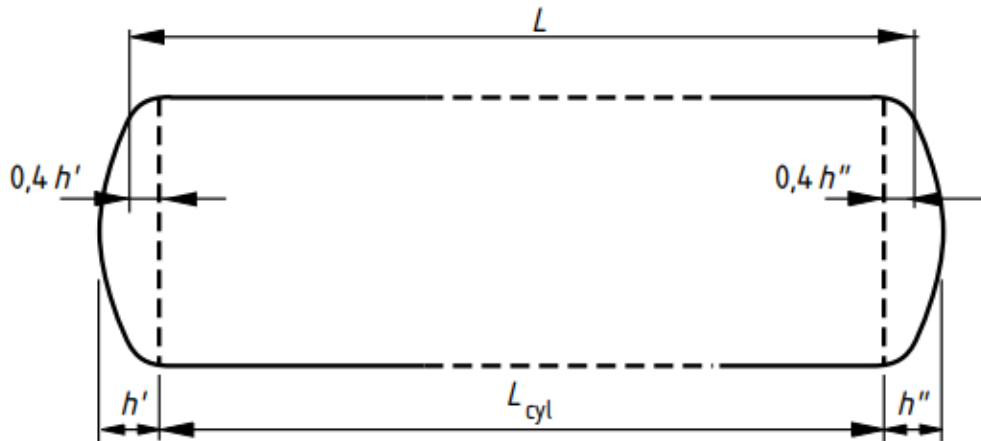


Figure 3.7: Cylinder with heads

of a perfect cylindrical, conical or spherical shell, from the following equation using the same assumed value for  $e_a$  :

$$P_m = \frac{E \cdot e_a \cdot \epsilon}{R} \quad (3.12)$$

where  $E$  is the value of the modulus of elasticity and  $\epsilon$  is the mean elastic circumferential strain at collapse and has obtained by the following graphic shown in Fig.3.8. Following the graphic the value of  $\epsilon$  is 0,0004.

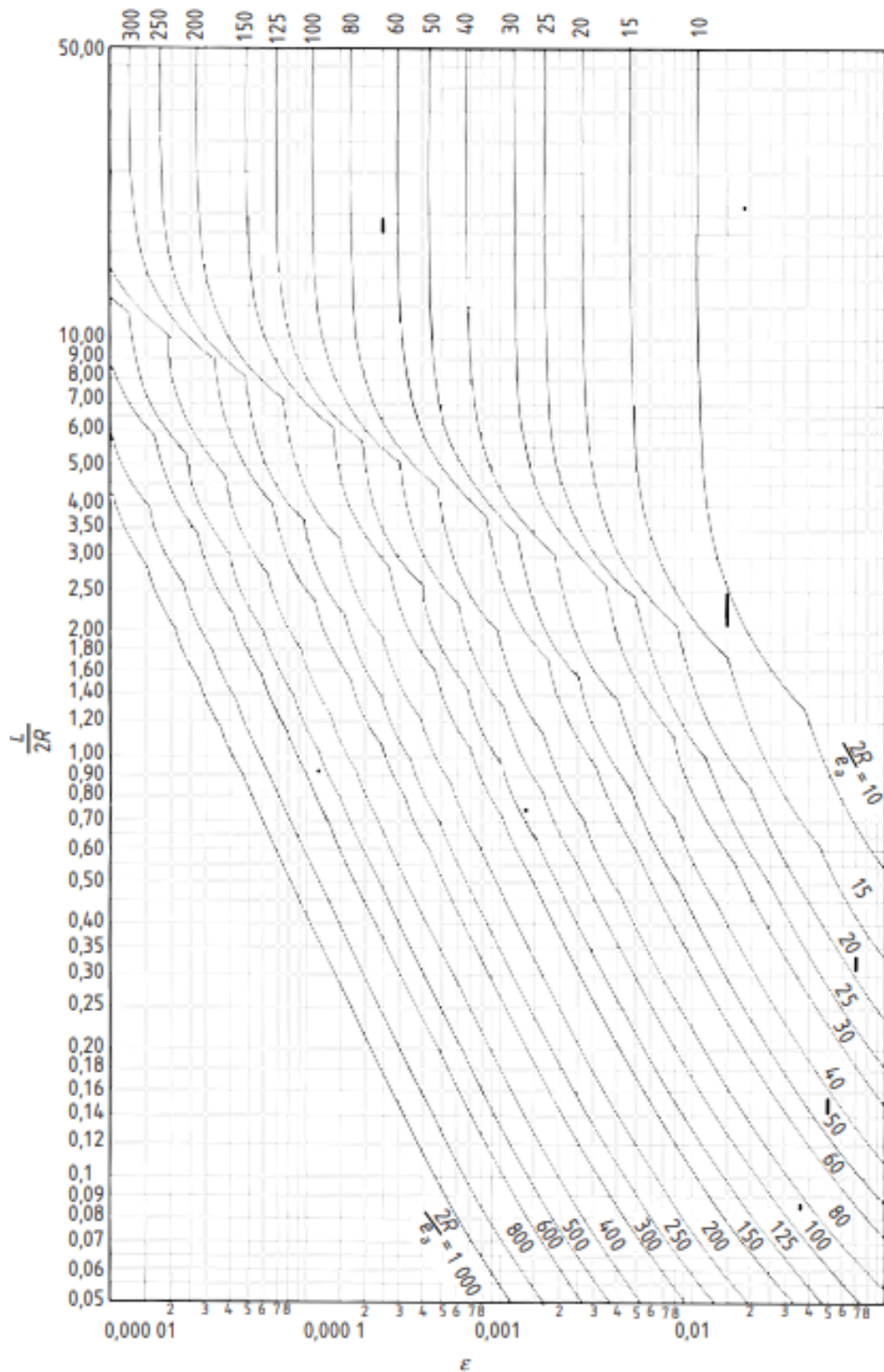
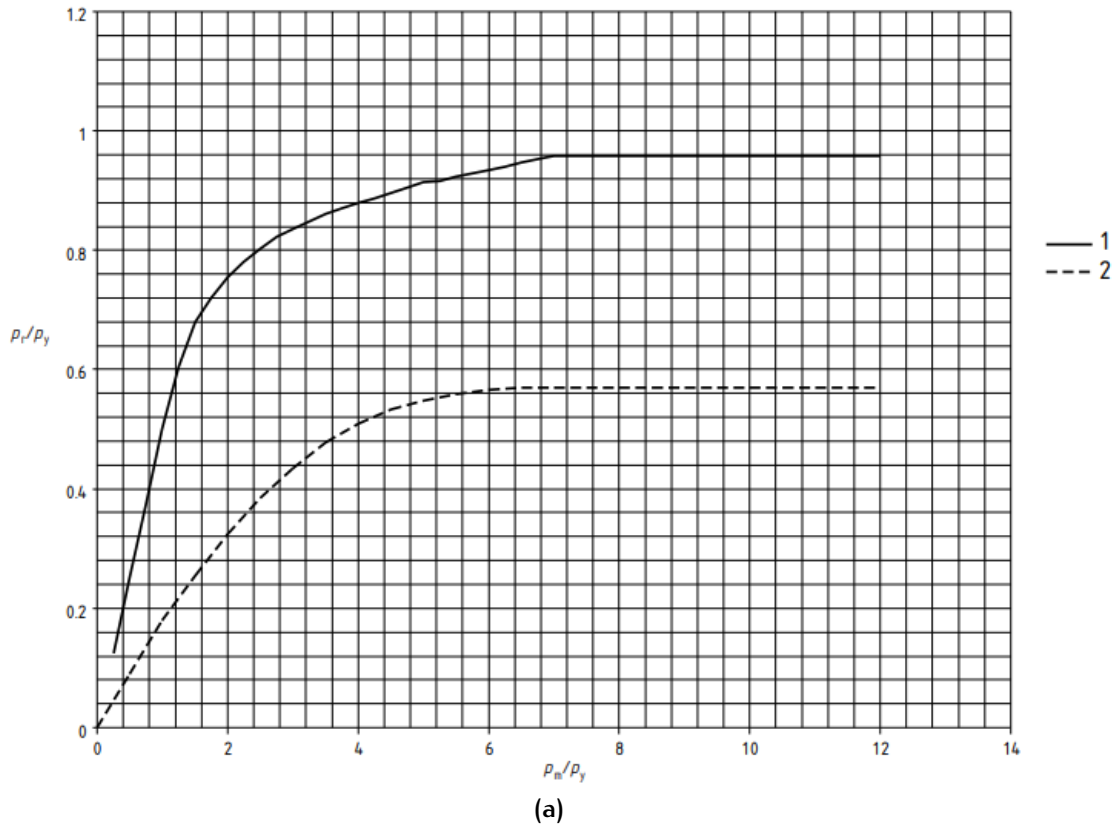


Figure 3.8: Value of  $e$

After that  $\frac{P_m}{P_y}$  has been calculated and  $\frac{P_r}{P_y}$  has determined from the first curve in Fig3.9 through a linear interpolation using the table in Fig.3.9.



1 - Cylinders and cones

$P_m/P_y$	0	0,25	0,5	0,75	1,0	1,25	1,5	1,75	2,0	2,25	2,5	2,75	3	3,25	3,5
$P_r/P_y$	0	0,125	0,251	0,375	0,5	0,605	0,68	0,72	0,755	0,78	0,803	0,822	0,836	0,849	0,861
$P_m/P_y$		3,75	4,0	4,25	4,5	4,75	5,0	5,25	5,5	5,75	6,0	6,25	6,5	6,75	$\geq 7,0$
$P_r/P_y$		0,87	0,879	0,887	0,896	0,905	0,914	0,917	0,923	0,929	0,935	0,941	0,947	0,953	0,959

(b)

Figure 3.9: Values of  $\frac{P_m}{P_y}$  versus  $\frac{P_r}{P_y}$

Thanks to Fig.3.9 it is possible to obtain  $P_r$  which is the lower bound collapse pressure. However, it is necessary that following equation shall be satisfied:

$$P < \frac{P_r}{S} = 0,25MPa \tag{3.13}$$

The external  $P$  is the ambient pressure 0,1 MPa and  $S= 1,5$  is the minimum safety factor applied in design conditions, so the 3.13 was successfully satisfied.

### Torispherical ends

Torispherical ends shall be designed as spherical shells of mean radius  $R$  equal to the external dishing or crown radius. Following the equations:

$$P_y = \frac{2\sigma_e \cdot e_a}{R} \tag{3.14}$$

and

$$P_m = \frac{1,21E \cdot e_a^2}{R^2} \quad (3.15)$$

In this case from Fig.3.9 it is used the curve "2" to calculate  $P_r$  and then the following equation shall be satisfied:

$$P < \frac{P_r}{S} = 0,8\text{MPa} \quad (3.16)$$

There are the same conditions of the outer vessel and the same values for  $P$  and  $S$  so the 3.16 has been satisfied.

### 3.2.4 Flanges

This part gives requirements for the design of circular bolted flange connections. Flanges with full face and narrow face gaskets, subject to internal and external pressure are included. In flange tightening there is a gasket of thick 4 mm large, made of NBR 70 that must ensure the sealing of the lid and the permanence of the fluid inside the tank.

#### *Bolts sizing*

For bolts sizing an empirical formula allows to calculate the minimum required number of bolts, given by:

$$N_b = \frac{D_i[\text{mm}]}{40} + 4 = 29,5$$

where  $D_i$  is the inner diameter of the inner vessel. the value of  $N_b$  is rounded up as a multiple of four so its value is 32.

An analysis was done about a tensile stress due the pressure of the vessel, stress is taken to be 20% higher considering several factors, as bending.

$$\sigma_b = \frac{1,2F_{b0}}{A_{cor}} = \frac{1,2p\frac{\pi}{4}\frac{D_{mg}^2}{N_b}}{\frac{\pi d_{cor}^2}{4}} \leq \frac{R_{p0,2,bolt}}{\eta} \quad (3.17)$$

$D_{mg}$  is the mean diameter of the O-ring gasket which has got a known size of 1035 mm and 4 mm thick. As first verification, from 3.17 we can obtain the minimum value of bolts' core diameter. The bolt class chosen for the Test facility is A2-70, an austenitic hardened steel, with a  $R_{p0,2} = 450$  MPa.

$$d_{cor} \geq 7,3\text{mm}$$

#### *Clamping force*

The first tightening has the purpose of making gasket yield in order to not escaping the fluid when it's inside the vessel. However, the bolts yield is the superior limit of the clamping force, so:

- minimum clamping force required by the gasket:

$$F_{0,\min} = R_{p0,2,g} A_{mg} = R_{p0,2,g} \frac{\pi D_{mg} b}{N} = 10,16 \text{ kN} \quad (3.18)$$

the number of bolts used in the commissioning  $N$  (44) and gasket thickness  $b$  are given known.

- maximum clamping force required by the bolts: the bolts dimension is already known from design so it is possible to obtain the core diameter and the area by reference to the table in the Fig.3.10:

Diametro nominale di filettatura (vedere punto 1) e diametro esterno $d=D$			Paso $P$	Diametro medio $d_2 = D_2$	Diametro di nocciolo della vite $d_3$	Diametro della vite all'inizio del raccordo $d_1$	Diametro di nocciolo della madre vite $D_1$	Profondità dei filetti della vite $h_3$	Ricoprimento $H_1$	Raggio arrotondamento fondo filetto della vite $r$	Sezione resistente (vedere punto 4) $\text{mm}^2$	Sezione di nocciolo $\text{mm}^2$
Colonna 1	Colonna 2	Colonna 3										
10			1,5	9,026	8,180	8,376	8,376	0,920	0,812	0,217	68,0	62,3
		11	1,5	10,026	9,180	9,376	9,376	0,920	0,812	0,217	72,3	65,9
12			1,75	10,863	9,853	10,106	10,106	1,074	0,947	0,253	84,3	76,2
	14		2	12,701	11,546	11,835	11,835	1,227	1,083	0,289	115	105
16			2	14,701	13,546	13,835	13,835	1,227	1,083	0,289	157	144
	18		2,5	18,376	14,933	15,294	15,294	1,534	1,353	0,361	192	175
20			2,5	18,376	16,933	17,294	17,294	1,534	1,353	0,361	245	225
	22		2,5	20,376	18,933	19,294	19,294	1,534	1,353	0,361	303	282
24			3	22,051	20,319	20,752	20,752	1,840	1,624	0,433	353	324
	27		3	25,051	23,319	23,752	23,752	1,840	1,624	0,433	459	427
30			3,5	27,727	25,706	26,211	26,211	2,147	1,894	0,505	561	519
	33		3,5	30,727	28,706	29,211	29,211	2,147	1,894	0,505	694	647
36			4	33,402	31,093	31,670	31,670	2,454	2,165	0,577	817	759
	39		4	36,402	34,093	34,670	34,670	2,454	2,165	0,577	976	913
42			4,5	39,077	36,479	37,129	37,129	2,760	2,436	0,650	1 120	1 050

Figure 3.10: Bolts size

$$F_{0,\max} = R_{p0,2,b} A_{cor} = 64,85 \text{ kN} \quad (3.19)$$

We have 44xM16 bolts made of A2-70, these bolts have a  $A_{cor} = 144 \text{ mm}^2$ . The favorable conditions are close to 3.18, so  $F_0 = F_{0,\min}$ .

### ***Bolts and gasket total load in operating condition***

The total load on bolts and gasket depends on the  $\Delta F$  caused by pressure so it is necessary to calculate the contribution due to pressure  $p$ :

$$P = p \cdot A_{mg} = p \frac{\pi D_{mg}^2}{4} = 250,45 \text{ kN} \quad (3.20)$$

Now we can estimate the single bolt load as a function of  $N$ :

$$F_p = \frac{P}{N} = 5,7 \text{ kN} \quad (3.21)$$

For the  $\Delta F$  estimation we have to consider the components' stiffness:

- gasket stiffness

$$k_g = E_g \frac{\pi D_{mg} b}{b} = 768,3 \frac{\text{N}}{\text{mm}} \quad (3.22)$$

- bolt stiffness

$$\frac{1}{k_b} = \frac{1}{k_{bf}} + \frac{1}{k_{bl}}$$

we have to consider the thread length:

$$l_{bt} = \frac{1}{3} l_{tot} \quad ; \quad l_{bl} = \frac{2}{3} l_{tot}$$

$$k_{bf} = E_b \frac{A_{cor}}{l_{bt}}$$

$$k_{bl} = E_b \frac{A_{nom}}{l_{bl}} = E_b \frac{\pi d_{nom}^2}{4 l_{bl}}$$

$$k_b = 507,6 \frac{\text{kN}}{\text{mm}} \quad (3.23)$$

we can know  $\Delta F$  due to the pressure on the bolt and on the gasket:

$$\Delta F_g = \frac{F_p k_g}{k_b + k_g} = 8,6 \text{ N} \quad ; \quad \Delta F_b = \frac{F_p k_b}{k_b + k_g} = 5683 \text{ N} \quad (3.24)$$

Finally we can calculate the total load on single bolt and on the gasket:

$$F_g = F_0 - \Delta F_g = 10,15 \text{ kN}$$

$$F_b = F_0 + \Delta F_b = 15,84 \text{ kN}$$

To verify the seal of the NBR gasket the following equation must be true:

$$F_g \geq F_{g,lim}$$

$$F_{g,lim} = m p A_{mg} = 122 \text{ N}$$

where  $m$  is a gasket factor (0,5 for rubber material).

### ***Bolts static test***

The sealing gasket is verified and now we need to check stress components applied to the bolts. The axial stress component is affected by pressure and tightening, torsional stress by tightening while considering the eccentricity between bolt and gasket, we'll also have a bending component.

- **Axial component**

$$\sigma_{ax} = \frac{F_b}{A_{cor}} = 110 \text{MPa} \quad (3.25)$$

- **Torsional component**

Depends on the moment of tightening, consisting of two tightening torques, the first due to friction between nut and flange and the second one due to friction between the threads. The first contribution under operating conditions is negligible and then we have:

$$M_s = M'_s + M''_s = 0 + V_0 \frac{d_m}{2} \tan(\alpha + \phi) \quad (3.26)$$

where:

- $V_0$  is the initial clamping force
- $d_m$  is mean bolt diameter ( $0,9d_{nom}$ )
- $\alpha$  is the angle between threads ( $\arctan(\frac{p}{\pi d_m})$ )
- $\phi$  will hinge on the thread's profile ( $\arctan(0,15)$ )

The second tightening torque is:

$$M''_s = 11696 \text{Nmm}$$

Therefore, the torsion component is equal to:

$$\tau_{tor} = \frac{16M''_s}{\pi d_{nom}^3} = 23,97 \text{MPa} \quad (3.27)$$

- **Bending component**

The bending component depends on the eccentricity, so to the rotation of the flange by the effect of the load. The eccentricity  $e$  (from design) is equal to 54 mm. The bending moment per unit length is:

$$m = \frac{V_0 e}{\pi(D_{mg} + e)} = 251 \text{N} \quad (3.28)$$

Now we have to consider the flange rotation:

$$\theta_{fl} = \frac{m D_{mf}^2}{4EJ_{fl}} = \frac{m D_{mf}^2}{4E \frac{1}{12} b^3 h^3}$$

The bending component, considering a total rotation of  $\theta = 0,15\theta_{fl}$ , is:

$$\sigma_{flex} = \frac{\theta E d_{nocc}}{2l_b} = 60,47 \text{MPa} \quad (3.29)$$

Taking a safety coefficient of  $\eta = 2$  we can verify through Von Mises:

$$\sigma_{VM} = \sqrt{(\sigma_{flex} + \sigma_{ax})^2 + 3\tau_{tor}^2} = 175,38\text{MPa} \quad (3.30)$$

$$\sigma_{VM} \leq \frac{R_{p0,2,b}}{\eta} = 225\text{MPa}$$

### 3.2.5 Vertical vessels with skirts

This clause is part of the chapter on additional loads and gives rules for the design of support skirts for vertical vessels. There are several skirts type, that one taken into account is a cylindrical stand with frame connection on knuckle area, shown in Fig.3.11. We need to check the three sections shown in Fig.3.11. Checking

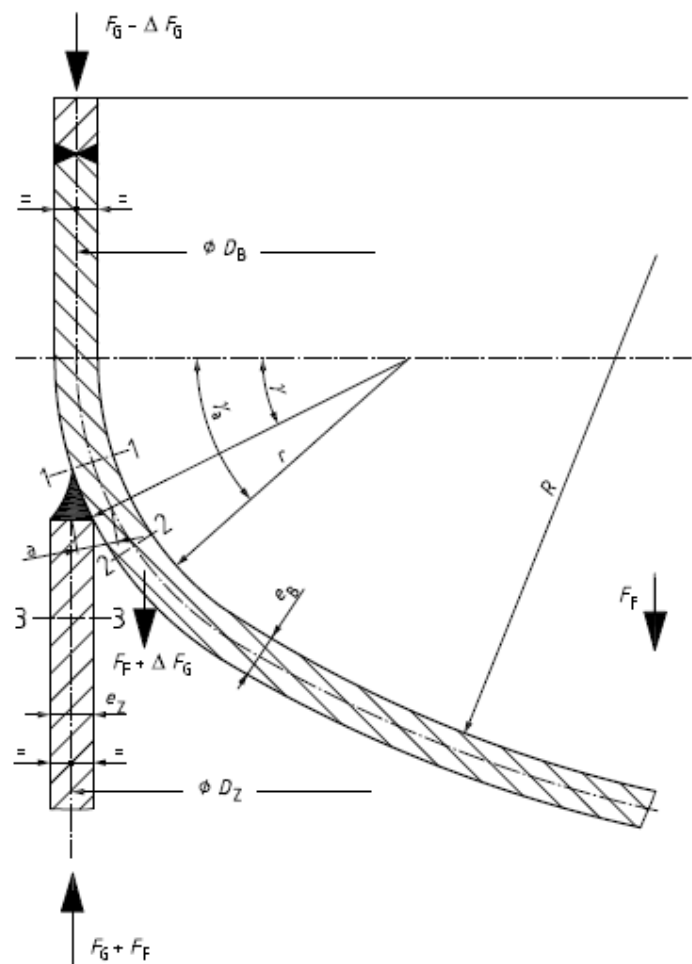


Figure 3.11: Skirt connection in knuckle area

is required for the membrane and the total stresses, while only the respective longitudinal components are being taken into account. The section force  $F_Z$  in the skirt in the region of the joint depends on the position: position  $q$  where the mo-

ment strengthens the load component; position  $p$  where the moment weakens the load component.

$$F_{Zp} = -F_1 - F_G - F_F + 4 \frac{M_1}{D_z} = 4,1 \text{ kN} \quad (3.31)$$

$$F_{Zq} = -F_1 - F_G - F_F - 4 \frac{M_1}{D_z} = -47 \text{ kN} \quad (3.32)$$

Where:

- $F_Z$  is the equivalent force in the considered point ( $p$  or  $q$ ) in the skirt.
- $F_1$  is the global additional axial force in section 1 – 1, considering membrane theory of axisymmetric shells:

$$F_1 = \gamma(V_1 + V_2)$$

- $F_G$  is the weight of vessel without content.
- $F_F$  is the weight of content.
- $M_1$  is the resulting moment due to external loads in section 1 – 1 above the joint; between the pressure loaded shell and skirt.

### Membrane stress

The membrane stresses, with  $P = 0,3 \text{ MPa}$  as maximum operating pressure, at point 1 – 1 are:

$$\sigma_{1p}^m = \frac{F_{Zp} + \Delta F_G + F_F}{\pi D_B e_B} + \frac{P D_B}{4 e_B} = 23,59 \text{ MPa} \quad (3.33)$$

$$\sigma_{1q}^m = \frac{F_{Zq} + \Delta F_G + F_F}{\pi D_B e_B} + \frac{P D_B}{4 e_B} = 13,84 \text{ MPa} \quad (3.34)$$

where  $D_B$  and  $e_B$  are the mean diameter and the thickness of outer vessel. The membrane stress in section 2 – 2 is:

$$\sigma_2^m = \sigma_{2p}^m = \frac{\Delta F_G + F_F}{\pi D_B e_B} + \frac{P D_B}{4 e_B} = 21,06 \text{ MPa} \quad (3.35)$$

In section 3 – 3 of the skirt, the membrane stresses are equal to:

$$\sigma_{3p}^m = \frac{F_{Zp}}{\pi D_z e_z} = 1,05 \text{ MPa} \quad (3.36)$$

$$\sigma_{3q}^m = \frac{F_{Zq}}{\pi D_z e_z} = -3 \text{ MPa} \quad (3.37)$$

All membrane stresses need to satisfy this condition:

$$|\sigma^m| < f = 167 \text{ MPa}$$

### **Bending stress**

The eccentricity  $a$  of the shell wall centreline causes a bending moment:

$$M_p = aF_{Zp} \quad M_q = aF_{Zq}$$

with:

$$a = 0,5\sqrt{e_B^2 + e_Z^2 + 2e_B e_Z \cos(\gamma)}$$

$$\cos(\gamma) = 1 - \frac{D_B + e_B - D_Z + e_Z}{2(r + e_B)}$$

where  $r$  is the inside knuckle radius of torispherical end. The corresponding bending stresses in sections 1-1 to 3-3 at the outer surface (a):

$$\sigma_{1a}^b(a) = \sigma_{2a}^b(a) = C \frac{6M_p}{\pi D_B e_B^2} = 5,19 \text{MPa} \quad \sigma_{1q}^b(a) = \sigma_{2q}^b(a) = C \frac{6M_q}{\pi D_B e_B^2} = -14,81 \text{MPa} \quad (3.38)$$

$$\sigma_{3a}^b(a) = C \frac{6M_p}{\pi D_Z e_Z^2} = 3,32 \text{MPa} \quad \sigma_{3q}^b(a) = C \frac{6M_q}{\pi D_Z e_Z^2} = -9,48 \text{MPa} \quad (3.39)$$

Within the range  $0,5 < \frac{e_B}{e_Z} < 2,25$ , the correction factor  $C$  can be taken approximately equal to:

$$C = 0,63 - 0,057\left(\frac{e_B}{e_Z}\right)^2$$

In the region of sections 1 – 1 to 2 – 2 the above bending stress components are superimposed by the bending effect caused by the internal pressure in the knuckle.

$$\sigma_1^b(p) = \sigma_2^b(p) = \frac{(P + P_H)D_B}{4e_B} \left(\frac{\gamma}{\gamma_a} \alpha - 1\right) = -6,44 \text{MPa} \quad (3.40)$$

where:

- $\alpha$  is the stress intensification factor due to  $y$ :

$$\alpha = y = 125 \frac{e_B}{D_B}$$

- $P_H$  is the hydrostatic pressure.

As membrane stress the bending stress has to verify this condition:

$$|\sigma^b| < f = 167 \text{MPa}$$

### **Total stresses and strength conditions**

The total stresses shall be obtained as follows:

- section 1 – 1:

– position "p":

inner surface:

$$\sigma_{1,pi}^{tot} = \sigma_{1,p}^m - \sigma_{1,p}^b(a) + \sigma_1^b(p) = 11,96\text{MPa}$$

outer surface:

$$\sigma_{1,po}^{tot} = \sigma_{1,p}^m + \sigma_{1,p}^b(a) - \sigma_1^b(p) = 35,22\text{MPa}$$

– position "q":

inner surface:

$$\sigma_{1,qi}^{tot} = \sigma_{1,q}^m - \sigma_{1,q}^b(a) + \sigma_1^b(p) = 22,2\text{MPa}$$

outer surface:

$$\sigma_{1,qo}^{tot} = \sigma_{1,q}^m + \sigma_{1,q}^b(a) - \sigma_1^b(p) = 5,47\text{MPa}$$

- section 2 – 2:

– position "p":

inner surface:

$$\sigma_{2,pi}^{tot} = \sigma_{2,p}^m + \sigma_{2,p}^b(a) + \sigma_2^b(p) = 19,80\text{MPa}$$

outer surface:

$$\sigma_{2,po}^{tot} = \sigma_{2,p}^m - \sigma_{2,p}^b(a) - \sigma_2^b(p) = 22,31\text{MPa}$$

– position "q":

inner surface:

$$\sigma_{2,qi}^{tot} = \sigma_{2,q}^m + \sigma_{2,q}^b(a) + \sigma_2^b(p) = -0,19\text{MPa}$$

outer surface:

$$\sigma_{2,qo}^{tot} = \sigma_{2,q}^m - \sigma_{2,q}^b(a) - \sigma_2^b(p) = 42,31\text{MPa}$$

- section 3 – 3:

– position "p":

inner surface:

$$\sigma_{3,pi}^{tot} = \sigma_{3,p}^m - \sigma_{3,p}^b(a) = -2,27\text{MPa}$$

outer surface:

$$\sigma_{3,po}^{tot} = \sigma_{3,p}^m + \sigma_{3,p}^b(a) = 4,37\text{MPa}$$

– position "q":

inner surface:

$$\sigma_{3,qi}^{\text{tot}} = \sigma_{3,q}^{\text{m}} - \sigma_{3,q}^{\text{b}}(\mathbf{a}) = 6,48\text{MPa}$$

outer surface:

$$\sigma_{3,qo}^{\text{tot}} = \sigma_{3,q}^{\text{m}} + \sigma_{3,q}^{\text{b}}(\mathbf{a}) = -12,48\text{MPa}$$

All total stresses verify the following equation:

$$|\sigma^{\text{b}}| < f = 167\text{MPa}$$

### 3.3 FINITE ELEMENT ANALYSIS

In this session a FEA study of the cryostat is presented. Ansys Workbench, a commercial FEA software, has been used. The goal of the analyses is to simulate the mechanical behaviour of the cryostat and compare the obtained results with the findings using the code formulas. Thermal and pressure loads have been considered. Also buckling verifications have been carried out, in particular for the external vessel subject to vacuum condition.

As first step it was necessary to simplify the cryostat's 3D CAD model to make the simulation more operational and lighter. The simplification was done with Ansys's 3D modeling software SpaceClaim. All the parts, except for the flanges, could be considered as thin elements (one dimension much smaller than the other two) therefore were simplified as surface elements.

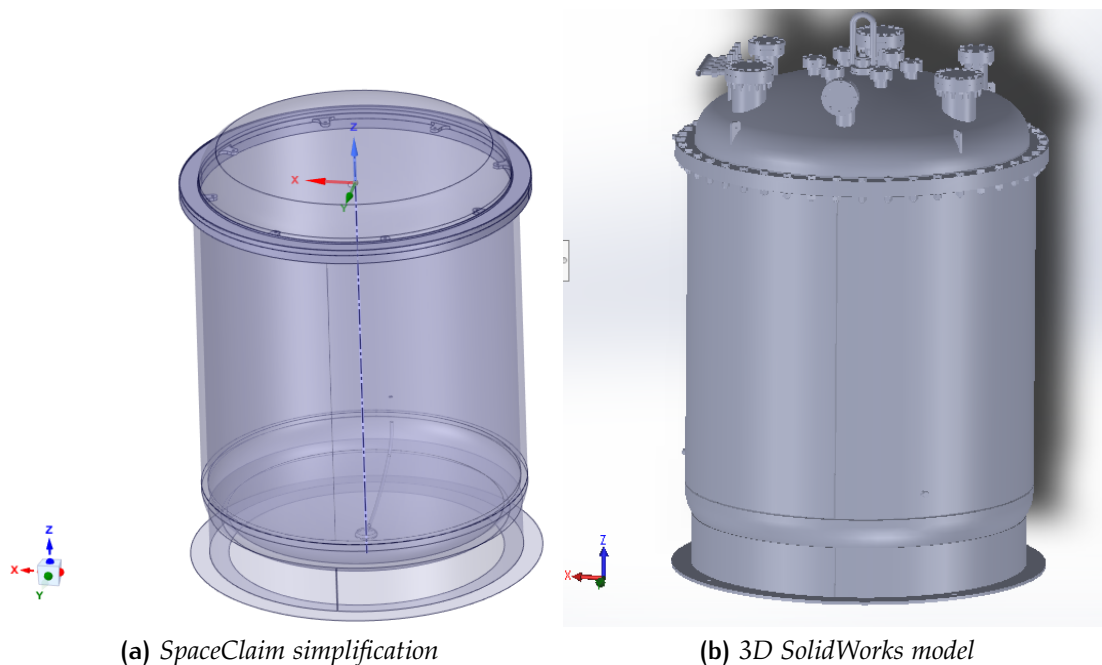


Figure 3.12: Cryostat's 3D modelling and development

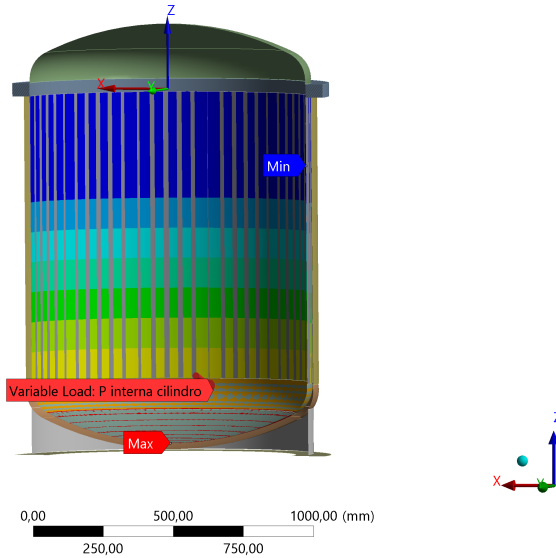
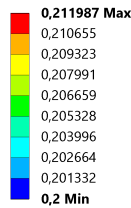
As shown in Fig.3.12 the 3D model was simplified by removing all fittings and the mechanical inner structure. The geometry has been then imported in Ansys Mechanical, a finite element solver.

After setting the material (AISI 304L stainless steel) and the mesh, it is necessary to set the boundary conditions in terms of loads and relevant for the structure. An outer pressure of 1 absolute bar has been set considering the normal ambient condition of the clean room. The inner pressure was set considering a maximum allowed pressure of 2 relative bar and the hydrostatic pressure due to LN<sub>2</sub>.

In Fig.3.13 shows that the hydrostatic pressure was set considering a maximum distance of 30 cm between the flange and LN<sub>2</sub> level. Solutions show stress and deformation behaviour in line with what was expected, the inner vessel is subject to greater stresses and deformations, which do not exceed the value  $f$

**B: Static Structural**

P interna cilindro  
 Time: 1, s  
 Unit: MPa  
 01/12/2021 12:16

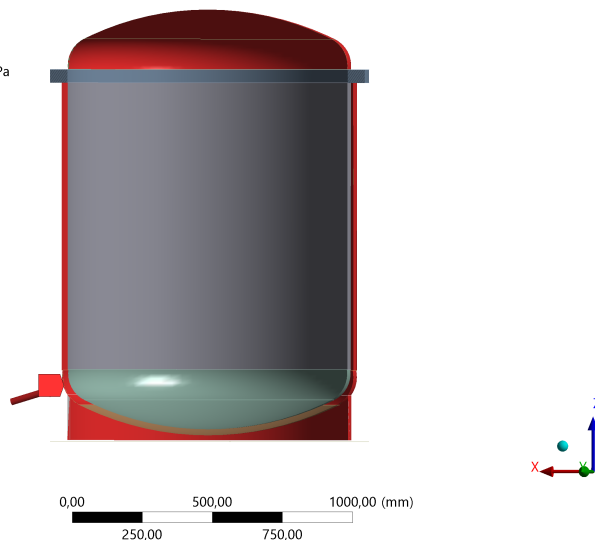


(a) Inner pressure: gas overpressure + hydrostatic pressure

**B: Static Structural**

Pressione Esterna Cilindro  
 Time: 1, s  
 01/12/2021 12:19

Pressione Esterna Cilindro: -0,1 MPa



(b) Outer pressure

Figure 3.13: Analysis settings

(3.2). The outer vessel being supported directly from the skirt has lower stress values. The bottom of the inner vessel as shown in Fig.3.15 and Fig.3.13, undergoes towards the bottom deformations. The highest stresses to which the inner vessel is subject are focused in the knuckle radius area of the torispherical end. While the cylindrical part, of both inner and outer vessel, has low and constant stress and deformation values.

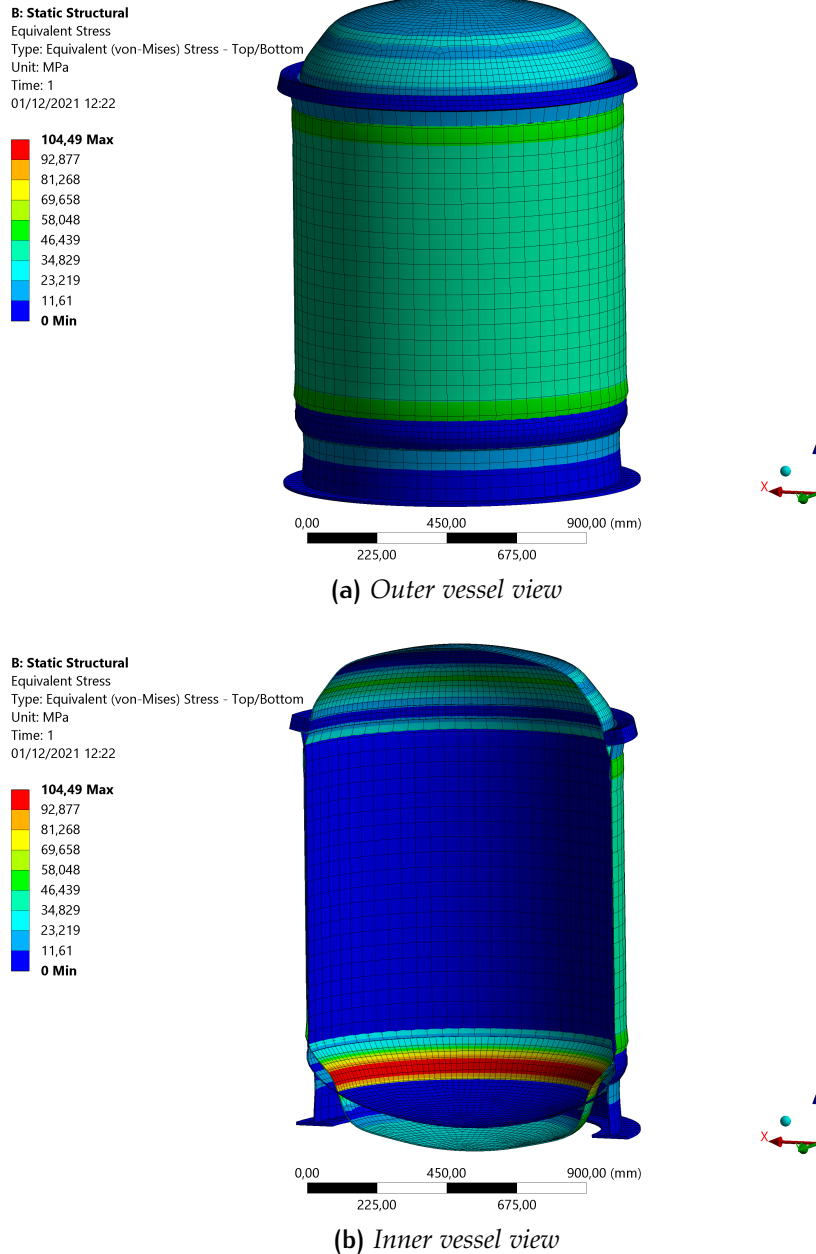
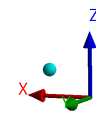
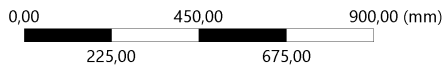
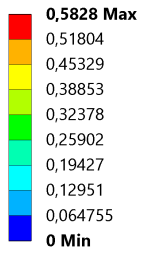


Figure 3.14: Equivalent stress solution

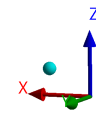
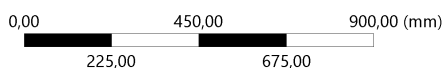
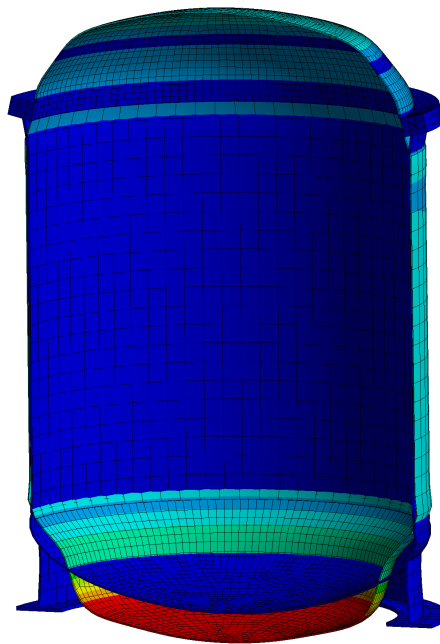
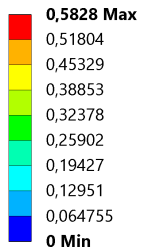
For a steady-state thermal analysis was added several thermal conditions at the cryostat. It was considered the state of the cryostat as if it was in operating conditions: The external temperature is the clean room temperature (set to 22°C); The inner vessel is completely filled during the operation phase so I set the T inside the cryostat to -196°C (LN<sub>2</sub> temperature) up to a height 30 cm from the flange, above the LN<sub>2</sub> level I set an ambient temperature due to the three circular plates inside the cryostat as thermal shields. As results, see Fig.3.16, the steady-state thermal solution shows a constant temperature of 22°C outside the cryostat and this should ensure a safe working condition during testing.

**B: Static Structural**  
 Total Deformation  
 Type: Total Deformation  
 Unit: mm  
 Time: 1  
 01/12/2021 12:23



(a) *Outer vessel view*

**B: Static Structural**  
 Total Deformation  
 Type: Total Deformation  
 Unit: mm  
 Time: 1  
 01/12/2021 12:23

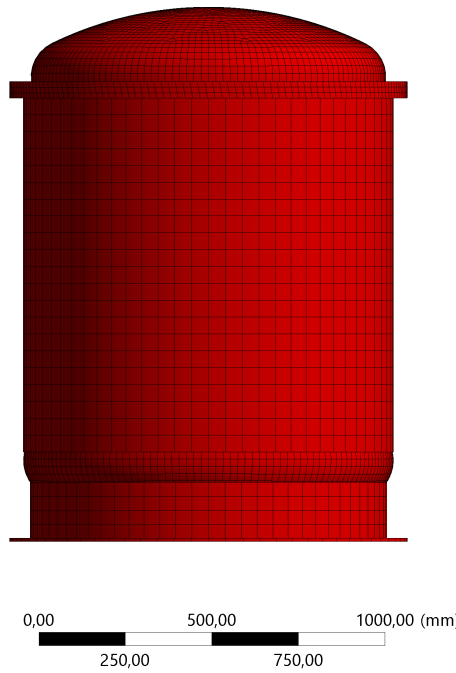
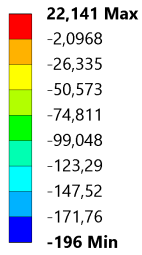


(b) *Inner vessel view*

Figure 3.15: Total deformation solution

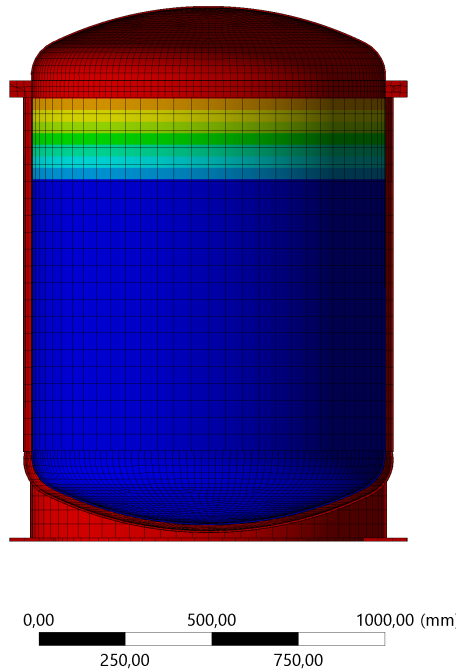
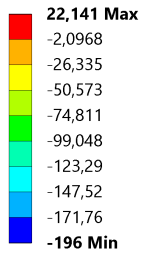
To the steady-state thermal settings are added the loads previously used giving a new solutions for stress and deformation, shown in Fig.3.17 & Fig.3.18.

**D: Steady-State Thermal**  
 Temperature  
 Type: Temperature  
 Unit: °C  
 Time: 1  
 01/12/2021 12:33



(a) Outer vessel view

**D: Steady-State Thermal**  
 Temperature  
 Type: Temperature  
 Unit: °C  
 Time: 1  
 01/12/2021 12:33



(b) Inner vessel view

Figure 3.16: Steady-state thermal solution

As we can see from the previous pictures (3.18) the main stressed and deformed zone is the bottom of the inner vessel, the outer vessel is subject to low deformations, in particular long z axis, due to the skirt.

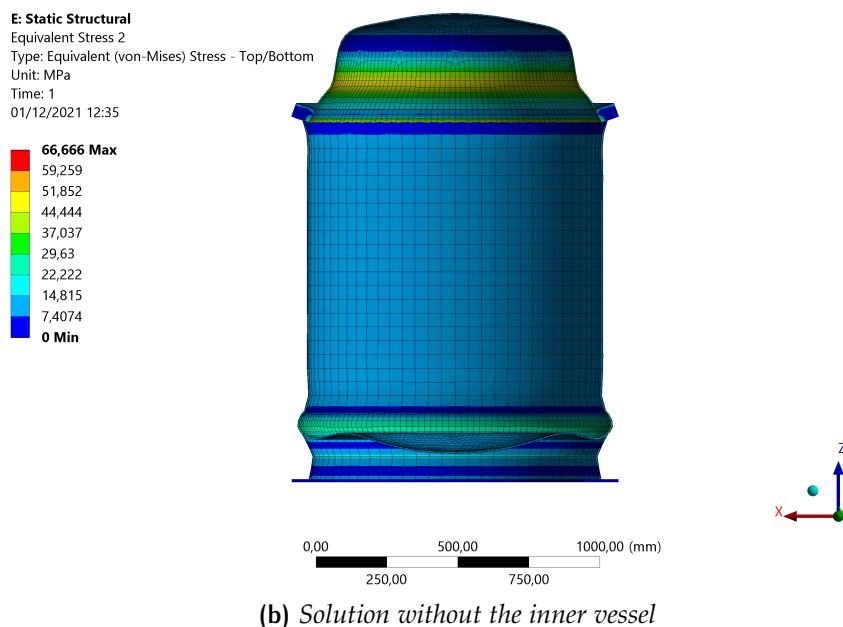
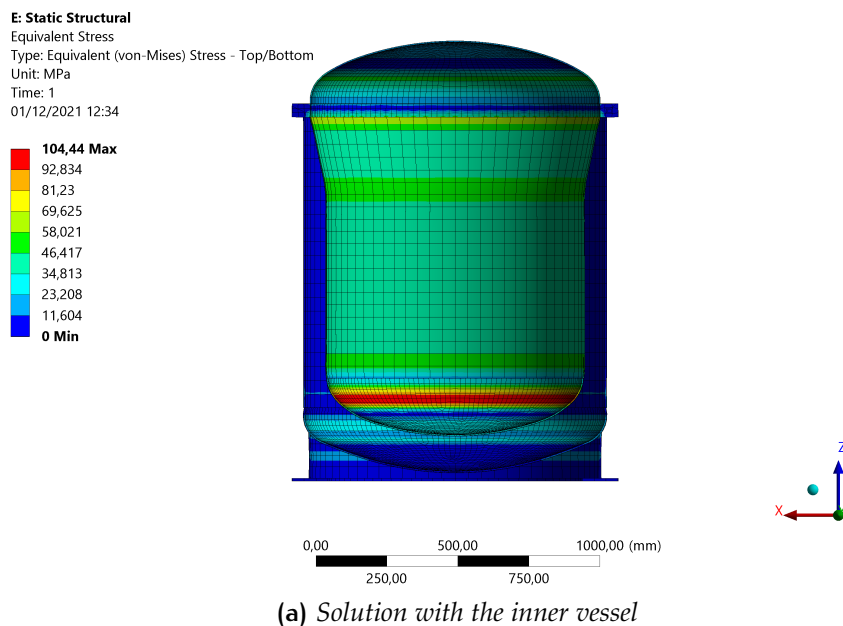


Figure 3.17: Equivalent stress solution

The final step was an Eigenvalue buckling test which is generally used to estimate the critical buckling loads of stiff structures. Stiff structures carry their design loads primarily by axial or membrane action, rather than by bending action. Their response usually involves very little deformation prior to buckling. However, even when the response of a structure is nonlinear before collapse, a general eigenvalue buckling analysis can provide useful estimates of collapse mode shapes.

A buckling, or stability, analysis is an eigenvalue-problem. The magnitude of the scalar eigenvalue is called the “buckling load factor”, BLF or load multiplier. The computed displacement eigen-vector is referred to as the “buckling mode” or mode shape. The buckling load factor (BLF) is an indicator of the fac-

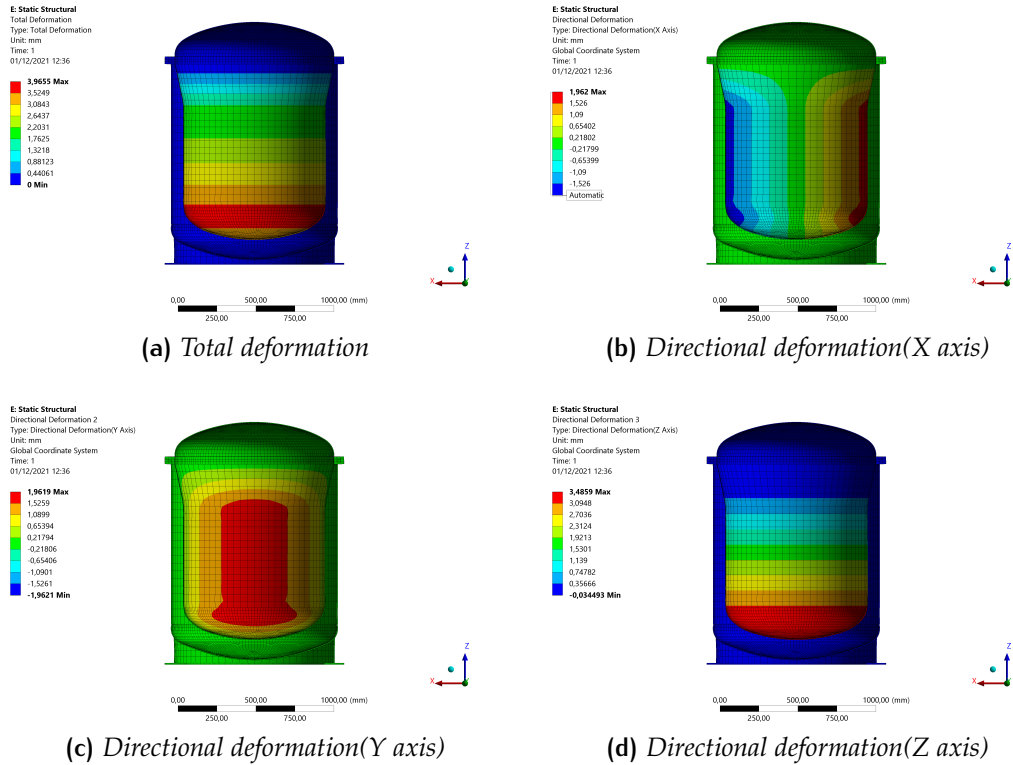


Figure 3.18: Deformation solution

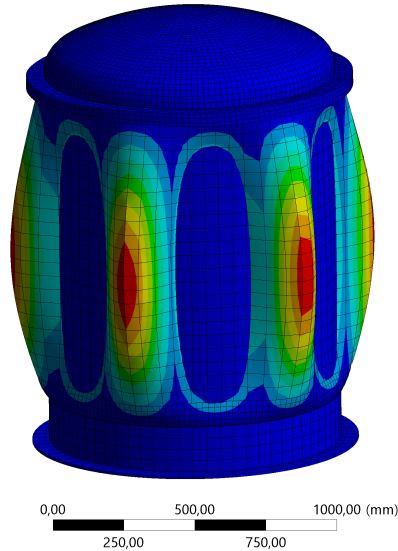
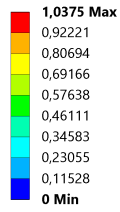
tor of safety against buckling or the ratio of the buckling loads to the currently applied loads. After setting the number of buckling modes to search for, in this case it was set 3 modes to find, ANSYS calculates the load multiplier for each mode (BLF). If you applied the real load in the Static Structural system, then the load multiplier is the factor of safety outer vessel stress with respect to that load.

The solution of the buckling analysis shows a load multiplier of at least 9 for each mode shape, see Tab.5, this means that the applied loads are less than the estimated critical loads. Buckling shape have similar deformations so was reported only one in Fig.3.19 and it can be seen how the outer vessel is the most unstable part of the cryostat.

Table 5: Load multiplier values

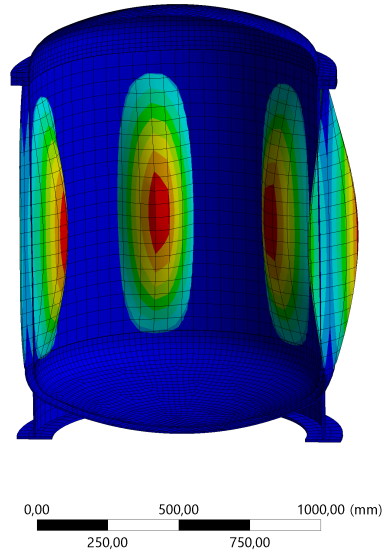
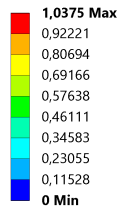
Mode shape	Load multiplier
1	9,1062
2	9,1087
3	9,7512

**F: Eigenvalue Buckling**  
 Total Deformation  
 Type: Total Deformation  
 Load Multiplier (Linear): 9,1062  
 Unit: mm  
 01/12/2021 12:38



(a) full cryostat

**F: Eigenvalue Buckling**  
 Total Deformation  
 Type: Total Deformation  
 Load Multiplier (Linear): 9,1062  
 Unit: mm  
 01/12/2021 12:38



(b) sectioned cryostat

Figure 3.19: Buckling analysis solution

# 4

## ASSEMBLY AND COMMISSIONING

After examining all aspects of the Test Facility, from design process to mechanical design, there was the assembly and commissioning of the system. In this chapter I'm going to describe single components, their functionality and how they were installed, describing all fittings showed in the facility.

There will be then describe how the Slow Control LabView based program has been implemented to automate the process and how it has affected manual steps by describing the commissioning steps. As a final step there will be a brief report about the preliminary tests carried out and a comparison with the design expectations.

### 4.1 ASSEMBLY WORK

This session is dedicated to the manual assembly of the Test Facility. I will describe each element of the assembly, chronologically, and I will analyze the type of connection between the various components. Starting from a first layout of the system, see Fig.4.1, we tried to place components respecting the space limits of the clean room.

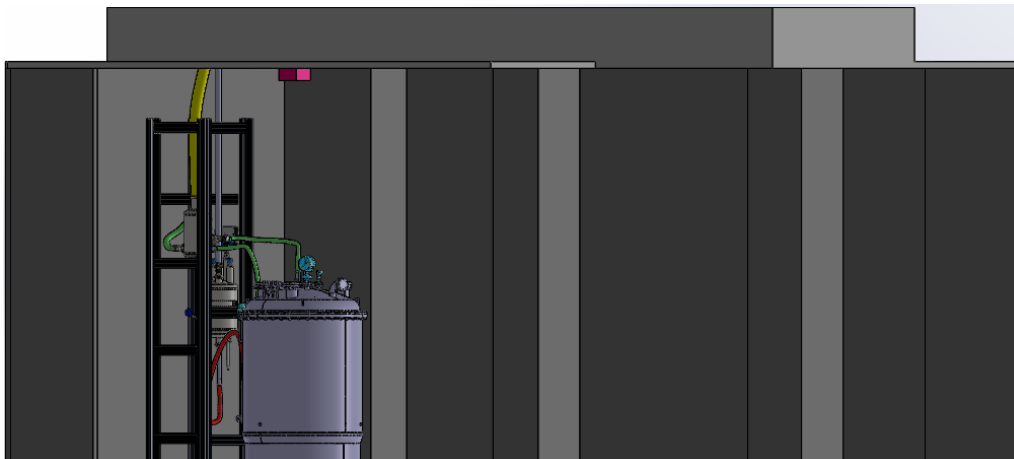
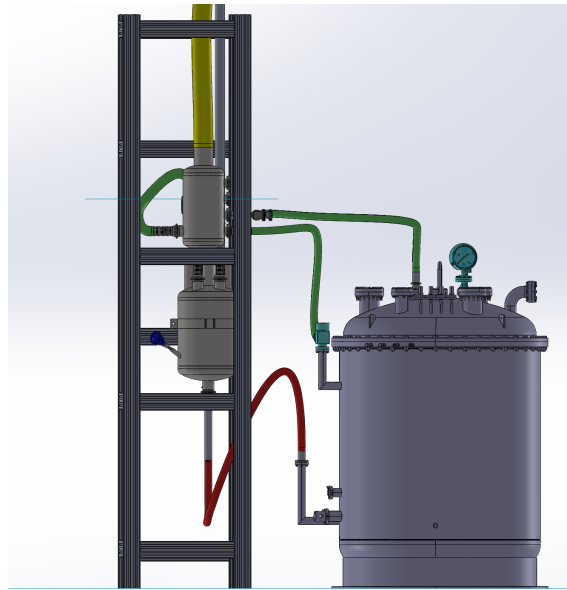


Figure 4.1: Test Facility's first 3D layout

It was important to place the Bosch profile structure and Demaco's cryostat, first. The profile structure (built around the the LN<sub>2</sub> line) is used as a support to contain several components of the facility and protect the LN transfer and gas vent lines.

In order to reduce the distance between the cryostat and the LN<sub>2</sub> feed line, the Demaco vessel should be positioned close to this tower structure. The link between the two is done by the 2.5 meter flexible vacuum insulated transfer line,

see Fig.4.2. Its positioning was constrained, as mentioned previously, also by electric hoist which can be used to lift the flange.



(a) 3D preliminary layout. red pipe: double-wall transfer line; yellow pipe:vent line; green lines: $N_2$  gas lines.



(b) Cryostat's assembly

Figure 4.2: Cryostat and profile tower layout

Then we moved to the cold box and manifold installation, fabricated by the Criotec, which were mounted by hooking them to the tower. The cold box is the first element linked to the outdoor system, it is connected on the top with the bayonet coupling to the  $LN_2$  double-wall line coming from the outside thanks to a KF50 fitting.

ISO-KF is a quick release flange used in vacuum systems. It consists of two symmetrically distributed KF flanges, one O-Ring and centering brackets inside clamps. No additional tool is needed, but simply unscrew the flat nut by hand to loosen or press the connection. The ISO-KF vacuum fittings exist of the following nominal diameter sizes include DN 10, 16, 25, 40, 50. The flange material is usually 304, 316 stainless steel, etc. ISO-KF vacuum joints are usually made of flange, clamp, o-ring and centering ring, as shown in Fig.4.3.

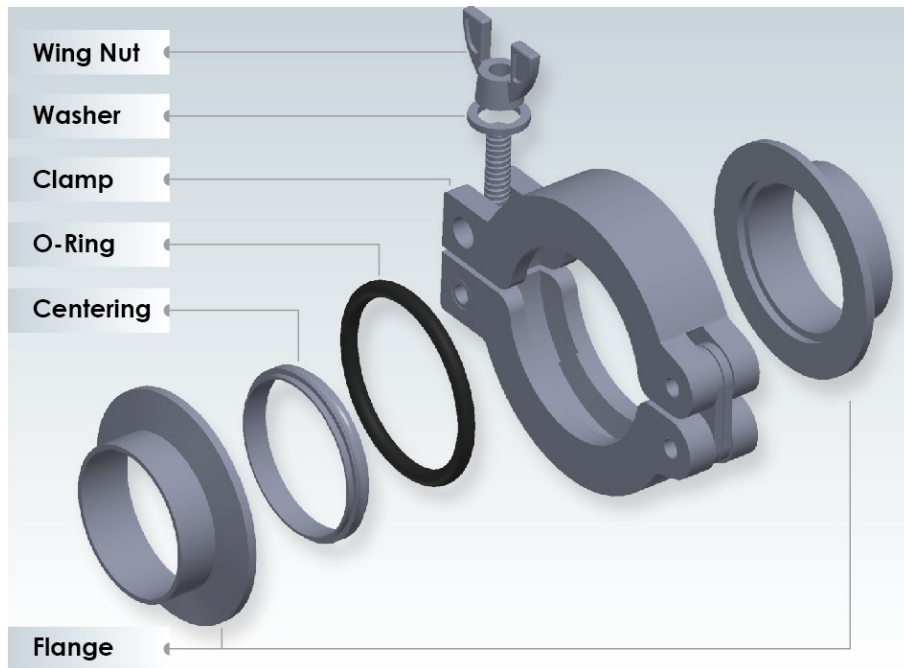
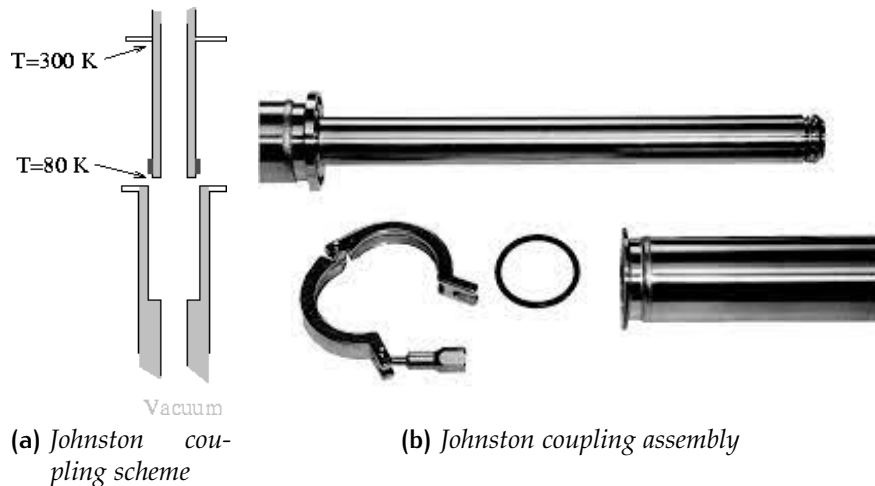


Figure 4.3: KF flange connection mode

An additional single wall flexible line link the cold box on the top with the vent manifold, this connection is also done with KF type of flange (KF50). The LN<sub>2</sub> feed line exit the cold box on the bottom in the form of male bayonet. This element belongs to very diffuse type of cryogenic connections, namely Johnston coupling (red line in Fig.4.2 pic. "a").

Johnston coupling is a very easy and very reliable coupling, shown in Fig.4.4.



(a) Johnston coupling scheme

(b) Johnston coupling assembly

Figure 4.4: Johnston coupling

The pipes are installed by sliding the male part of one pipe into the corresponding female part of the next line. The couplings are sealed and secured with KF flanges with an O-ring and a hinged clamp or bolted flanges. There is no welding necessary between pipes. In this case the flexible double-wall line has one female fitting, linked to the male fitting of the cold box, and a male one, inserted in the female connection of the cryostat via CF40 fitting. The female part

of the flexible transfer line connected to the cold box from its bottom then continues and ends with another male bayonet welded to the CF40 flange in order to fit the Demaco LN<sub>2</sub> inlet port (see fig. 4.5). The Fig.4.5 shows the double-wall hose and its connections with cryostat and coldbox. The CF flange (originally



(a) Johnstone coupling on the coldbox's bottom (b) CF40 for male transfer line's connection

Figure 4.5: Double-wall transfer line between coldbox & cryostat

called ConFlat) is a type of connection where both flanges are identical. Typical flange materials are austenitic stainless steel types 304L, 316L, 316LN. The seal mechanism is a knife-edge that is machined below the flange's flat surface. As the bolts of a flange-pair are tightened, the knife-edges make annular grooves on each side of a soft metal gasket. The extruded metal fills all the machining marks and surface defects in the flange, yielding a leak-tight seal, see Fig.4.6. The CF seal operates from 1013 mbar to  $1.3 \times 10^{-13}$  mbar, and within the temperature range  $-196^\circ \text{C}$  to  $450^\circ \text{C}$  (depending on material). The gasket material sealing two flanges determines the joint's maximum temperature and, to an extent, the base pressure of the vacuum volume. Metal gaskets are impermeable to gases and withstand moderately high temperatures indefinitely. The normal gaskets for stainless steel CF flanges are punched from  $\frac{1}{4}$  hard, high purity, oxygen-free (OFHC) copper stock.

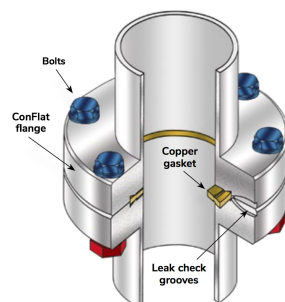


Figure 4.6: CoFlat flange assembly

As explained in section 2, the manifold has 4 input lines and 1 vent line. 3 input lines, we will see them later, come from the cryostat and one comes from the coldbox. The big vent line is a plastic pipe 10 cm diameter, attached with a metal cable ties, that brings the gas  $N_2$  out of the clean room by discharging it to the ambient, see Fig.4.7.



Figure 4.7: Plastic line to the vent

As concerns the internal structure's installation, the PDUs holding structure has not yet been mounted but we have provided a temporary structure designed to host 2 PDUs for the first tests. This simple structure consists of two aluminum plates. The top one serves to hold the PDUs, while the bottom one is used as the illumination plat that provide the fibers connectors fixed to the plate and illuminate the PDUs above, are currently installed on 4 threaded bars, see Fig.4.8.



Figure 4.8: Actual inner structure

After having placed the cryostat we proceed with the installation of the following equipment on the top flange, shown in Fig.4.9:

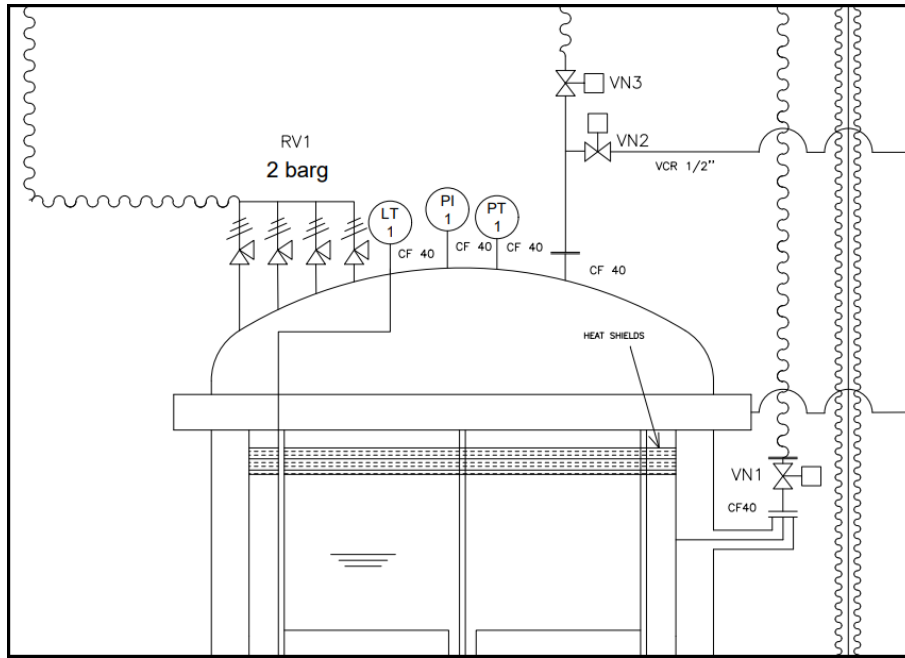


Figure 4.9: Fittings on the upper flange

- 1 CF40 fitting for the relative Pressure Indicator (PI1) and 1 CF40 fitting for the absolute Pressure Transducer (PT1):

PT1 and PI1 were installed to monitor pressure inside the cryostat, one is accessible through LabView program and the other allow the direct local monitoring of the relative pressure inside the cryostat, they are shown in Fig.4.10.



Figure 4.10: Pressure indicator (PI1) on the left; pressure transducer (PT1) on the right.

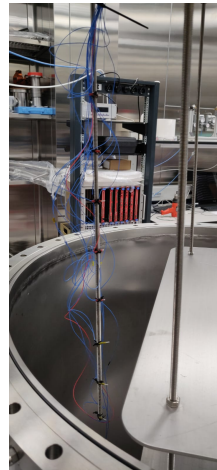
- 1 CF40 fitting for the Level Transducer (LT1):

The Level Transducer lets us to determine the LN<sub>2</sub> level position inside the vessel thanks to the nine PT100 thermal-resistor sensors used. The level sensor is composed of nine PT100 sensors mounted on the 1 m threaded

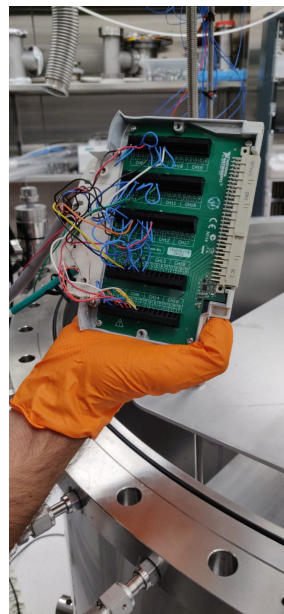
rod connected to the top flange. All sensors are then read out by the dedicated NI board of the PXI system. Inside the vessel PT100s were placed along a threaded bar at different heights as shown in Fig.4.11 "a & b". The very first sensor (PT100 n.9 in Fig.2.21 of Chapter 2) is located on the bottom of the vessel and therefore show the moment when the LN start to get in, after a 20 cm distance, I placed PT100s every 10 cm until "level 1". I place the first PT100 at 40 cm far from the top flange.



(a) First PT100 placement



(b) 9 PT100s placement



(c) PT100s installation inside the motherboard



(d) PXI of NI

Figure 4.11: PT100 installation

- 1 CF40 fitting for the connection between vessel, manifold and the pressure reducers panel and for the nitrogen gas intake:

Another element of the top flange assembly allow to maintain constant the pressure inside the cryostat and give the possibility to create the pressure

during the draining phase. This assembly is composed of two Swagelok manual valves with VCR fittings mounted on the CF40 flange see Fig.4.12.



Figure 4.12: 3-way fitting with two manual valves VN2 & VN3

This type fitting was provided by Swagelok, a company which supports industrial companies building and operating small bore fluid system providing necessary components. Swagelok's VCR fitting offer the high purity of a metal-to-metal seal, providing leak-tight service from vacuum to positive pressure. The seal on a VCR assembly is made when the gasket is compressed by two beads during the engagement of a male nut or body hex and a female nut, see Fig.4.13.

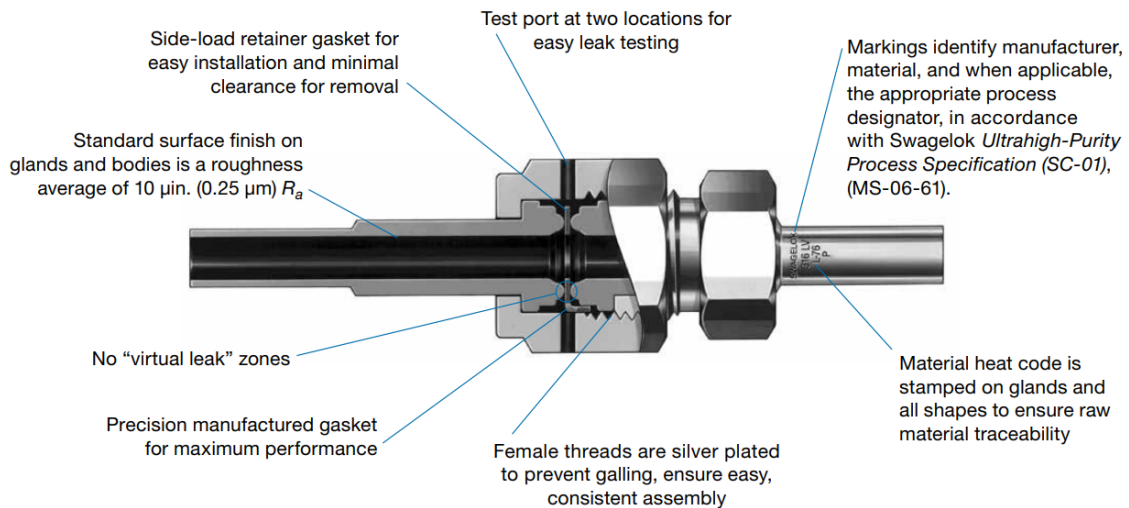


Figure 4.13: Swagelok's VCR fitting

The two lines are decoupled thanks to 2 Swagelok manual valves. One line is connected via CF40 and a flexible metal line to the manifold. This line before reaching the manifold is intercepted by a relief valve (globe valve RV02) used to set the pressure inside cryostat, see Fig.4.14. The other line is linked to pressure reducers panel through by Rilsan's thermoplastic pipe and serves to pressurise the cryostat during draining.

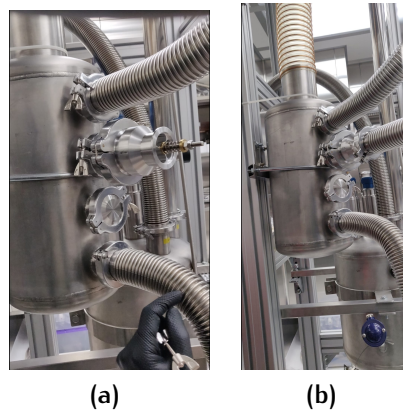


Figure 4.14: Relief valve RV2

- 1 CF100 fitting for the feedthroughs intake inside the vessel and 1 CF40 fitting for optical fibers that will illuminate the PDMs during the test.



Figure 4.15: CF40 for optical fibers

- 1 KF40 fitting between the safety valves and the manifold:

The four safety devices outputs, present on the Demaco cryostat top flange, are grouped together. This output then get connected by the flexible metal line to the main vent collector for exhaust, see Fig.4.16.



Figure 4.16: KF40 metal hose from 4 safety valves

- 1 CF40 where an angular metal manual valve is placed (VN1):

The last connection between the cryostat and the vent manifold allow to remove the cold gas from the cryostat during the filling phase. This is a CF40 flange based connection that includes all metal valve and the KF40 flexible metal line, see Fig.4.17.



Figure 4.17: Manual angle valve VN1

## 4.2 SLOW CONTROL SYSTEM

To make the Test facility processes automated is of the up most importance. The process must be able to work for long periods and to be controlled remotely, it must be able to work outside working hours. For this reason the Test Facility is controlled by the NI PXIe-8861 based Slow Control system.

During this autumn the Naples Test Facility has hosted several scientists from all over the world to work on the tests, they must be able to work comfortably and safely on the system and this is possible thanks to the Slow Control System.

Let's see in detail the steps to start the test and electronic components controlled by Slow Control, in the Table 6 :

Table 6: Facility's electronic components

P&ID Name	Component	Brand	Model	Placement
EV01 – 3	Solenoid-valve	Emerson, Asco	Solenoid Valve: SCE222F003	outdoor, Linde Supply Tank N <sub>2</sub>
EV21	Solenoid-valve	Emerson, Asco	Solenoid Valve: SCE222F003	outdoor, bottle's room
PT1	Pressure transducer	WIKA	S20	vessel's flange, clean room
LT1	Level transducer	PT100x9	DC-LS-50	vessel's flange, clean room
VC1	Proportional manual valve	Criotech	-	cold box, clean room

### *Pre setting and checking operations*

It is necessary to carry out several pre setting and checking operations in order to operate under ideal conditions. The following steps are planned:

- Check the sensors correct operation: LT1, PT1, PI1, VC1.
- Check insulation vacuum values in the cryostat: Vacuum Pumping station.
- Closed cryostat: flushing with N<sub>2</sub> to reduce moisture or perform 3 cycles of Pump cycles (down to 10<sup>-2</sup> mbar) & Purge (with N<sub>2</sub>).

### *Filling Phase*

Once pre setting operations are done it is possible to start filling the cryostat. In order to fill the cryostat, the V22 valve (LN supply tank) will be opened manually, while the EV03 solenoid-valve (see Fig.4.18), and the VC1 proportional valve (cold box) will be controlled by LabView. Finally, the VN1 all metal valve must



Figure 4.18: Solenoid-valve EV03

be gradually and manually opened in order to release the cold  $N_2$  gas from the cryostat and avoid the pressurization of the vessel in the process of filling.

The proportional valve (VC1), shown in Fig.4.19, is opened after the VS1 (the first manual valve of the cold box). So first the valves outside are opened, then VS1 on the cold box, then VN1 (to discharge the gas from the cryostat), and then the VC1 is gradually opened to bring it to 50% – 60% opening.



Figure 4.19: Proportional valve VC1 linked to the PXIe and controlled by Slow Control

It is necessary avoid pressure increases, controlling the VN1 and monitoring pressure sensor (PT1) value through the Slow Control system. First of all manual valve VS1 on the coldbox must be opened to supply  $LN_2$ . The other vent line, connected to the manifold too, remains insulated by keeping the manual valve VN3 closed.

In order to start the actual fill phase it is necessary to act on the coldbox as follows:

- open EV03 and V22 outside the clean room
- open VS1
- open VN1 to discharge the N<sub>2</sub> outside the cryostat
- gradually open VC1

The aims during filling operation are to reach the first PT100's level (40 cm far from the upper flange) and to maintain pressure set to atmospheric pressure, these can be resumed by the following Tab.7.

Table 7: Set point values

Point to check	Set point valure
PT1	1 bar
TT1	77 K

### *Testing phase*

First steps to do during this phase are:

- close VN1
- open VN3

In the future the test phase the proportional valve VC1 on the cold box will suppose to read the LT1 signal, in particular, should be checked the TT1 value by LabView program (check if is  $> 77$  K), in order to keep the LN level well above the PDUs (all PDUs covered by LN<sub>2</sub>). At the same time, the RV2, placed on one of the vent line to the manifold, guarantees a pressure inside the cryostat not exceeding 1,2 bar. If necessary, it can be possible to act on the proportional valve VC1 to refill if the level of liquid nitrogen is not stable, normally in this phase the VC1 has an opening degree of 0%.

### *Emptying phase*

In this phase as first steps:

- close VN3
- open VN2 introducing N<sub>2</sub> gas from PRs panel to increase pressure inside the cryostat up to 3 bar



Figure 4.20: Electro-valve EV02 and the vent

- open completely VS1 and VC1 to let the LN<sub>2</sub> flow back through the bi-directional double wall transfer line
- open EV02, shown in Fig.4.20, to let N<sub>2</sub> reaches the vent

The liquid will flow back through the bidirectional transfer line and thanks to the non-return valve NVR02 it will pass through the evaporator VA02 until it reaches the vent. Fig.4.21 shows the flow diagram of the control loops during phases.

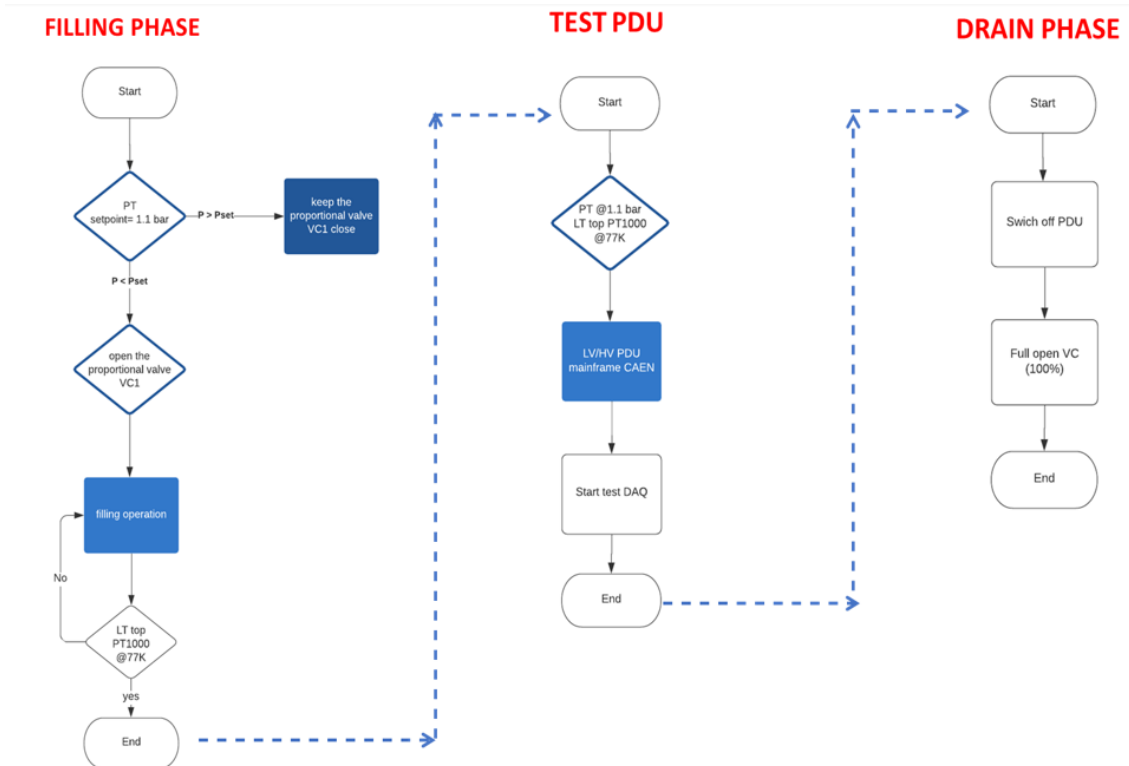


Figure 4.21: Control loop

Fig.4.22 shows the program's interface which has been done with LabView. The program allows us to read the PT100s temperature and pressure inside the cryostat at the same time. On the left of the front panel an acquisition rate can

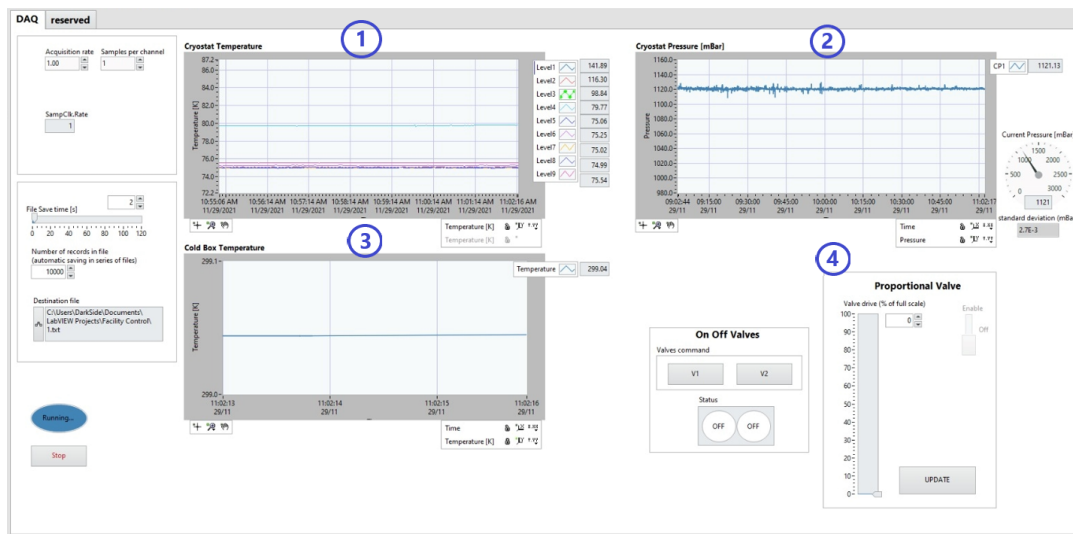
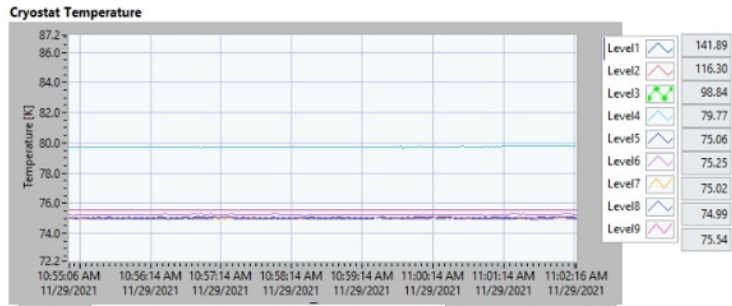


Figure 4.22: LabView's interface

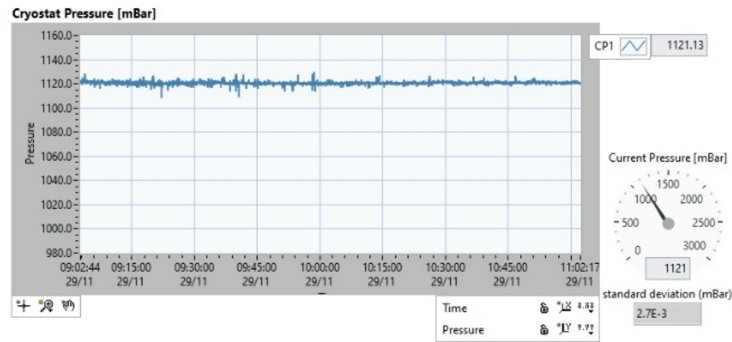
be set as well as the number of files saved for a range of seconds. There is a section to indicate the name and location of the saved data file. Looking closer at this interface example, Fig.4.23 pic *a* shows a temperature-time graph which plots the 9 PT100 trend. In this case 5 PT100 (from level 9 to 5) are stably below the nitrogen liquid (a temperature of 75 K is read), level 4 having a T of 79 K, so it is close to reaching the liquid, then levels from 3 to 1 are out of scale, we can change the visible temperature range on the chart.

Fig.4.23 pic. *b* shows instead the course of the read pressure transducer PT1, in figure it has a stable course to 1120 mbar which means that it isn't in emptying or filling phase. In the last graph, Fig.4.23 pic. *c*, there is another PT100 supplied with connection head located in the cold box that let to read its temperature in order to free the cold box from the excess cold gas opening VS2.

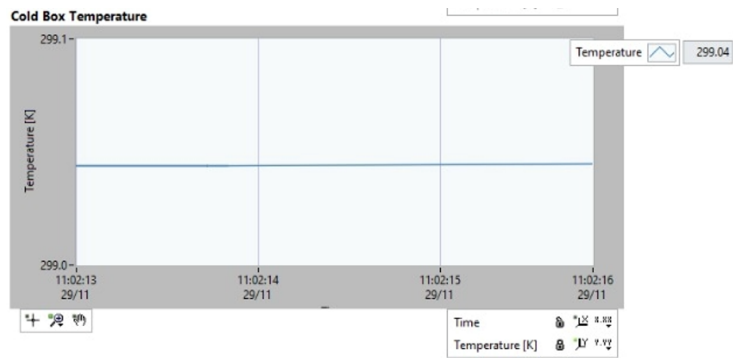
Pic. *d* of Fig.4.23 shows the front panel dedicated to the facility valves control. On the left there is the simple on/off of the EV01 and EV02 solenoid valves, respectively used for the low pressure  $N_2$  gas inlet and for the vent line. On the right there is the panel for the gradual opening of the proportional valve VC1, in the example it is closed because no refill of the cryostat is coming.



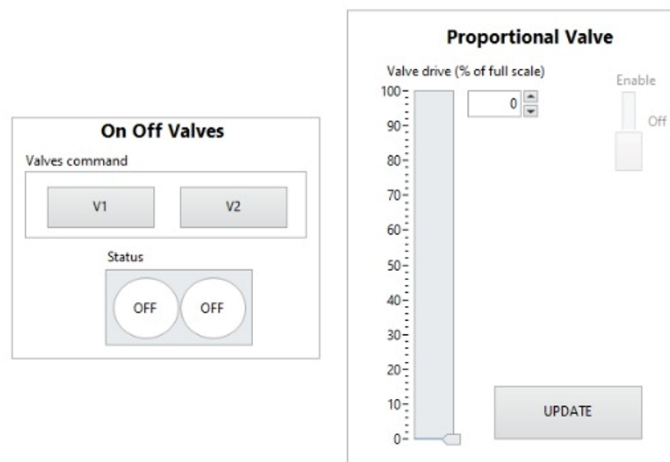
(a) PT100 Temperature chart



(b) Pressure Transducer PT1 chart



(c) PT100 cold box Temperature chart



(d) Valves front panel

Figure 4.23: Proportional valve VC1 linked to the PXIe and controlled by Slow Control

In Fig.4.24, instead, there is the Labview control station that turns out to be very close to the Test Facility system which makes it easy to switch between manual actions and remote work. However, the control station is used by the staff inside the clean room but it is also accessible by PC authorized outside the laboratory so that it can be possible to act on the system even outside working hours.



Figure 4.24: Slow control station

### 4.3 TEST FACILITY'S TESTS

After assembly phase and the pre setting of the system and slow control's realization me and team have run the Test Facility and started the first tests. In this section I will give a brief description of the tests that was carried out and results obtained, comparing them to the design expectations and objectives set.

#### *First test*

The first test was carried out in August, after checking states of the involved valves the filling started by opening EV03 and VC1 as scheduled. Having the proportional valve fully opened VS1, manual valve on the coldbox, was gradually opened to make the fluid flow slowly inside cryostat and at the same time VN1 was opened not to raise the pressure of the cryostat.

The layout of PT100s was slightly different from the current one, the PT100 on the bottom was 50 cm from the next PT100. Once the liquid has finally reached the first sensor (exactly 12 minutes from the test's start) it took 52 min to reach the second. So was estimated a filling rate of almost  $1 \frac{\text{cm}}{\text{min}}$ . During the filling phase the manifold, vent line and the hose following the VN1 were frozen, see Fig.4.25.

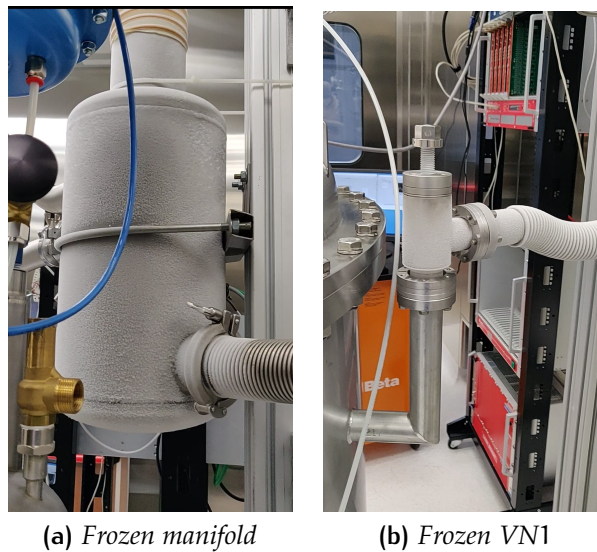


Figure 4.25: Proportional valve VC1 linked to the PXIe and controlled by Slow Control

LN<sub>2</sub> level reached the last PT100 after 1 hour and 35 min, filling speed met design expectations. The drain procedure starts opening the manual valve close to the vent and completely open VS1 in order to let the LN<sub>2</sub> flow back easily. Then I closed VN3 and operated on VN2 flowing N<sub>2</sub> gas from PRs panel to increase the pressure. The pressure of the cryostat rose up to 2,7 bar (near the maximum allowed by the safety valves 3 bar). Draining the cryostat completely it was found that at the maximum emptying speed under pressure the drain phase takes about 7 hours, with an average rate of  $0,2 \frac{\text{cm}}{\text{min}}$ .

### Following tests

The goal of subsequent tests was to evaluate an evaporation rate obtained from a no-pushed drain phase, therefore without the use of N<sub>2</sub> to increase the pressure. Alternative solutions have been adopted compared to previous test, such as the use of a heating cable to be placed on the line next to VN1, to prevent its and manifold icing, see Fig.4.26.

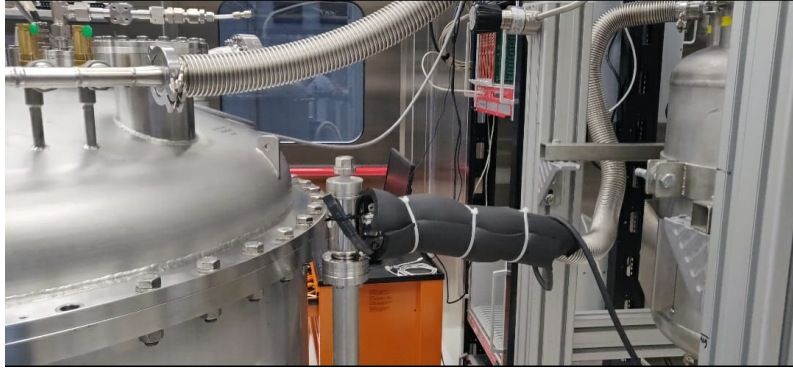


Figure 4.26: Heating cable

During one of the drain tests was left the cryostat inactive, without operating on any component, to look for the natural evaporation rate of the system. LN<sub>2</sub> level took 3254 minutes to evaporate from one PT100 to another (I read from data log when the 2 PT100 reached a temperature much higher than 77 K to understand when they were outside of liquid fluid) and knowing the distance between sensors we estimated an evaporation rate of  $0,004 \frac{\text{cm}}{\text{min}}$ .

The main requirement of the Test Facility is to work continuously and independently. During the tests, PDUs have to be totally submerged by liquid nitrogen. The facility has to operate for a long period (weeks) and has to keep operational condition even during periods when no one has access to the clean room. The most common problem that could happen working with cryogenic fluids is the fluid's evaporation. In this case the fluid's evaporation would result in PDUs spill from LN<sub>2</sub>, compromising the test. This is the reason why it was necessary estimate an evaporation rate, firstly in theory and then through the tests creating a comparison between the results. Theoretically this rate was calculated by carrying out a thermodynamic analysis of the system. Is it possible to make some thermodynamic hypotheses based on Dewar flask theory. The vacuum flask consists of two vessels, see Fig.4.27, one placed within the other and joined at the neck. The gap between the two vessels is partially evacuated of air, creating a partial-vacuum which reduces heat conduction or convection. Heat transfer by thermal radiation may be minimized by silvering flask surfaces. Most heat transfer occurs through the neck and opening of the flask, where there is no vacuum, in this case through the top dome. As first hypothesis It was assumed that there aren't significant heat exchanges between lateral cylindrical wall of the cryostat and the fluid, as it is a double-walled vessel with vacuum insulation in the cavity, see Fig.4.27. LN<sub>2</sub> evaporates due to the heat provided by the overlying gas layer, in particular through convective and diffusive heat exchange. The N<sub>2</sub> layer

instead receives heat by radiation, convection and conduction from the upper dome which has single-wall and unable to thermally insulate the upper part of the vessel.

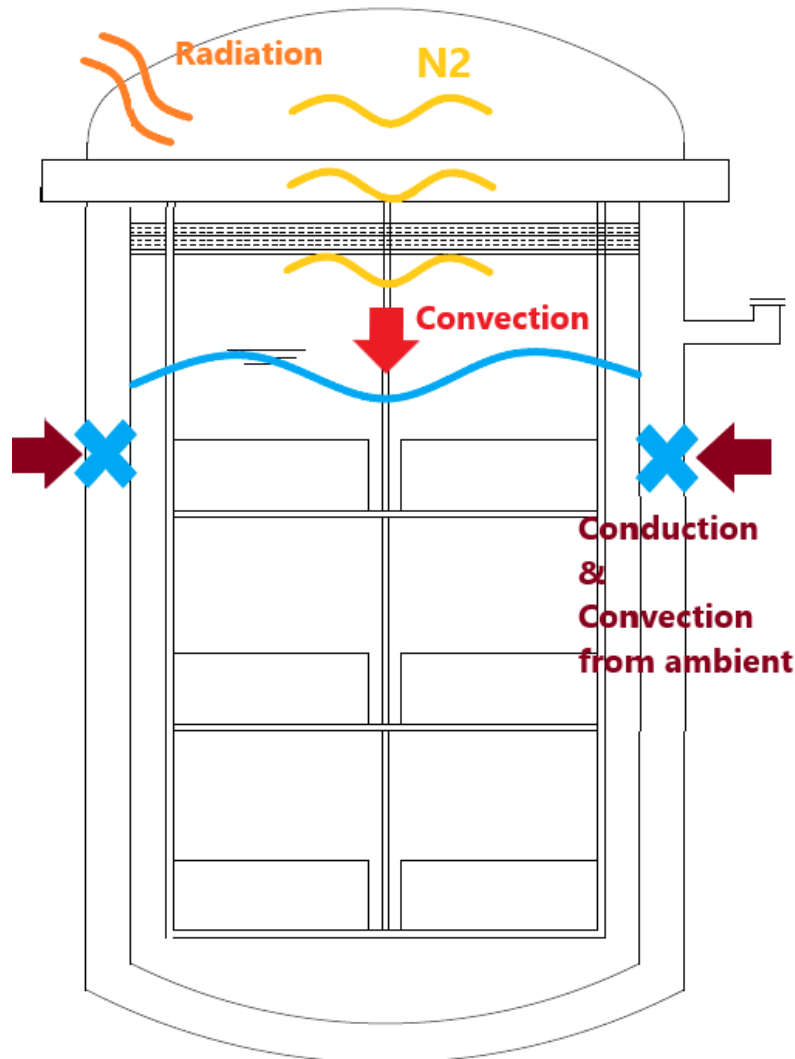


Figure 4.27: LN<sub>2</sub> and N<sub>2</sub> heat exchanges

As a result of this theoretical assessment, an amount of liquid evaporated in  $\frac{\text{cm}}{\text{min}}$  was evaluated. The evaporation rate that was estimated is  $0.0039 \frac{\text{cm}}{\text{min}}$ , very close to that obtained from the reported tests. The results seem to be comparable with the theoretically estimated calculations. The tests were carried out without placing the 3 heat shields which should further reduce the evaporation rate. The 3 heat-shields at the upper flange's height serve as thermal insulation because the upper part of the cryostat is single-walled (the dome) and more exposed to heat exchange, they will be installed in the cryostat for the future test.

After first test I reconfigured the layout of the sensors, arriving at 9 sensors (first layout mentioned), before arrival of several researchers of the DS collaboration. Once the system operation has been established the following tests were intended to test the first motherboards. Researchers who arrived at the INFN's laboratory are experts in reading data, especially data related to electrical signals sent by the PDU. The data is collected and plotted on the MIDAS software.

MIDAS is also able to collect PT100 data directly from the PXIe computer, see examples in the following figures. Fig.4.28 shows as on 22 October there was a complete filling of the cryostat, easily guessed from graphs, the 9 curves related to the 9 PT100 have a constant decrease until reaching 77 K. The data collected on 27 October show a drain procedure under pressure, in fact on the same lines (brown) in Fig4.29 and Fig4.30 there is respectively an increase of cryostat's pressure up to 2287 mbar and a gradual increase of PT100's temperatures. The data

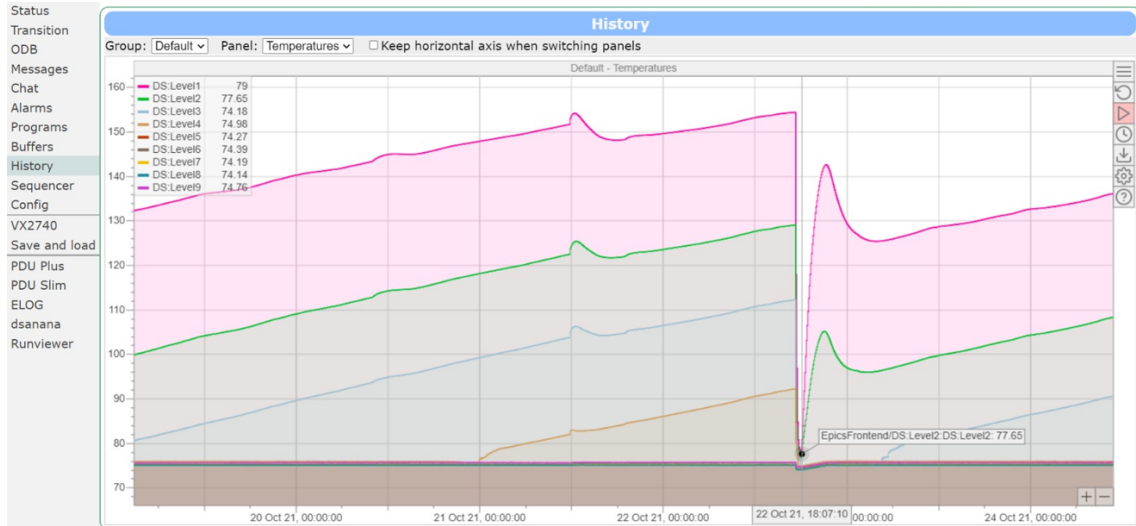


Figure 4.28: MIDAS's interface, data handling 22 October

collected on 27 October show a drain procedure under pressure, in fact on the same range of time (from 12 am to 8 pm on 27 October and from 10 : 40 am to 7 pm on 28 October) in Fig4.29 and Fig4.30 there is respectively an increase of cryostat's pressure up to 2287 mbar and a gradual increase of PT100's temperatures.

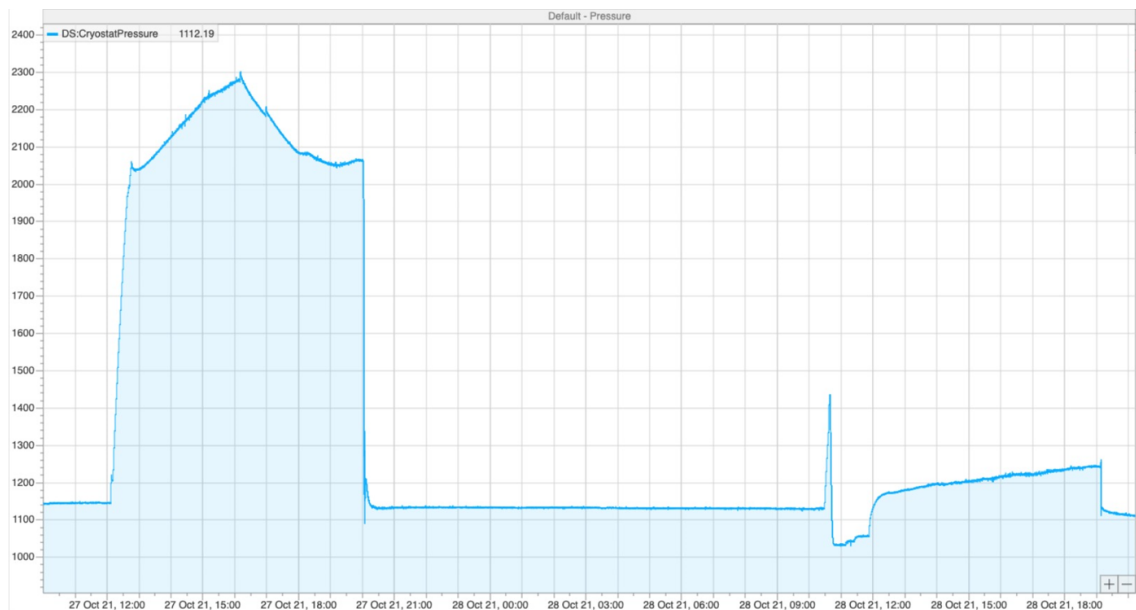


Figure 4.29: Pressure's trend, data handling 27 October

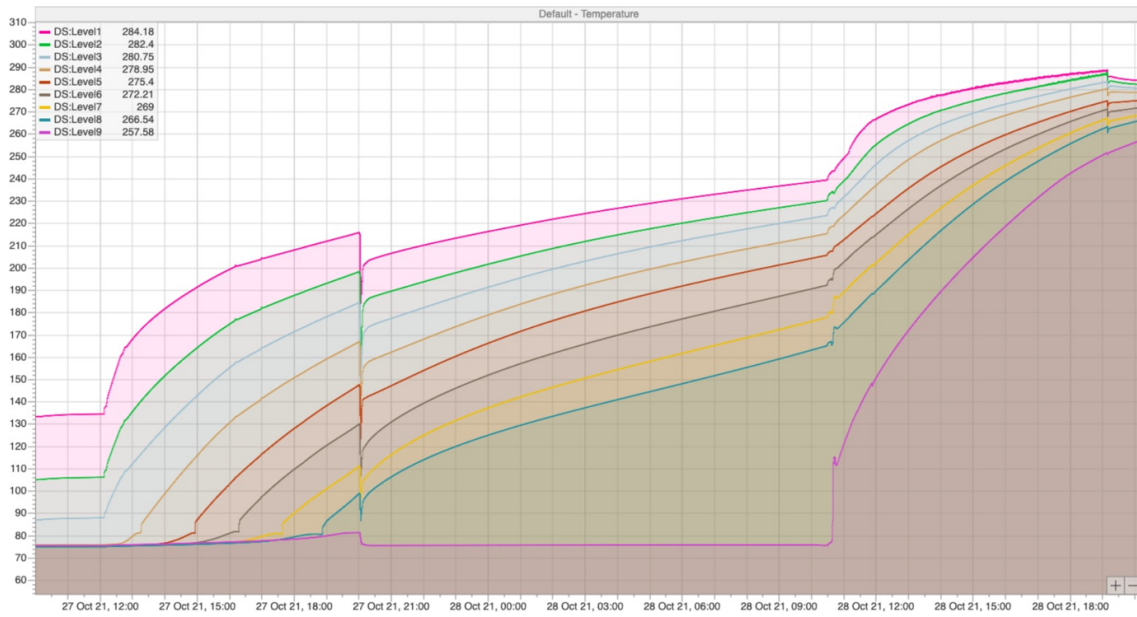


Figure 4.30: Temperature's trend, data handling 27 October

## CONCLUSION

All pre and post-production steps of the test facility have been reported in this thesis. The system is currently connected and functioning inside the clean room in the Physics department of Federico II, as shown.

The PDU Test Facility is active since mid of September 2021 and was used to test the other two versions of the PDUs: the PDU Plus (arrived to Naples on September 28th and was tested in LN<sub>2</sub> for 20 days) and the PDU slim (arrived to Naples on October 10th, and since 19th of October is under testing in LN<sub>2</sub>).

Naples Test Facility reliability has been amply demonstrated and the design objectives have been accomplished: its evaporation rate, theoretically and practically evaluated during the tests. Thanks to the first tests carried out were calculated:

- Filling speed:  $1 \frac{\text{cm}}{\text{min}}$
- Pressure emptying speed:  $0,2 \frac{\text{cm}}{\text{min}}$
- Evaporation rate:  $0,004 \frac{\text{cm}}{\text{min}}$

important data to better manage future PDU tests. The evaporation rate is sufficiently low ensuring that the PDU remain below the level of liquid nitrogen for long periods, about 2 days. The goal has been reached as this rate is in line with the design expectations. In the future, however, the 3 heat Shields will be mounted to further reduce the rate of evaporation.

The Slow Control system through LabView guarantees the use and control of the system remotely, its interface is easily manageable by all actual staff and by the staff of the DarkSide collaboration that will work in the clean room in the future.

Currently Test Facility needs only small improvements to the mechanical structure that supports the PDU, in the near future the 3-levels structure will be mounted as it was designed, so that it will support 12 PDU during a single test. With these goals achieved and continuous improvements to the slow control system, the Test Facility will finally enter its final phase of testing, the facility will be able to test a large number of PDU continuously so as to ensure their use in the experiment Darkside-20k.

## BIBLIOGRAPHY

- [1] DarkSide Collaboration, *DarkSide-20k Design Report*, April 2021, TDR 2021 DarkSide project.
- [2] J.G. Weisend II, *Cryostat Design*, Case Studies, Principles and Engineering Editors 2016.
- [3] Regulation (EU) No 652/2014 of the European Parliament and of the Council of 15 May 2014, Official Journal of the European Union 27 June 2014.
- [4] Quick Reference Guide Intertek, *Six Steps to Determine the Category and Modules of Pressure Equipment*, Pressure Equipment Directive 97/23/EC.
- [5] European standard EN 13445 – 1 : 2014 (version 1 : 2014 – 09), *Unfired pressure vessels — Part 1: General*.
- [6] European standard EN 13445 – 2 : 2014 (version 1 : 2014 – 09), *Unfired pressure vessels — Part 2: Materials*.
- [7] European standard EN 13445 – 3 : 2014 (version 1 : 2014 – 09), *Unfired pressure vessels — Part 3: Design*.
- [8] European standard EN 13445 – 5 : 2014 (version 1 : 2014 – 09), *Unfired pressure vessels — Part 5: Inspection and testing*.
- [9] Joe Woodward, *Eigenvalue Buckling and Post-buckling Analysis in ANSYS Mechanical*, September 10, 2018.
- [10] DarkSide Collaboration, *DarkSide-20k Design Report*, April 2021, TDR 2021v. 2.5 DarkSide project.
- [11] ASSOGASTECNICI, *Progettazione, installazione, collaudo e gestione di sale criobiologiche*, Edizione 215 September 2015.
- [12] Bernhard Schwingenheuer MPI Heidelberg, *Cryogenic Infrastructure*, Ringberg castle, 11 Febr 07.
- [13] IKS Technology, *Specifiche e differenza di tre flange di vuoto comuni (CF, KF, ISO)*, 8 June 2018.
- [14] BNL/MERIT Magnet Analysis Repor, *Vacuum Jacket Design*, Page 11.0 – 11.
- [15] B. Baudouy, *Heat Transfer and Cooling Techniques at Low Temperature*, CEA Saclay, France.
- [16] Prof. Stefano Lanzini, *Recipiente in pressione*, International Conference on Esercitazione II.

- [17] *Pressure Equipment Directive (PED) - Conformity Assessment*, <https://www.intertek.com/technical-inspection/pressure-equipment-assemblies/>
- [18] *Swagelok VCR Fittings and VCO Fittings Explained*, <https://edmontonvalve.swagelok.com/blog/bid/325525/the-advantages-of-swagelok-vcr-and-vco-fittings>
- [19] *PRODUCT SHEET JOHNSTON COUPLING*, [https://demaco-cryogenics.com/wp-content/uploads/2021/01/EN-Johnston-Coupling-2\\_hq-02-2018-1.pdf](https://demaco-cryogenics.com/wp-content/uploads/2021/01/EN-Johnston-Coupling-2_hq-02-2018-1.pdf)
- [20] *ConFlat(CF) UHV Flanges & Components Technical Notes*, [https://www.lesker.com/newweb/flanges/flanges\\_technicalnotes\\_conflat\\_1.cfm](https://www.lesker.com/newweb/flanges/flanges_technicalnotes_conflat_1.cfm)
- [21] *VCR FITTINGS Metal Gasket Face Seal Fittings*, <https://www.swagelok.com/downloads/webcatalogs/en/ms-01-24.pdf>
- [22] *Vacuum Flask - Wikipedia*, [https://en.wikipedia.org/wiki/Vacuum\\_flask](https://en.wikipedia.org/wiki/Vacuum_flask)
- [23] *Vacuum Flange - Wikipedia*, [https://en.wikipedia.org/wiki/Vacuum\\_flange](https://en.wikipedia.org/wiki/Vacuum_flange)
- [24] *Buckling - Wikipedia*, <https://en.wikipedia.org/wiki/Buckling>